OSMOSE

OPTIMAL SYSTEM-MIX OF FLEXIBILITY SOLUTIONS FOR EUROPEAN ELECTRICITY

Final Report on demo execution results

D5.5

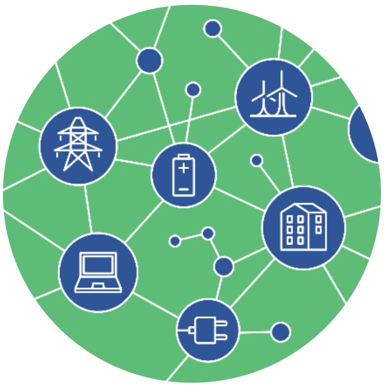

Contact: www.osmose-h2020.eu

The project has received funding from the European Union’s Horizon 2020 research and innovation programme under grant agreement No 773406

Document properties

Project Information

Programme	**O**ptimal **S**ystem-**M**ix **O**f Flexibility **S**olutions For **E**uropean Electricity
Project acronym	OSMOSE
Grant agreement number	773406
Number of the Deliverable	5.5
WP/Task related	5/5.5

Document information

Document Name	Osmose D5.5: Final Report on demo execution results
Date of delivery	31/03/2022
Status and Version	Final Version
Number of pages	99

Responsible

Document Responsible	Terna
Author(s)	Giuseppe Lisciandrello, Francesco Silletti, Alessio Siviero, Gino Albimonti, Leonardo Petrocchi (Terna); Guido Coletta, Dario Ronzio, Elena Collino (RSE); Marilena Lazzaro (ENG); Marco De Ieso, Giovanna Camorali (IBM); Christian Noce, Riccardo Klose, Martina Radicioni (Enel); Andrea Guzzetti, Stefano Bedogni (Edison); Riccardo Riva, Roberto Bazzani, Mauro Dalla Francesca (Compendia); Alberto PESCE (HITACHI-ABB); Davide Poli, Alfredo Vaccaro, Antonio Pepicello (ENSIEL)
Reviewer(s)	Gorazd Azman (ELES) / Alberto Escalera (REE)
Approver	Nathalie GRISEY (RTE)

Dissemination Level

Type (distribution level)	☒ PU, Public ☐ CO – full consortium, Confidential, only for members of the consortium (including the Commission Services) ☐ CO – some partners, Confidential, only for some partners

	(list of partners to be defined)

Review History

Version	Date	Reviewer	Comment
V1	31/03/2022	Nathalie GRI-SEY	

Table of content

0 Executive summary 8
1 Introduction 9
2 Zonal - Energy Management System (Z-EMS) 11
2.1 Test planning and execution....11
2.1.1 Overview 11
2.1.2 Detailed report of the most relevant sessions 12
2.2 Main Results 15
2.2.1 Z-EMS results 15
2.2.2 Results of the forecasting software (PREVEL) 22
2.2.3 Conclusions on the Z-EMS 26
3 Demand Side Response (DSR)....28
3.1 Introduction 28
3.2 Congestion Resolution 29
3.2.1 Test planning and execution 29
3.2.2 Main results 31
3.2.3 Conclusions on congestion management from DSR 50
3.3 Automatic Voltage Control (AVC) 50
3.3.1 Test planning and execution 50
3.3.2 Main results 51
3.3.3 Conclusions on voltage regulation from DSR 55
4 Dynamic Thermal Rating (DTR) 56
4.1 Test planning and execution....56
4.1.1 Overview 56
4.2 Main Results 56
4.2.1 Sensor-based DTR 56
4.2.2 Weather-based DTR 58
4.2.3 Conclusions Sensor-based DTR 62
4.2.4 Conclusions Weather-based DTR 62
5 Renewable Energy Systems (RES)....64
5.1 Introduction 64
5.2 Automatic Voltage Regulation 64
5.2.1 Test Planning and Overview 64
5.2.2 Main Results 66

5.2.3 Conclusions on voltage regulation from wind power plants 69
5.3 Synthetic Inertia 69
5.3.1 Test Planning and Overview 69
5.3.2 Main results 70
5.3.3 Conclusions on inertia from wind power plants 74
6 Overall conclusion from WP5 demonstrator..........75
7 Annex 1 – Zonal – Energy Management System..........77
7.1 Dashboard 77
7.2 Report of Z-EMS test sessions..........79
8 Annex 2 – Demand Side Response..........82
8.1 DSR Congestion Resolution Test Calendar..........82
8.2 DSR Congestion Resolution Test Results 84
8.2.1 Compendia 84
8.2.2 Enel X 89
8.2.3 Edison 91
9 Annex 3 - RES 93
9.1 AVC tests in Vaglio 93
9.2 AVC tests in Pietragalla..........98
9.3 Synthetic inertia control device parameters (Pietragalla) 99

List of acronyms and abbreviations

You can find in the table below the list of the acronyms and abbreviations used in this document.

Acronym	Meaning
aFRR	Automatic Frequency Restoration Reserve
ARIMAX	Auto-Regressive Integrated Moving Average Model with eXogenous input
AVC	Automatic Voltage Control
BDE	Regulation command sent by Terna operator to BSP
BSP	Balancing Service Provider
DB	Database
DC-OPF	Direct Current Optimal Power Flow
DSR	Demand Side Response
DTR	Dynamic Thermal Rating
ECMWF	European Centre for Medium Range Weather Forecasts
EMS	Energy Management System
FTP	File transfer Protocol
GFS	Global Forecast System
HD	Hard Disk
IFS	Integrated Forecast System
KPI	Key Performance Indicator
MOS	Model Output Statistics
NOAA	National Oceanic and Atmospheric Administration
NWP	Numerical Weather Prediction
OPF	Optimal Power Flow
PREVEL	Previsioni Elettriche (electric forecasts)
RAM	Random Access Memory
RAMS	Regional Atmospheric Modeling System
RES	Renewable Energy System
RF	Random Forest
SCCT	Sistema Controllo, Comando e Conduzione Terna (Terna control system)

SW	Software
VPN	Virtual Private Network
VST	Very-Short Term
WRF	Weather Research and Forecasting Model
Z-EMS	Zonal Energy Management System
CSET	Cyber Security Evaluation Tool
NIST	National Institute of Standards and Technologies
OU	Organisational Unit

0 Executive summary

This document summarizes the main results of the experimentation conducted within the Italian demonstrator (Work Package 5) of the OSMOSE project. The experimentation was conducted in a 150kV portion of the South-Italian grid, affected by large presence of renewable energy sources capacity and grid congestions. The overall test campaign lasted for about 9 months of 2021 in a real operation environment and tackled the investigation of several flexibility sources, such as 1) grid flexibility from innovative dynamic thermal rating (DTR) sensors coupled with advance dispatching and load forecast techniques, 2) flexibility from large industrial loads (DSR) and 3) flexibility from utility scale wind power plant. The document starts with a brief introduction that recall all the previous stages of the demonstrator, from the planning and design up to the physical implementation and software developments that were necessary to make the tests possible. Afterwards, there is a chapter dedicated to each main aspect of the demonstrator that illustrate the duration and the settings of each test, the mathematical formulation of the KPIs and their evaluation over the campaign tests, with some insights and technical conclusions derived from the numerical evidences. The first chapter shows how effectively the Zonal Energy Management system was able to detect and solve congestions, also by exploiting the load forecast models developed, for which accuracy levels are provided. The second one shows the results of more than 300h of aggregated use of the industrial loads for congestion management and Automatic Voltage Control provision, showing that slower regulation were more reliable than faster ones. The third one shows how significatively current power lines can be overloaded up to 300% of their standard ratings with smart and less invasive DTR technologies. Then, results on the control of wind power plants, with and without electrochemical storage, for the provision of voltage regulation and inertia are shown, illustrating how much wind power plants can contribute to system stability. Finally, a last chapter summarizes once again the conclusion derived from each technical chapter, by giving it a perspective from a system point of view as well as some insights for further developments. Three annexes complete the document with more graphs and detailed reports of each test session.

1 Introduction

Work Package 5 has undergone several stages: in 2018, at the start of the OSMOSE project, the area of the demo was selected in a relevant portion of the south Italian high voltage grid between Puglia and Basilicata. The flexibility to be tested was declared during the project proposal as follows:

- Flexibility from the grid to improve congestion management on HV grids and maximize RES production by coordinated use of Dynamic Thermal Rating (DTR) short-term forecasts and Demand Side Response (DSR) resources
- provision of Synthetic Inertia (SI) and Automatic Voltage Control (AVC) by single or aggregated large renewable power plants
- provision of Frequency Restoration Reserve (FRR) and AVC by single or aggregated large industrial loads in coordination with traditional power plants

Work Package 5 spent then a considerable effort into identifying the resources to be involved for testing the aforementioned flexibility:

- seven high voltage line were selected for the test of two innovative DTR solutions
- 20 industrial loads were initially selected for the participation in the DSR tests. By the start of the experimentation, 7 of them signed to take active part in the experimentation as linked third parties. However, two of them resigned in the 2021, compromising the possibility to test a-FRR. AVC and congestion management have been nonetheless tested
- Two wind power plants, owned by the project partners, were successfully involved in the demo. Hydroelectric and photovoltaic plants initially identified as possible linked third parties were afterwards discarded. Tests were performed on wind rotors and coupled BESS, when present

After identifying the electrical and geographical perimeter of experimentation (described in D5.1 and D5.2), 2019 was mostly devoted to the specification of all the necessary action to develop all the software and hardware assets in order to enable the tests, as well as the services definitions (set points, ramps, dead bands, etc.). This refers to all the ICT infrastructure needed for the development of a Zonal Energy Management system used for the congestion detection and resolution, the development of DTR sensors and relative master nodes, the physical and software upgrades to the control systems of industrial and RES power plants, as well as cybersecurity analyses. Then, up until the first months of 2020, the partners engaged in the actual implementation of all the demo components. The complexity of this task was already high given by the heterogenous pool of technologies and actors involved in the demo, such as plant owners, aggregators, software developers, hardware providers, researchers and the TSO personnel, including operative staff on the field and in the control rooms. The organization of technical and administrative tasks was further strained by the advent of the Covid-19 pandemic, which delayed by four months the implementation activities, in order to take into account health and authorization issues. Nevertheless, thanks to the relentless and diligent effort dedicated by all partners, the demo implementation was done by the start of 2021, as described in D5.3 and D5.4, and the experimentation started officially in February 2021. Since then, several pieces of the demo entered in the operative stage:

- The DTR systems were fully installed before 2021, however their testing had to wait the completion of the Z-EMS that is responsible for their handling
- The Z-EMS infrastructure was already running tests in February 2021. Further updated version of the systems add-ons, such as the dashboard and the DTR integration became operative shortly after
- The RES power plants started connection tests and first AVC tests in February 2021 as well. The tests requirements and specifications were perfected ever since. Synthetic Inertia tests were conducted in the last months of the experimentation
- Industrial power plants proved to be the most challenging part of the demo, due to the heavy retrofit in some cases. By February 2021, two out of the seven selected sites were ready to go, the other followed shortly after, except for two sites that gave up the experimentation due to authorization issues

Experimentation of all the flexibilities resources has been carried out until November 2021, producing a huge amount of data for the many technologies involved. Indeed, Work Package 5 tackled the techno-economic feasibility of flexibility services from many point of views, giving the Consortium the opportunity to get an holistic overview on many possible solutions.

Finally, December 2021 and January 2022 have been spent to collect and analyse the performances of each solution, thus producing this document, deliverable D5.5, which describes all the important key findings of WP5 demo. Therefore, we present in the next chapters the details of each executed tests, main numerical results and computed KPIs. Conclusions for each technology and services are provided in each specific chapter, while general conclusions will be provided at the end of the document.

2 Zonal - Energy Management System (Z-EMS)

2.1 Test planning and execution

2.1.1 Overview

The experimentation was made by several sessions. Duration and goals of each session were arranged and confirmed by all partners before the start of the session. Indeed, the WP5 demo relies on different components working together in order to achieve the expected goals. These components are under responsibility of different partners and a coordination activity was performed in order to properly address the experimentation. As a reminder, the main software components of WP5 demo are the following:

- Zonal Energy Management System Z-EMS (IBM): aims at detecting and solving future congestions in the sub-trasmission grid.
- Hand of Data - HoD (ENG) responsible for data retrieving and trasformation, Z-EMS activation and managing of its outputs.
- PREVEL (RSE) is the forecast chain that provides some meteorological variables and the active and reactive loads for each node in the network.
- Two innovative Dynamic Termal Rating methods (ENSIEL): DTR Weather-Based and DTR Sensor-Based. The needed business logic for allowing the proper execution of both this method is implemented by Wrapper (ENG).
- EMS Dashboard (ENG) put at disposal of Terna Operator in order to monitor the Z-EMS congestion management, utilization of DSR and RES plants for the other flexibility services, BDE creation and submission.

Moreover, as anticipated in D5.4 deliverable, the WP5 Demo relies on the ICT Infrastructure of figure below:

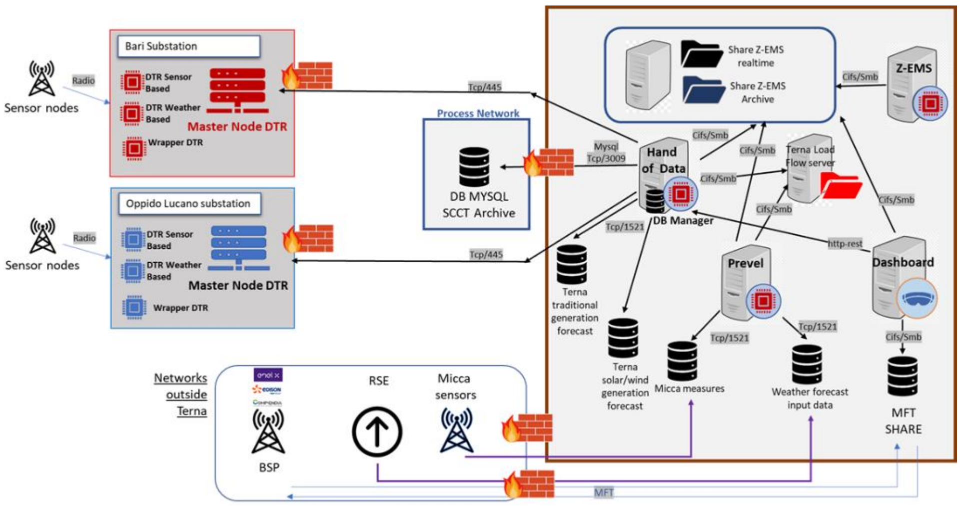

Regarding the EMS Dashboard, the functional specification provided in D5.4 was finalised after the deliverable submission. ENG has therefore developed this tool that was deployed in Operational Environment (Esercizio) in order to be used by TERNA during the experimentation and the test execution. A recap of main functionalities provided by the Dashboard are reported in Appendix 1.

In order to properly assess the correct operation of each component, four kinds of tests have been defined and carried out:

1) **Preliminary tests**, whose aim is to test ICT communication and basic functionalities
2) **DTR – DSR integration tests**, to include DTR and DSR into Z-EMS application, Dashboard included as well
3) **In-vitro tests**, to verify the Z-EMS congestion management algorithm with fake forced congestion by forcing selected lines ampacity to a very small value;
4) **Full tests**, with full Z-EMS, DTR and Dashboard functionalities; DSR is included only when BSP aggregators are available.

Since the experimentation lasted for several months, the amount of results is in large quantity for each type of tests, therefore, only the most relevant sessions will be reported in the main body of the document. A full report of test sessions can be found in Annex 1.

2.1.2 Detailed report of the most relevant sessions

Long full test 06/08 - 13/08

Scope

1) To assess the long-term Z-EMS operation in real conditions (no forced congestion, DTR and DSR inputs included)
2) To verify the final Z-EMS version

Description

On 30/07, the last Z-EMS version (v2.3) was uploaded in *Esercizio*. In this new version the tolerance for the congestion detection, previously set at 5%, is now set at 0,1 A, in order to detect more congestions, even small ones. It was decided that this will be the final Z-EMS version delivered for the OSMOSE Project.
During the 7 days long test, the weather-based DTR is running, there are no forced congestions and the BSPs don't send any offers. Taking into account that the Z-EMS operates within 00:00 and 20:59 each day, the number of available quarter of hours (qh) per day is 21*4 = 84.

Main results

Here we report the number of successful runs and the number of runs executed day by day. The average percentage of successful runs (meaning that the Z-EMS outputs are correctly saved) per day is 75 %, while the average percentage of successful run respect to the number of executed runs per day is 96 %. The difference between these two percentage is due to the failed creation and uploading of the Z-EMS input files by Hand of Data, PREVEL or Terna systems. You can see very low number of executed runs.

Date	Succesful runs	% successful runs/runs day	Executed runs	% successful runs/runs
06/08	82	97,6	82	100
07/08	82	97,6	83	98,7
08/08	39	46,4	40	97,5
09/08	29	34,5	29	100
10/08	66	78,5	79	83,5
11/08	81	96,4	82	98,7
12/08	64	76,2	65	98,4

For what concerns quality performance of the new Z-EMS version, it detects many more congestions than previous versions.

In-vitro test with BSPs 07/10

Scope To send commands to BSP/industrial loads

Description During the day, all 3 BSPs (Compendia, Edison, Enel X) are available, having previously sent their offers. Indeed, weather-based DTR is running.
Congestions are forced in 3 lines.
At 9:30, the Dashboard shows the first Z-EMS results: all 3 line congestions have been detected and the algorithm recommends to send 3 commands to BSP (see Fig. 2-1).
During the day, 3 commands are sent:
to Compendia (-0,48 MW) at 09:30
to Edison (-0,05 MW) at 10:45
to Enel X (-4,5 MW) at 13:45

Main results Commands are quickly sent, even if in some quarter of hours (qh) the Z-EMS results are shown very late on the Dashboard (one minute before the end of the qh), for example at 9:30. Apart from those rare cases, results are usually shown 3 minutes before the end of the qh, giving the operator enough time to decide which command to send.
At 10:00, Z-EMS detects a real congestion (118 %), too, in one line, correctly shown on the Dashboard.

Reference Table in paragraph 2.1.2, test number 3.5

In-vitro test with BSPs 28/10

Scope To send commands to Enel X and activate its industrial loads

Description Enel X offers 6 MW (downlift), available from 14:00 to 18:00 for at least 1 hour and not more than 2 hours, activation time is 1 hour. During the in-vitro test, weather-based DTR is running and congestion are forced on lines that are close to Enel X plant.
At 12:30, Z-EMS detects all forced congestion, except for two qh. In the same qh, Enel X offer is shown on the Dashboard and BDE is sent to activate the industrial load from 14:00 to 15:30 (see Fig. 2-2).

Main results BDE is correctly sent by Terna and received by Enel X. Further analysis about the power modulation will be executed by Terna and Enel X.

Reference Table in paragraph 2.1.2, test number 3.5

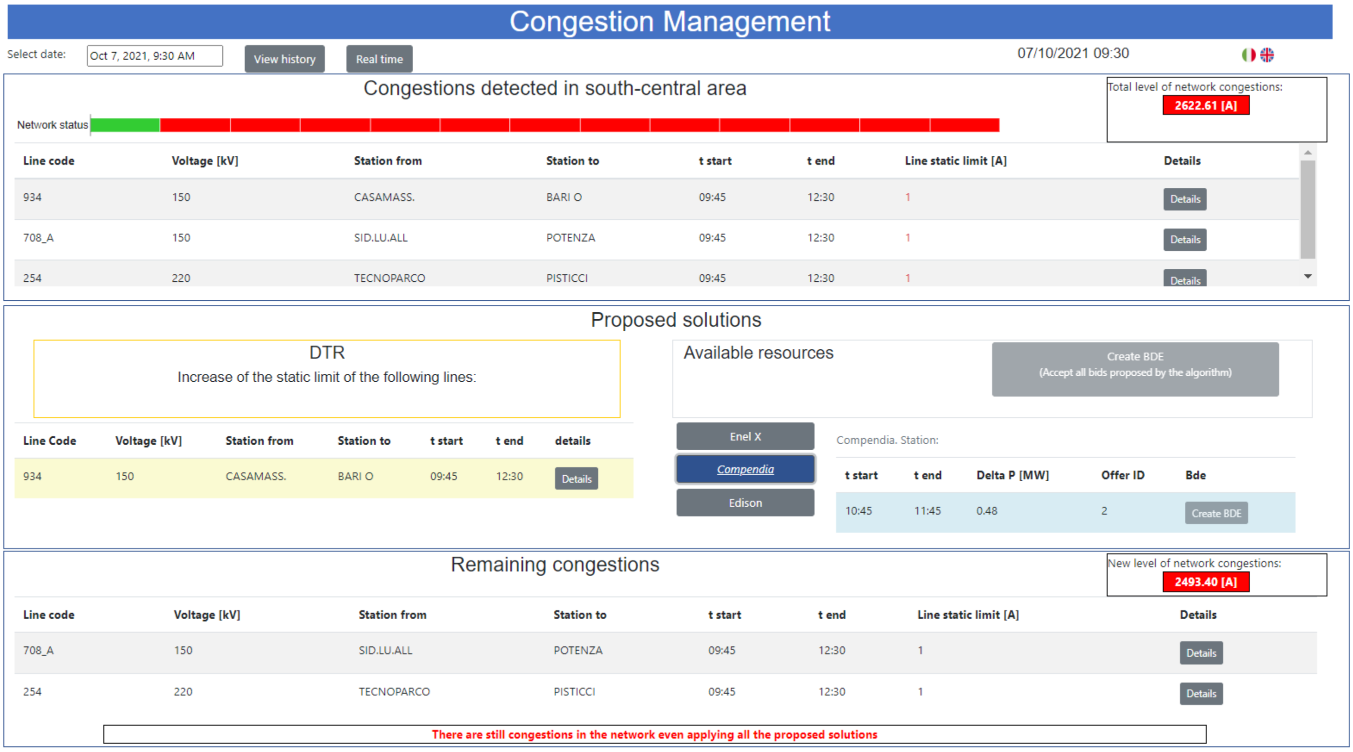

Figure 2-1 - Dashboard on 07/10/21 at 9:30

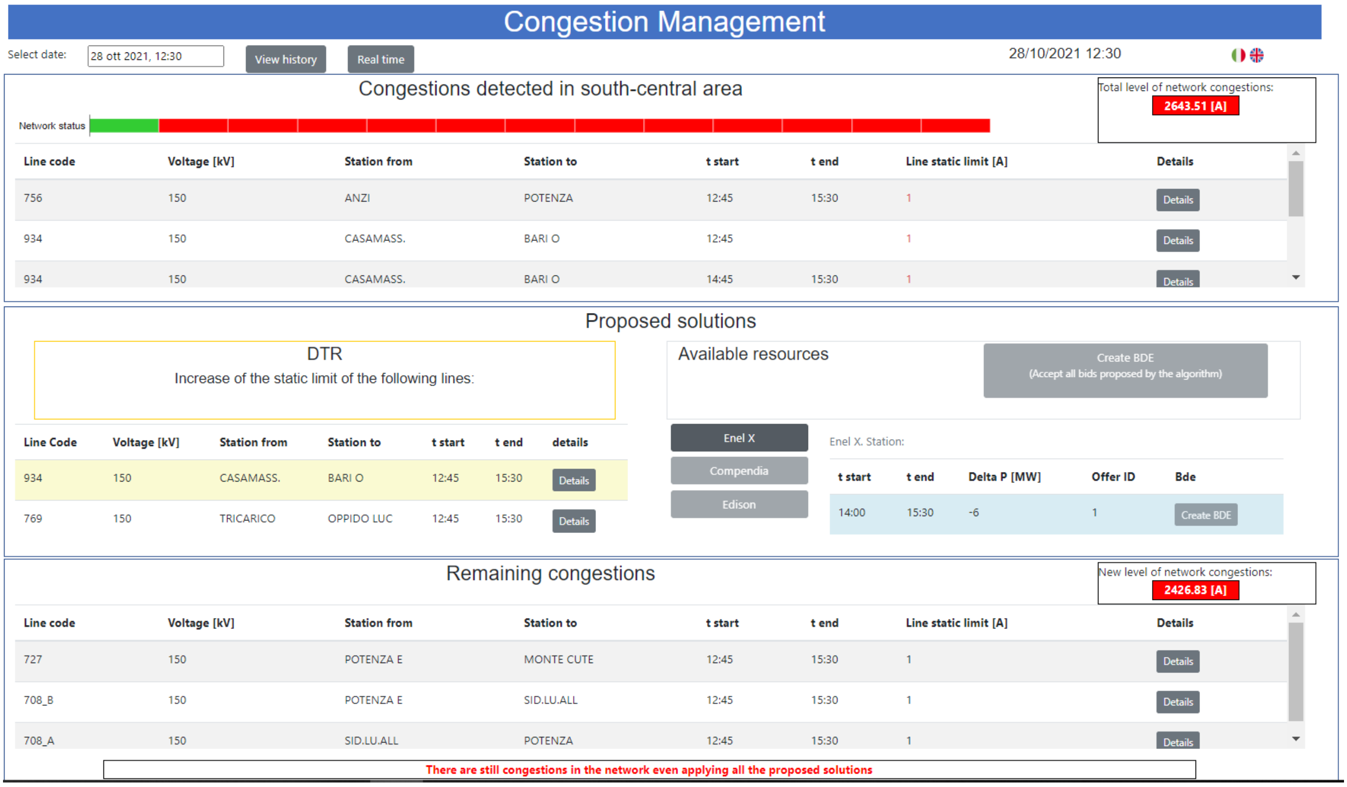

Figure 2-2 - Dashboard on 28/10/21 at 12:30

2.2 Main Results

2.2.1 Z-EMS results

2.2.1.1 KPIs general overview

The performances of the Z-EMS are evaluated based on several KPIs. A part of them are computed online and tend to summarize the goodness of each Z-EMS execution. Another group of KPIs is computed offline, which aims to assess the performances of the Z-EMS over a specified time period. Moreover, the KPIs are computed both on the so-called extended area, $\mathcal{L}$, which is the portion of the electric network in the south of Italy selected to take into account the boundary effects, and on the restricted area, $\mathcal{L}^0 \subset \mathcal{L}$, which is the proper demonstration area, which includes most of Puglia and Basilicata regions. The four KPIs are evaluated on the Full Test sessions executed from August to November 2021.

K1 - Reliability

The first KPI, $K1$, measures the input data reliability and it can be computed as:

$$K1 = \frac{\sum_{t \in \mathcal{T}} \zeta_t}{n} \cdot 100 \quad (1)$$

where n is the number of quarter of hours in the considered time interval and $\zeta_t \in 0{,}1$ is an indicator assigned at each Z-EMS execution that is 1, if input data are considered suitable by Z-EMS and the execution starts, and 0, otherwise.

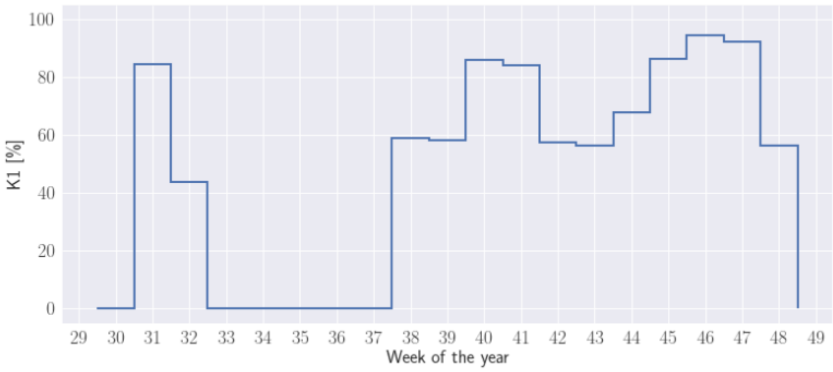

Figure 2-3 - K1 weekly profile

Figure 2-3 depicts the K1 indicator computed over each weekly time interval starting from June 01 up to November 30. The Z-EMS ran almost continuously in this period, except for a long interruption due to cyber security issues occurred in August 12 (week 32nd) and solved in September 21. Those cyber security issues were not related to the Z-EMS itself, but to one of the partners involved in the experimentation. Being compliant with Terna's best practice, the experimentation had to be stopped until all due verification were completed. Anyway, it is worth noting that, within the normal operation of the Z-EMS, K1 is always above 60%, with peaks of 80-90%. On the average and excluding the weeks from 32 to 37, K1 is 71.3%.

K2 - Convergence

A second KPI, $K2$, measures the Z-EMS ability to converge within the 15-min time step available for each instance. This KPI can be computed as:

$$K2 = \frac{\sum_{t \in \mathcal{T}} \psi_t}{n} \cdot 100 \quad (2)$$

where n is the number of quarter of hours in the considered time interval and $\psi_t \in 0{,}1$ is an indicator assigned at each Z-EMS execution that is 1, if model M1 data is reliable and its execution is completed within the 15-min time slot and 0, otherwise.

The analysis shows that just 2 out of 5,712 instances did not correctly converge within the 15-min time step. Hence, it is possible to affirm that the Z-EMS is able to provide useful pieces of information to the operator, given a reliable set of data.

K3 - Network Congestions Prediction

The third KPI, $K3$, is actually a group of indicators that measure the ability of the Z-EMS to correctly predict the occurrence of a network congestion. Hence, $K3$ is a vector of 12 triplets, $(K_{3,1}, \dots, K_{3,12})$, which measures the accuracy, the precision and the recall of the Z-EMS algorithm for each forecasting horizon.

At each correct execution of the Z-EMS the triplet (t_0, r, r_tot) is stored, where t_0 is the time stamp of the model instance and r (resp. r_tot) is an indicator which is equal to 1 if congestion occurs at $(t_0, \mathcal{L}^0)$ (resp. $(t_0, \mathcal{L})$) and 0, otherwise. Moreover, at each execution of model $M2$ a new n-tuple (t_0, $t_0 + i \cdot 15'$, s, s_tot) where s (resp. s_tot) is equal to 1 if the network is predicted to be congested at $(t_0 + i \cdot 15', \mathcal{L}^0)$ (resp. $(t_0 + i \cdot 15', \mathcal{L})$) and 0 otherwise.

Based on these data, it is possible to define four indicators:

- True Positive $\mathrm{TP}_{i,t}$: this indicator is 1, if there is **congestion** at t (according to Terna load flow data), and the Z-EMS algorithm predicted a **congestion** at t when executed at $t - i$ and 0, otherwise.
- True Negative $\mathrm{TN}_{i,t}$: this indicator is 1, if there is **no congestion** at t and the Z-EMS algorithm predicted **no congestion** at t when executed at $t - i$ and 0, otherwise.
- False Positive $F\mathrm{P}_{i,t}$: this indicator is 1, if there is **no congestion** at t, and the Z-EMS algorithm predicted a **congestion** at t when executed at $t - i$ and 0, otherwise.
- False Negative $F\mathrm{N}_{i,t}$: this indicator is 1, if there is **congestion** at t, and the Z-EMS algorithm predicted **no congestion** at t when executed at $t - i$ and 0, otherwise.

Hence, it is possible to compute the four classical indicators of the confusion matrix:

- $TP_i = \sum_{t \in T} TP_{i,t}$
- $TN_i = \sum_{t \in T} TN_{i,t}$
- $FP_i = \sum_{t \in T} FP_{i,t}$
- $FN_i = \sum_{t \in T} FN_{i,t}$

The triplet $K_{3,i}$ is defined as:

$$Accuracy_i \coloneqq \frac{\mathrm{TP_i + TN_i}}{\mathrm{TP_i + TN_i + FP_i + FN_i}} \tag{3}$$

$$\mathrm{Precision}y_i \coloneqq \frac{\mathrm{TP_{i,t}}}{\mathrm{TP_i} + \mathrm{F}P_\mathrm{i}} \tag{4}$$

$$\mathrm{Recall_i} = \frac{\mathrm{TP_i}}{\mathrm{TP_i + FN_i}} \tag{5}$$

The weekly evaluation of these KPI is shown in Figure 2-4.

Accuracy gives information about how well Z-EMS is capable of detecting the real behavior of the grid, detecting real congestions (TP) but also cases with no congestions (TN). Precision is the ratio between TP and the sum of TP and FP. Graphs in Figure 2-2 show that Accuracy is high, compared to Precision. This happens because TN is high (in the grid, in fact, real congestions are rare because Terna central EMS is working, too) and FP is high too (meaning that Z-EMS detects a lot of false congestions).

It's worth noting that line limits used by Z-EMS are partially different from those used by Terna central EMS. In Terna, in fact, two kinds of line limits are adopted: the first one is the safety limit, the second one is the operational limit that is few amperes below the safety limit. Indeed, these limits are changed seasonally: during the summer they are lower than during the winter. For Z-EMS, during all tests, only summer operational limits (the lowest ones) have been adopted, in order to be conservative.

Recall is the ability to detects real congestions, since it's the ratio between real congestions detected (TP) and total congestions happened in the grid (TP+FN). Concerning the extended area $\mathcal{L}$, Z-EMS Recall is well (0.78-0.79) and Accuracy and Precision are discrete, due to the fact that Z-EMS detects many false congestions while in the grid there are very few congestions. Indeed, comparing values for $\mathcal{L}$ with values for $\mathcal{L}^0$, it's worth noticing that the former are better than the latter, meaning that Z-EMS performances are better in the whole extended area than in the demo area. This could be due to input data quality.

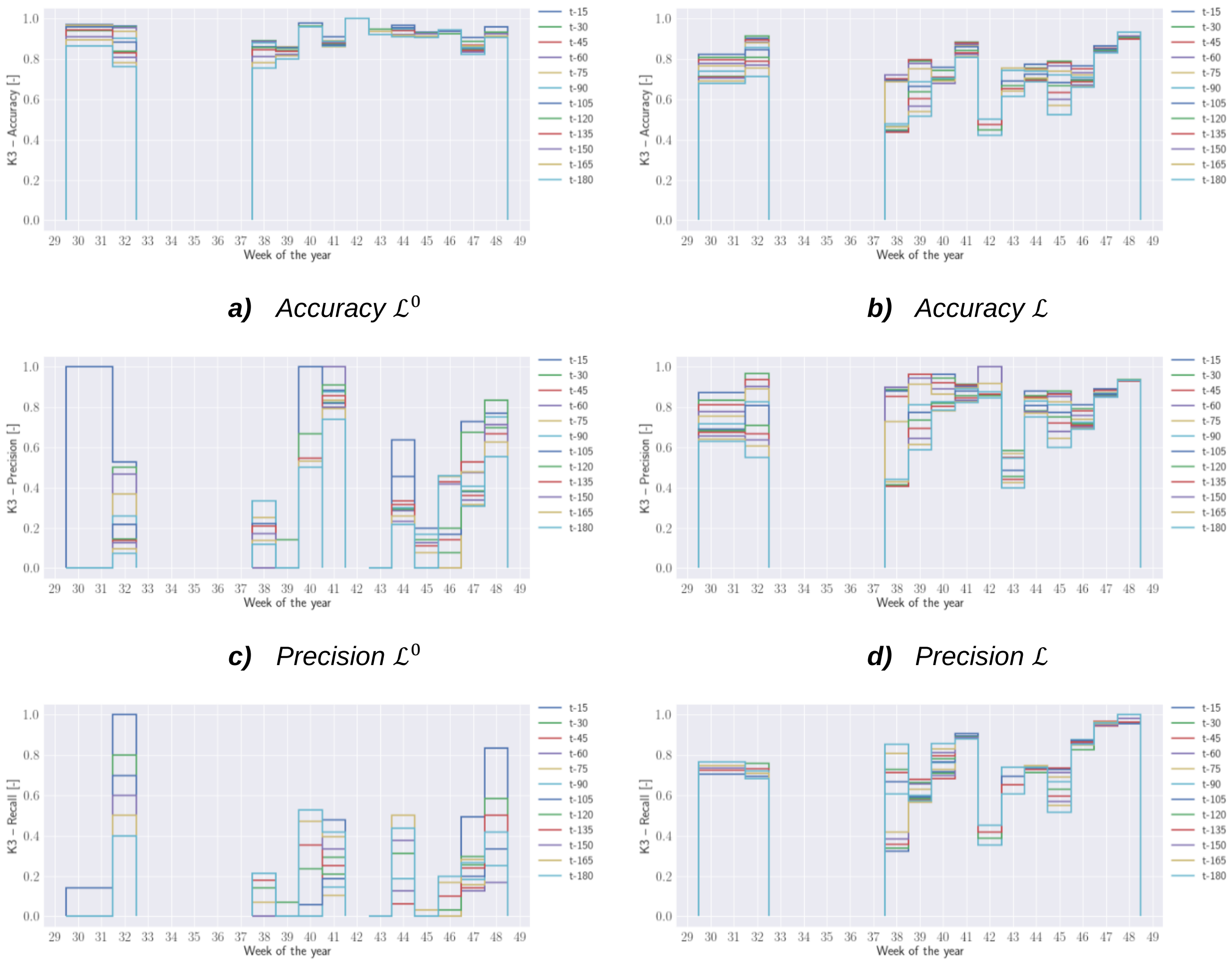

a) *Accuracy $\mathcal{L}^0$* ***b)*** *Accuracy $\mathcal{L}$*

c) *Precision $\mathcal{L}^0$* ***d)*** *Precision $\mathcal{L}$*

e) *Recall $\mathcal{L}^0$* ***f)*** *Recall $\mathcal{L}$*

Figure 2-4 – K3 weekly profiles

Table 2-2-1 – K3 values for the entire experimentation period.

	Accuracy $\mathcal{L}$	**Accuracy $\mathcal{L}^0$**	**Precision $\mathcal{L}$**	**Precision $\mathcal{L}^0$**	**Recall $\mathcal{L}$**	**Recall $\mathcal{L}^0$**
t-15	0,801	0,932	0,888	0,610	0,779	0,322
t-30	0,795	0,922	0,880	0,491	0,778	0,186
t-45	0,787	0,920	0,868	0,419	0,779	0,103
t-60	0,778	0,918	0,853	0,380	0,781	0,090
t-75	0,769	0,916	0,835	0,364	0,786	0,106
t-90	0,741	0,913	0,790	0,342	0,797	0,130
t-105	0,726	0,911	0,774	0,333	0,795	0,153

t-120	0,715	0,905	0,760	0,305	0,797	0,179
t-135	0,703	0,903	0,747	0,307	0,794	0,206
t-150	0,693	0,893	0,734	0,279	0,798	0,239
t-165	0,685	0,886	0,725	0,261	0,799	0,256
t-180	0,674	0,877	0,714	0,232	0,799	0,252

K4 - Local Network Congestions

The fourth KPI, K4, is somehow similar to the previous one. Indeed, it measures the ability of the Z-EMS to correctly predict the occurrence of a congestion on a specific line. Hence, $K4$ is a vector of 12 triplets, $(K_{4,1}, \dots, K_{4,12})$, which measures the accuracy, the precision and the recall of the Z-EMS algorithm in predicting the congestion of each specific line and for each forecasting horizon.

At each correct execution of the Z-EMS the triplet $(t_0, r, r$_tot) is stored, where t_0 is the time stamp of the model instance and r (resp. r_tot) is an indicator which is equal to 1 if congestion occurs at $(\mathrm{t}_0, \mathcal{L}^0)$ (resp. $(t_0, \mathcal{L})$) and 0, otherwise. Moreover, at each execution of the model a new n-tuple (t_0, $t_0 + i \cdot 15'$, s, s_tot) where s (resp. s_tot) is equal to 1 if the network is predicted to be congested at $(t_0 + i \cdot 15', \mathcal{L}^0)$ (resp. $(t_0 + i \cdot 15', \mathcal{L})$) and 0 otherwise.

Based on these data, it is possible to define four indicators:

- $\mathrm{TP}_{\mathrm{l,i,t}}$: this indicator is 1, if the line l is congested at t (according to Terna load flow data), and the Z-EMS algorithm predicted that congestion at t when executed at $t - i$ and 0, otherwise.
- $\mathrm{TN}_{\mathrm{l,i,t}}$: this indicator is 1, if the line l is not congested at t and the Z-EMS algorithm predicted no congestion at t when executed at $t - i$ and 0, otherwise.
- $F\mathrm{P}_{\mathrm{l,i,t}}$: this indicator is 1, if there the line l is not congested at t, and the Z-EMS algorithm predicted a congestion at t when executed at $t - i$ and 0, otherwise.
- $F\mathrm{N}_{\mathrm{l,i,t}}$: this indicator is 1, if the line l is congested at t, and the Z-EMS algorithm predicted no congestion at t when executed at $t - i$ and 0, otherwise.

Hence, it is possible to compute the four classical indicators of the confusion matrix:

$$TP_i = \sum_{l \in \mathcal{L}} \sum_{\mathrm{t} \in T} TP_{l,i,t}$$

$$TN_i = \sum_{l \in \mathcal{L}} \sum_{\mathrm{t} \in T} TN_{l,i,t}$$

$$FP_i = \sum_{l \in \mathcal{L}} \sum_{\mathrm{t} \in T} TF_{l,i,t}$$

$$FN_i = \sum_{l \in \mathcal{L}} \sum_{\mathrm{t} \in T} FN_{l,i,t}$$

The triplet $K_{3,i}$ is defined according to (3)/

The weekly evaluation of these KPI is shown in Figure 2-5.

Performances are lower than K3's, as expected: Z-EMS has got some difficulties in determining the right congested line when a congestion occurs in a specified quarter of hour. Apart from that, same comments about Accuracy, Precision and Recall already described for K3 are valid for K4. Even in this case, performances for extended area $\mathcal{L}$ are better than in demo area $\mathcal{L}^0$.

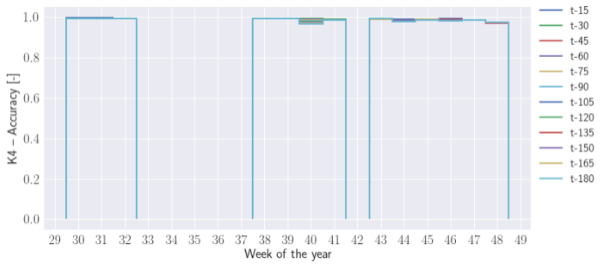

a) Accuracy $\mathcal{L}^0$

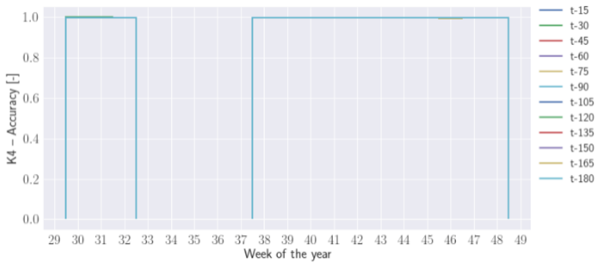

b) Accuracy $\mathcal{L}$

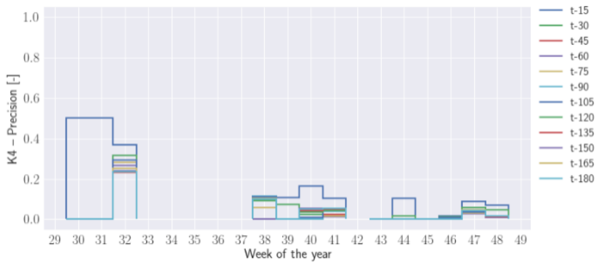

c) Precision $\mathcal{L}^0$

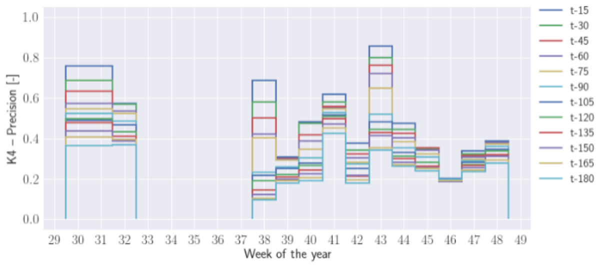

d) Precision $\mathcal{L}$

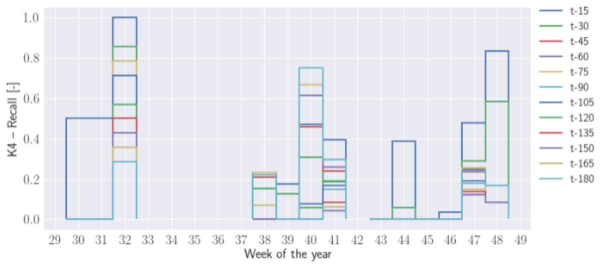

e) Recall $\mathcal{L}^0$

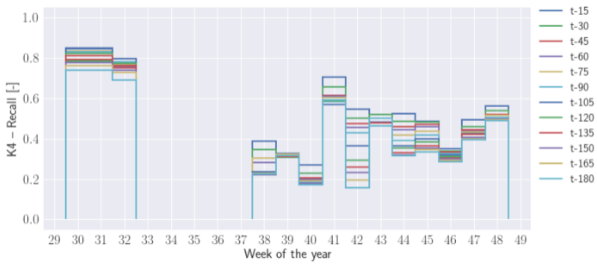

f) Recall $\mathcal{L}$

Figure 2-5 - K4 weekly profiles

Table 2-2 – K4 values for the entire experimentation period.

	Accuracy $\mathcal{L}$	Accuracy $\mathcal{L}^0$	Precision $\mathcal{L}$	Precision $\mathcal{L}^0$	Recall $\mathcal{L}$	Recall $\mathcal{L}^0$
t-15	0,997	0,990	0,361	0,092	0,456	0,363
t-30	0,997	0,989	0,345	0,052	0,428	0,199
t-45	0,997	0,989	0,332	0,026	0,412	0,099
t-60	0,997	0,988	0,323	0,022	0,405	0,084
t-75	0,997	0,988	0,312	0,027	0,397	0,107
t-90	0,997	0,988	0,298	0,033	0,385	0,142
t-105	0,997	0,987	0,287	0,033	0,377	0,154
t-120	0,997	0,987	0,279	0,037	0,372	0,176
t-135	0,997	0,986	0,270	0,037	0,367	0,191
t-150	0,997	0,986	0,259	0,039	0,360	0,206
t-165	0,997	0,985	0,250	0,039	0,354	0,212
t-180	0,997	0,985	0,241	0,038	0,347	0,211

K5 - Local Network Congestions (extended version)

This KPI has been formulated after noticing that sometimes congestions were detected by Z-EMS in lines that are close to actual congested lines. So, K5 is like an extension of K4. In fact, in this case

$TP_{l,i,t}$ is 1 even if the line, where congestion is detected by Z-EMS, is connected to the same node where is connected the real congested line (according to Terna load flow).

The results, as expected, are better than K4. This demonstrates that Z-EMS is capable of detecting congestions with a very small error (just one node next) in the location. Comparing K5 values in Table 2-3 with K4 values in Table 2-2, there is an improvement of Precision and Recall for the area $\mathcal{L}$ of 2-3 %, which means that 2-3 times out of 100 cases the congestion is detected in one line that is one node far from the real congested line.

Table 2-3 – K5 values for the entire experimentation period.

	Accuracy $\mathcal{L}$	Accuracy $\mathcal{L}^0$	Precision $\mathcal{L}$	Precision $\mathcal{L}^0$	Recall $\mathcal{L}$	Recall $\mathcal{L}^0$
t-15	0,997	0,990	0,389	0,096	0,475	0,372
t-30	0,997	0,989	0,371	0,056	0,446	0,211
t-45	0,997	0,989	0,359	0,031	0,431	0,116
t-60	0,997	0,988	0,349	0,026	0,423	0,101
t-75	0,997	0,988	0,339	0,032	0,416	0,126
t-90	0,997	0,988	0,324	0,035	0,405	0,148
t-105	0,997	0,987	0,313	0,033	0,398	0,154
t-120	0,997	0,987	0,307	0,037	0,394	0,176
t-135	0,997	0,986	0,300	0,037	0,392	0,191
t-150	0,997	0,986	0,287	0,039	0,385	0,206
t-165	0,997	0,985	0,278	0,039	0,379	0,212
t-180	0,997	0,985	0,269	0,038	0,372	0,211

2.2.1.2 Some deeper analysis and comments

In this section some critical instances will be analysed in detail to go deeper in the evaluation of the Z-EMS performances. To this end, critical instances characterized by at least five congested lines have been selected (see Table 2-4).

Number of congestions may seem low, but it is high considering that Terna central EMS works in order to solve them, too.

Table 2-4 – Critical instances characterized by five congested lines.

Critical instances	Number of congested lines
2021-09-27 09:15:00	8
2021-09-27 16:15:00	7
2021-09-27 17:00:00	6
2021-09-27 15:45:00	6
2021-09-27 17:15:00	6
2021-09-27 09:45:00	6
2021-09-27 17:30:00	6
2021-09-28 07:45:00	5
2021-08-10 18:00:00	5
2021-09-27 17:45:00	5
2021-09-27 16:45:00	5
2021-09-27 18:00:00	5
2021-09-27 16:30:00	5
2021-09-28 07:00:00	5
2021-09-27 16:00:00	5
2021-09-27 08:45:00	5
2021-09-28 08:45:00	5
2021-09-28 08:00:00	5
2021-09-29 08:30:00	5

Event 2021-09-27 09:15:00

According to Terna load flow output, in this quarter of hour there are eight congested lines, as shown in Table 5.

Table 2-5 – Congested lines at 2021-09-27 09:15:00.

SezID_N1	SezID_N2	I [A]	limit [A]
FON________VVVNET__	SSI________VVVNET__	708.02	432
FON________VVVNET__	PSG________VVVNET__	572.03	432
CRL________VVVNET__	AGR________VVVNET__	366.53	296
AZI________VVVNET__	CRL________VVVNET__	354.27	296
MRZ________VVVNET__	MTS________VVVNET__	139.29	129
TRC________VVVNET__	MAR________VVVNET__	395.10	370
TRC________VVVNET__	BUS________VVVNET__	394.17	370
RAM________VVVNET__	PSG________VVVNET__	453.71	432

The Z-EMS managed to find congestions at this time instant as shown in Table 2-. A closer look to Table and Table 2- brings out that one out of eight congested lines was predicted at 08:00:00 (1.25 hours in advance) and two at 08:45:00 (0.5 hours in advance).

Table 2-6 – Congested lines detected by the Z-EMS at 2021-09-27 09:15:00.

t0	SezID_N1	SezID_N2	I [A]
08:00:00	FON________VVVNET__	SSI________VVVNET__	436.47
08:45:00	FON________VVVNET__	SSI________VVVNET__	437.37
08:45:00	AGR________VVVNET__	CRL________VVVNET__	298.71
08:45:00	CEN________VVVNET__	BUS________VVVNET__	436.31
08:45:00	MRT________VVVNET__	APE________VVVNET__	108.07

The congestions on the other lines are not detected, while two false positives are found at 08:45:00 (0.5 hours in advance).

Even in this case, it should be taken into account that Terna central EMS works to solve congestions in parallel to Z-EMS using traditional congestion resolution methods (i.e. generating units re-dispatch, RES curtailment, grid topology re-configuration) so that some of congestions foreseen by Z-EMS happens not to be real congestions because they are solved by Terna central EMS in real-time.

This closer look demonstrates what K3 and K4 already showed: Z-EMS detects more congestions than real ones, some of them are true while the most of them are false. Even in this case, Terna central EMS operations should be taken into account, since it affects number and location of real-time line congestions.

2.2.2 Results of the forecasting software (PREVEL)

Bearing in mind that in order to efficiently manage flexibility resources one must have a representation of the state of the grid a few hours in advance, the aim of this activity is to verify the possibility of predicting the load at nodal level up to 3 hours in advance in a better way than persistence, and to identify which categories of loads are instead difficult to predict.

The forecast system implemented provides the weather forecast for the DTR and the load forecast for each node of the grid every 15' and with a time horizon of 3 hours ahead.

Concerning the load forecast, two relevant aspects need to be stressed: the grid state changes at each run time, and the forecast variable is the difference between demand and generation after the application of an AC load flow. Since the grid state is kept constant during the 3 hours of prediction, a first error occurs due to this discrepancy. Furthermore, the demonstrator has been implemented in such a way that it directly forecasts the total load in each subnets (primary stations), and not the individual load. The choice of providing forecasts for the aggregation of the loads in each node of the grid was made because the average number of loads is 1700 compared to an average value of 1000 nodes, and with this approach it was possible to reduce the number of elementary forecasts. In addition, spurious values, due to – probably – the AC load flow, are handled before building the forecasting models by trying to interpolate the outliers. These spurious values occur for a few consecutive time steps, and are not relevant for the short-term forecasts, which should predict the base load, nor for the very short-term forecasts. These values are not used in carrying out this analysis of results.

In addition, during the demonstration (since 01/06/2020 till 30/11/2021) the loads configurations changes over time, both considering subnets but also considering individual nodes (and thus using all the different combinations that occurred over time). The configurations grew from 1033 to 1470 (+42%), and so some of them are not populated enough to allow short-term predictions, since the predictive schemes adopted require a stable training set to look for a model describing the load trend. Many configurations have arisen for a few days or a few weeks, with no proxy to signal their forthcoming activation. For these cases, persistence was used as prediction. In particular, short (very short-) term forecasts were carried out for 90% (83%) of the subnets. Moreover, it is neither useful nor meaningful to use these configurations to assess the performance of forecasting methods.

But the biggest problem, and one that has proven to be very challenging to deal with, is the sudden change of the load baseline, due to a different use of the same (nominal) loads. These events do not depend on calendar days or the weather and are therefore not predictable from a physical point of view. This aspect should be further investigated as the performance of forecasting schemes strongly depends on the consistency and modelling of the input data.

On average, analysing the period from August to November 2020, very short-term forecasts were provided for 81% of the load configurations belonging to the DEMO area, and 78% of those belonging to the external area (extended area). The choice of configurations to be analysed was made by examining (by a human operator) the load trends.

The load forecasts have been calculated adopting a two-stages approach: once a day a short-term (ST) forecast, obtained applying a Random Forecast (RF) scheme with a 6-months training dataset, provides forecasts for all possible subnet configurations for two days ahead. This scheme uses as predictors some variables related to solar/wind generation (solar angles, radiative components, wind intensity at 10 and 75 m above ground) and some others related to demand (subjective temperature and relative humidity). Precisely because information on the type of generation and load for each node is not available, the forecasting scheme must be able to identify the features of both generation and demand. Once a week (on Saturdays), the RF models are calculated for each node configuration, for one and two days ahead, and for working days and holidays separately (about 4000 files and a total occupation of about 120 MB). The calendar day is not used as a predictor, as the models are built using homogeneous training datasets (only working days or only holidays). The RF scheme uses 350 trees to grow, 7 randomly sampled variables, and a validation set of 20% of the training. The training sets are made up using historical data, without any specific pre-processing to validate data.

RF performance is highly dependent on the node considered, in particular on the presence of generation (distributed, essentially photovoltaic), which manifests itself in a load trend characterised by a marked daily cyclicity (from an ex-post analysis). In this case, for forecast horizons longer than 105 minutes the short-term forecasts have smaller absolute errors than persistence. At 3 hours ahead, the rMAE[1] is 24.4% with respect to 36% of persistence, with an improvement of 32%.

The very short-term forecast (VST) scheme has the task of modifying the short-term forecast (which provides the baseline) on the basis of the most recent measurements. While the ST takes a few days (typically a week, when the RF models are updated) to adapt its forecast to a new baseline, the VST achieves this in a few hours. During the project, an ARIMAX (autoregressive integrated moving average with exogenous variables) and an Analog Ensemble (based on based on a search for past events similar to the current ones, shortly AnEn) schemes have been considered. The ARIMAX-based VSTs were not able to build a model for many subnets, and when they were able to do so, the output behaved like a persistence in most cases. The AnEn scheme is widely used to predict demand, generation and weather variables, but a physically reliable input is required. Baseline variations and spurious values introduce fast oscillations in the output, but rarely outside physical values, because the output AnEn is obtained by grouping selected past load values and only spurious values could provide outliers. This is particularly true for those subnets characterised by rapidly varying loads (about 1/8 in the DEMO area) but not large absolute variations in amplitudes (a few MW).

The AnEn predictors are the ST forecast, the zenith angle and the solar global irradiation, and the subjective temperature (the inclusion of the shifted measurements worsted the performance). The selection of the most similar past events is done considering each leadtime and the two adjacent ones (to intercept the trend), using the distance $d_{DM}(t,t') = \sum_{v=1}^{N_v} \left[\sum_{j=-\tilde{t}}^{\tilde{t}} \left(C_{v,t+\tilde{t}} - P_{v,t'+\tilde{t}}\right)^2\right]^{1/2} / \sigma_v$, where v represents each variable of the set of N_v predictors, $C_{v,t}$ the v-th component of the array of the current forecast for the forecast horizon t, and $P_{v,t'}$ the v-th component of the past forecasts relative to the same temporal horizon of $C_{v,t}$. Each variable used to evaluate the distance has been previously normalized using the standard variation σ_v of each variable inside the historical period considered.

If the ST is highly correlated with the measurements, and the VST failed, the ST prediction is used. If the measurement at the starting time (the freshest one) is available and does not differ by more than 2 standard deviations from its mean value, the prediction is bias-corrected using that measurement. Finally, as persistence is always the best prediction for the earliest time steps, the output of AnEn is weighted against persistence using a linear dependence (AnEn's contribution increases from 10% at t=+0 to 80% at t=+90, and then to 100 % at t=+180). Bearing in mind that a comprehensive analysis should examine performance at each node, some average indices obtained using the demonstration period (from August to November 2021) will be shown here. The analysis was carried out for both the DEMO area and the external area (EXTS in the following), i.e. for 159 (vs. 197, i.e. 81%) configurations in the former and 641 (vs. 917, i.e. 70%) in the latter (the lower number is the number of filtered subnets selected using the rules above, the higher numbers indicate the total number of subnets present in the areas). Forecasts were provided not only for loads belonging to sub-networks of the network, but also for some lines at the boundary of the considered domain. This is a very strong assumption, which should be removed when considering the whole of Italy. The capacity of substations is very variable and can range from a few kW to ±300 MW, and the power crossing the border lines can even vary between —1400 MW and 1000 MW. The most frequent maximum value is between 10 MW and 50 MW.

[1] rMAE is the mean absolute error normalized w.r.t. the average of the absolute measured load: $rMAE = \frac{1}{N}\sum_k |P_k^{fore} - P_k^{meas}| / \frac{1}{N}\sum_k |P_k^{meas}|$, where P_k^{meas} is the measured load and P_k^{fore} the corresponding forecast.

The error indicators used here are the MAE, the average of absolute errors, and the MAPE, the average of the percentage errors. MAE can be divided for the average (absolute) measurements obtaining the corresponding relative (percentage) errors rMAE.

Defining the error as $e_{sub}^{forec}(t) = P_{sub}^{forec}(d, t_{start}) - M_{sub}(d, t_{start} + forec)$, where P is the prediction for each substation at starting time t_{start} of the day d and the leadtime forec, M the corresponding measurement, and the percentage error as $p_{sub}^{forec}(t) = 100 \cdot e_{sub}^{forec}(t)/M_{sub}(d, t_{start} + forec)$, the scatter plots of the instantaneous percentage error p_{sub}^{forec} against the measurement M for two leadtimes, i.e. for +30 and +180 minutes, are shown in Figure 2-6 for the DEMO area and for the external area, because an objective of the analysis was to determine how much the performance of the forecast decays with the time horizon.

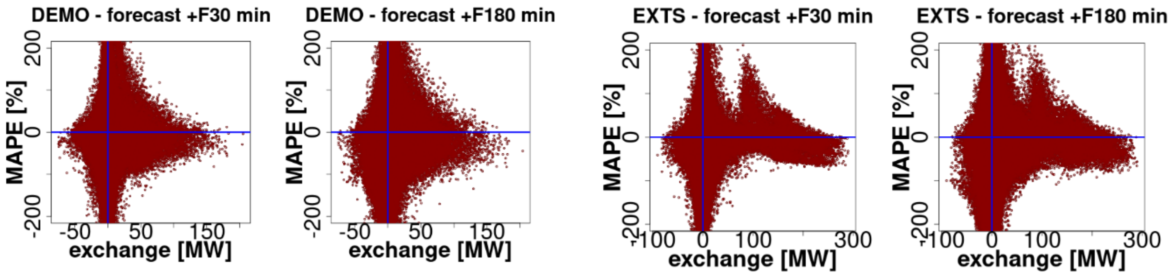

Figure 2-6 – Scatter plots for leadtimes +30 and +180 minutes. In abscissa the measured active loads, while in ordinate the instantaneous percentage error for the DEMO area (on the left) and for the external area (on the right) are shown. Boundary fluxes are not included.

The interesting feature that emerges from Figure 2-6 is the strong reduction of the percentage error with the size of the load for both positive and negative values, i.e. when load or generation are dominant respectively. The graphs show a general underestimation for positive loads, but it is important to be aware that p_{sub}^{forec} is a poor-accuracy indicator when small loads are involved, because of the insignificant amount used in the denominator to calculate the percentage.

In order to better understand the trend of errors with the amount of energy involved, the relative differential MAE has been calculated and reported in Figure 2-7-7 for the DEMO and the external area. The measurement series are divided into uniform intervals of power, and MAE is evaluated for each interval, considering only the forecasts associated with the measurements belonging to that interval. Relative values are calculated by normalising with respect to the average value of the same interval. Due to the fact that the population of each sub-interval differs considerably as the (absolute) value of the measures increases, only the indices of samples of at least 20 items are shown and a neighbourhood of the origin is masked, due to the presence of large errors associated to small denominators, with a little influence in terms of the energy moved. For larger values, errors show a more stable trend, oscillating around an rMAE of 7.5%÷15% (5%÷10%) for positive loads for the DEMO (external) area, and —40%÷15% (—30% ÷—10%) for the negative ones for the DEMO (external) area. Please note that normalisation is done with respect to the measured value on the x-axis. It is clear that the forecasting system based on Random Forest for ST and Analog Ensemble for VST is reasonably stable when varying the time horizon, and that the worsening of the performance with the temporal horizon is quite marginal.

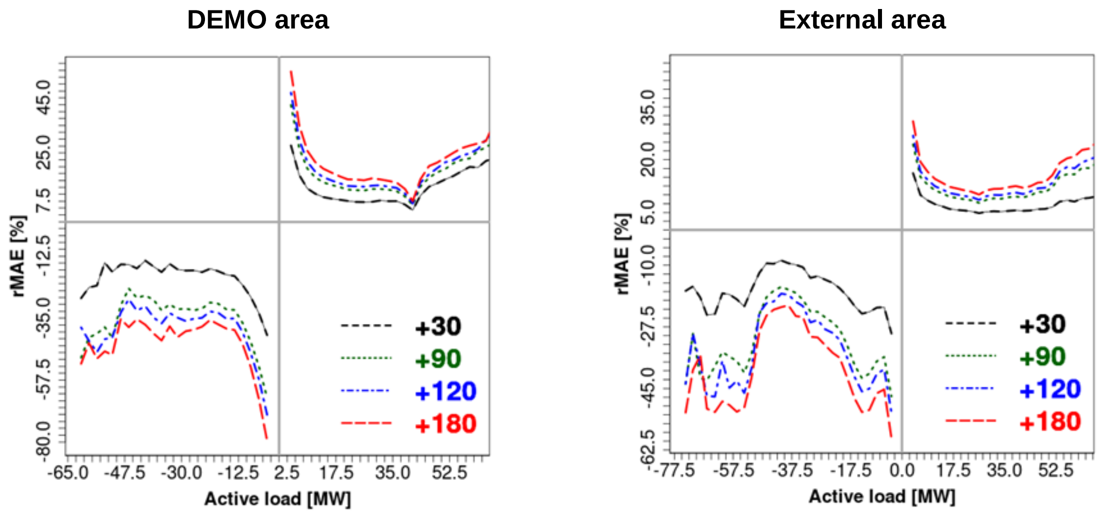

Figure 2-**7** – Relative percentage of rMAE for the DEMO area (on the left) and for the external area (on the right) for specific ranges of measurements. The error trend against exchange measurement is shown for four leadtimes with different colours. Sampling was carried out at a rate of 2.5 MW.

To analyse the daily variability for each leadtime, the absolute errors $\left|e_{sub}^{forec}(t)\right|$ have been represented by means of whiskers plots, by grouping data with respect to the daily quarter-hours. Figure 2-8 shows the boxplots for the last (+180') time horizon for the DEMO and for the external area. The worsening is more evident during the central hours of the typical day both in the interquartile range and in the 5th–95th quartiles, to which the forecast error of the distributed generation probably contributes. It is very interesting to observe that the distributions of the quantiles differ a lot both when considering VST versus persistence, and the DEMO area versus EXTS, and in particular the absolute errors and inter-quantiles are smaller for the EXTS area than for the DEMO area, due to the greater number of subnets in the former than in the latter, which implies that the number of subnets with large errors is a smaller percentage in the external area than in the DEMO area.

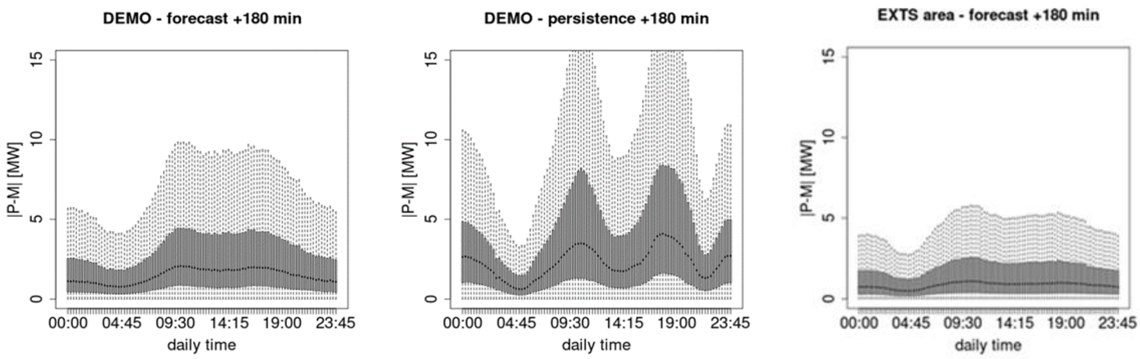

Figure 2-**8** – Quarter-hourly boxplots at leadtime +180 minute for the VST forecast (on the left), for persistence (on the middle) for DEMO area, and for VST forecast for the external area (on the right). There are shown the 5^{th} and 95^{th} quartile (longer dotted lines), the 25^{th} and 75^{th} (vertical rectangles), and the median values (black points). Outliers have been omitted.

Finally, a comparison of the MAE with respect to the time horizon for the two areas is shown in Figure 2-9. In this case the MAE is evaluated over the four months of the demonstration and is an average value per node, so that the total value of the MAE can be obtained by multiplying the average error by the number of (selected) nodes in the area (i.e. 167 for the DEMO and 675 for the outer area). In these plots the average error is shown without any normalisation, to avoid any masking due to different values at the denominator, as normalisation can vary with the time horizon (different data sets) and as the area varies. Then, the magnitude of this absolute error varies a lot with the areas, as noted above: better results are obtained when considering a larger area than a smaller one, because the number of relevant error sources in the outer area is smaller than in the whole (the outer area counts about 4 times the number of nodes in the restricted area), respectively a MAE of 281 MW for the DEMO and of 181 MW for the external area. The persistence is useful for leadtime less that 30', which introduces a greater imbalance between measurement and expected value, which increases monotonically with time. At 3 hours ahead the gain in the mean absolute error is of 86 MW/subnet for the DEMO area (i.e. a total gain of 14.3 GW), and of 55 MW/subnet (a total gain of 37 GW) for the external area, corresponding to an improvement of about 23.3% achieved by the VST for both the DEMO and the external area.

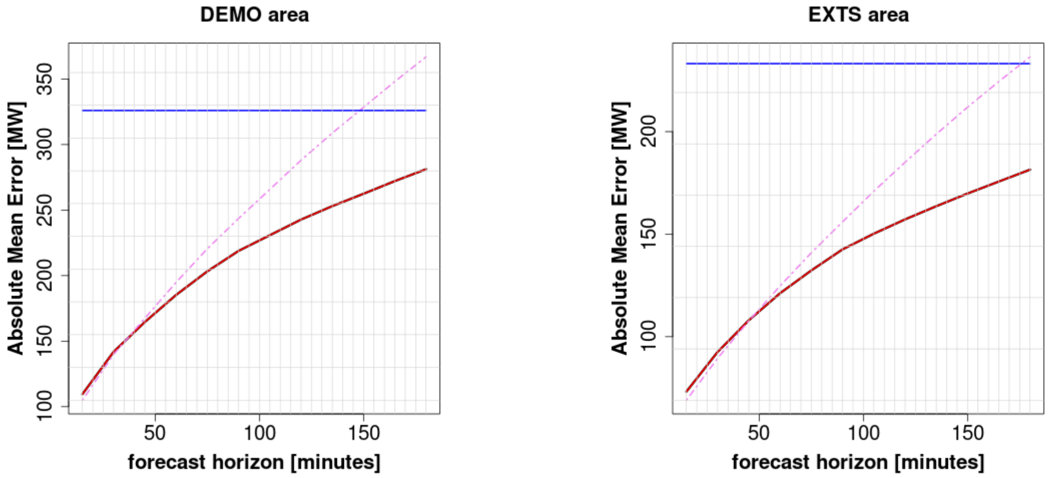

Figure 2-9 – Mean absolute error (MAE) for the DEMO (on the left) and EXTS (on the right) area. The horizontal (blue) lines refer to the ST forecast, the violet dotted ones to the persistence, and the solid red ones to the VST forecasts.

2.2.3 Conclusions on the Z-EMS

The Z-EMS developed within the OSMOSE project is a short-term congestion management tool based on the coordinated exploitation of flexibility services provided by DSR resources and DTR limits of existing interconnections. In this sense, the Z-EMS is the first practical large-scale application of optimal power flow techniques integrating DSR, RES and DTR technologies; its Technology Readiness Level is 8, since it is being tested and validated in a real operational environment.

As described, Z-EMS congestion detection ability is quite discrete: even though Accuracy and Precision are not so good, Recall is quite significant for 3 hours ahead OPF, also considering that it's working in parallel with Terna central EMS that solves congestions as well and that some important assumptions have been made during Z-EMS model development. To improve Z-EMS performances, the impact of these assumptions should be evaluated:

1) The DC-OPF formulation is missing the Q value. To overcome this limitation, the Q values from the input data at t0 are persisted along the entire time horizon. This persistence is a good proxy during the first steps, but the predictive power decays sharply after the first hour.

2) The forecast of loads and generation is affected by uncertainty.

3) The network is topologically unchanged during the 12 time steps (t1, …, t12). This assumption frequently doesn't hold in practice, as the incidence matrix or lines admittance values might change.

To overcome the first assumption, real Q forecast for both generation and load nodes should be used, so that the Z-EMS would be formulated as an AC-OPF. Regarding the second assumption, data quality of load and generation forecast can be improved by working on algorithms which are responsible for their provision.

In order to test the third assumption, the current deviations at a line/time step level over all the Z-EMS runs in September 27 have been analysed - all deviations normalized as a fraction of the current limit set for the line. A strong and significant correlation between the normalized absolute deviation and the number of changes in the network topology has been observed. The changes in network topology have been measured simply by summation, at each time step, of the number of lines or buses, which were present at t0 but were not listed at tn, and vice-versa. The behaviour of the median of the normalized deviation, given the # of topology changes, are shown in Figure 2-10.

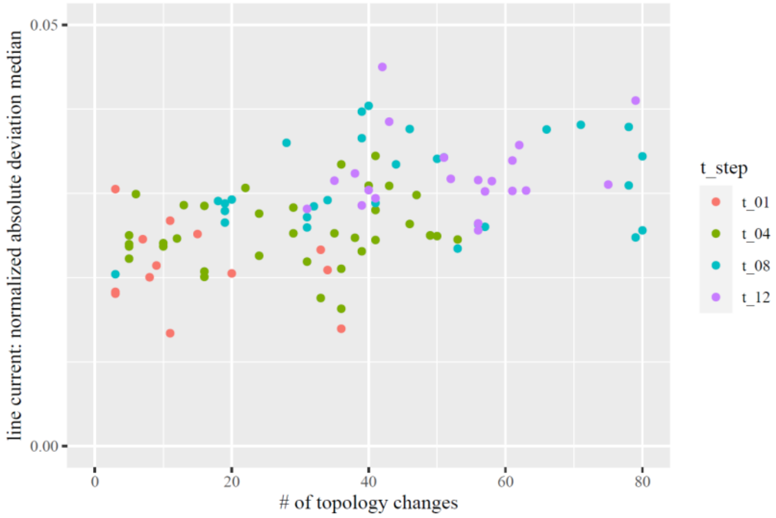

Figure 2-10

3 Demand Side Response (DSR)

3.1 Introduction

The experimentation phase of DSR involved 5 of the 7 industrial plants that initially agreed to participate in the demo activities as a third party.

With the Military site and the Car manufacturer there have been some slowdowns related to the letters of intent (LOI) which did not allow for any tests to be carried out in time with respect to the project deadlines. For the Military Site (Automatic Voltage regulation service), Terna and Enel X have preventively configured the plant in its own systems for the communication via IEC 60870-5-104. Unfortunately, the delays in obtaining the signature of the LOI did not allow to continue with the activities (communication tests, plant upgrade installations for service provision, tests).

For the Car Manufacturer (Congestion Resolution and automatic Frequency Restoration Reserve services) a definitive agreement about the content of the LOI has not been reached. For this reason, this industrial plant has decided to withdraw from the project although Edison and ABB had preventively configurated both RTU systems and the connection between aggregation platform and the site.

Table 3-1 provides an overview of all the partners and resources involved in the experimentation phase.

Table 3-1: Industrial DSR: Resources involved in the testing phase

BSP	***Plant ID***	***Industrial plant***	***Tested Resources***	***Flexibility service***	***Voltage level [kV]***	***Region***
Compendia	1	Industrial Park	Generator G5 Generator G6	Congestion resolution & Automatic Voltage Control	150	BASILICATA
	2	Steel mill	Blast Machine 1 Blast Machine 2 Decoring plant Compressor	Congestion resolution	220	APULIA
	3	Oil refinery	Heating System	Congestion resolution	150	APULIA
Enel X	4	Foundry	Furnace	Congestion resolution	150	BASILICATA
	5	Military site	Rephase systems	Automatic Voltage Control	150	APULIA
Edison	6	Powertrain industry	Cooling unit (Chillers)	Congestion resolution & automatic Frequency Restoration Reserve	150	APULIA
	7	Car manufacturer	Retired	Congestion resolution & automatic Frequency Restoration Reserve	150	APULIA

Test campaign mainly concerned the congestion resolution service, which it was possible to test on all the resources involved in different ways: increasing/decreasing loads consumption, increasing/decreasing generators production or load shifting.

Automatic Voltage Control (AVC) service was evaluated with local test sessions in the industrial park through the increase or decrease of the reactive power, in order to evaluate the voltage variations on the transmission grid.

Regarding Automatic Frequency Restoration Reserve (aFRR), some tests were to be carried out in the Powertrain Industry after the congestion resolution tests. Unfortunately, the latter have highlighted that it is not possible to quickly control the power absorption of a HVAC system by adjusting the temperature of the chillers due to the high inertia of the whole system and the unreliable control performed by an indirect dimension as temperature. Since aFRR is a continuous and fast power exchange with the grid based on a power signal received by the TSO, with the aim to restore the system emissions to the nominal frequency, it was not possible to perform tests for this service.

The following paragraphs describe the WP5 test results of Congestion Resolution service (3.2) and Automatic Voltage Control (3.3).

3.2 Congestion Resolution

3.2.1 Test planning and execution

Congestion Resolution tests entail a variation of energy exchange with the grid related to a certain period. Therefore, it was necessary to define an organizational methodology for the test campaign.

The first stage was the planning: at least 3 weeks in advance each BSP has communicated the availability days of the industrial plants. In this way, Terna's programming team could verify possible scheduled maintenance of the involved lines. If everything was ok Terna's territorial control room was informed, and if they did not detect any critical issues, a confirmation of the test days was communicated to the BSP. The second stage was the execution. In this phase BSPs presented day ahead a set of callable aggregated upward and downward offers, also including the baseline of the plants. During the test day, Terna selected the offers through the Dashboard and for those selected, regulation orders (BDE) were sent to the BSPs. Once a command is sent, Terna's territorial control room was informed another two times: the first one, immediately after sending the command, to communicate all the details of the test (moving power, starting time and duration), and the second time, to communicate the end of the test session. Details of communication between Terna, BSP and industrial plants were described in chapter 2.2 of the D5.3. The last stage was the ex-post Analysis, where BSP and Terna extracted and analysed all the data collected during the test.

As regards the bids submitted by the BSPs, they were of two types: Downward and Upward.

- Upward offer means a reduction of a load or an increase in the energy production in case of generation.
- Downward offer means an increase of the absorption of a load or a reduction of the energy production of a generator.

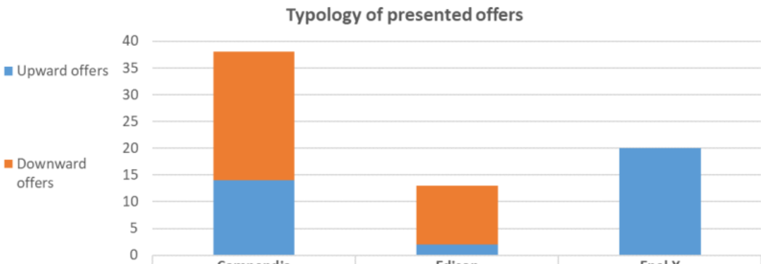

	Compendia	Edison	Enel X
Downward offers	24	11	0
Upward offers	14	2	20

Figure 3-1: Typology of presented offers for each BSP

Compendia presented a good mix of upward and downward offers (also aggregated). Most of the offers submitted by Edison were downward while Enel X presented only one type of offers (downward).

For each test day, offers were contained in a .xlsx file with the following key information:

- Availability hours: time slot within a day, in which the industrial plants are available to be called (eg: 09:00 AM - 02:00 PM).
- Minimum and maximum handling time.
- Activation time: minimum advance by which the bid must be called.

- Baseline: prediction of power exchange with the grid during the day.
- Minimum and maximum ΔP: amount of available regulating power.

The offers could be withdrawn, modified or updated even in real time (e.g. notification of failure to execute a command). Each bid could be called only once during the day with a flat power value between the minimum and the maximum offered.

Once the bids were accepted, based on the activation time, the BSPs received a command containing: the bid number selected (each offer file could contain up to 6 different bids), start and end time of displacement and power variation. Commands (BDE) were sent in agreement with the Z-EMS algorithm, when available, and using the Dashboard, described in Annex 1.

Figure 3-2 represents the command execution performance of the three BSPs. From the many offers presented by Compendia, around 85% were correctly executed, in 4 cases there were some problems with data acquisition or communication protocols, in 1 case an offer was retired and in 1 case a command was not executed due to some problems with the respective plant. With regards to Edison, in three cases commands were not executed, because, without notice by industrial client, the plant was not in operation at the test time and no regulation could be performed. The foundry controlled by Enel X instead, had successfully performed all commands.

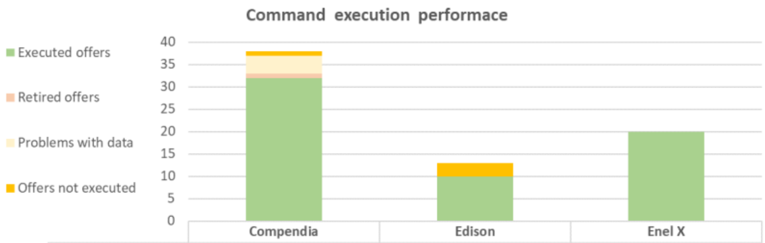

	Compendia	Edison	Enel X
Offers not executed	1	3	0
Problems with data	4	0	0
Retired offers	1	0	0
Executed offers	32	10	20

Figure 3-2: Command execution performance of the three BSPs

In terms of testing hours, Compendia and Enel X have far exceeded the 100 hours of availability, while Edison has almost reached the target (it was penalized by the withdrawal of the car manufacturer and numerous days of plant shutdown due to layoff of the Powertrain industry).

Table 3-2: Total amount of testing hours, for each BSP, of the congestion resolution campaign

BSP	***Availability hours***	***Callable hours***	***Called hours***	***Performed hours****
Compendia	129,75	37,75	36,25	30,25
Enel X	112	23,5	20,5	20,5
Edison	99	13	12,25	9,5

*Detracted hours in which command were not executed or data were not acquired

<u>Overall, for the congestion resolution test campaign, more than 114 MWh of energy were moved. The full calendar with the general information of all the tests is reported in Annex 2</u>

The performances of the resources involved in the experimentation were assessed on the basis of several parameters and indicators. Most of them are general and common to all the plants:

- Activation time: comparison with the standards reported in the Italian network code.
- Maximum duration offered.
- Ramp times.
- Average value of measured flexible power compared to the power required.

In addition, a first KPI evaluates the resources on the basis of the energy actually provided, understood as deviation and return to the starting condition (including ramps), compared to the called energy they should have supplied:

$$KPI1 = \frac{E_{real}\ [MWh]}{E_{theoretical}\ [MWh]}; \quad (6)$$

A variant of KPI1, called KPI1*, evaluates the energy provided with respect to that required but only in the time slot Δt within the call:

$$KPI1^{*} = \frac{E_{real\Delta t}\ [MWh]}{E_{theoretical}\ [MWh]}; \quad (7)$$

This variant was introduced for two reasons:

1. KPI1 could not be evaluated for all the plants involved, due to their particular power absorption profile.
2. With KPI1* it was possible to reduce the errors committed manually by the operators (e.g. delay in restoring the initial conditions) and understand the resource performances only from a technological point of view.

As explained in the following chapters, all BSPs had difficulties in predicting the baseline profiles of the industrial plants. Therefore, the term $E_{theoretical}$ in (6) and (7) was evaluated considering as power reference values (before and after the movements), an average of the measured power.

3.2.2 Main results

3.2.2.1 Compendia

a) Plants overview

The project involved three different sites: an industrial park, an oil refinery and a steel mill.

The tests were carried out without a baseline as it was impossible to characterize and quantify the specific consumption of the plants used for the project within its own site.

Industrial Park

The company offers services in energetic and environmental field, designs, builds and manages technological infrastructures, produces and distributes the utilities needed by companies in the industrial area of Basilicata.

The starting energy flexibility analysis analyzed all the types of plant present: plants used for electrical and thermal energy production, plants dedicated to utilities production for the industrial sector served and water purification plants. Only a few resources have been made available from all the systems, taking into account the infrastructure constraints and the related costs of connection to the remote-control network. Therefore, the following resources participated in the experimentation:

- n. 3 internal combustion engines fueled by palm oil each with a nominal power of 8,098 MW (G5-G6-G7).

The machines taken individually have an upward modulation potential that allows them to reach 4 MW of production in about 15 minutes and to be fully operational with 8 MW of production after 30 minutes. First tests execution showed instead that the operating point involves a withdrawal of approximately

7.98 MW which therefore becomes the basis of the offer. The shutdown command is implemented manually with a necessary notice time of at least 30 minutes.

Oil Refinery

The refinery ensures petroleum products supply for industrial and civil uses to a large area of the country. The possible sources of flexibility identified for the project are some plants marginally involved in production. Among these only the hot oil heater was suitable for carrying out the tests.

Differently from the analysis phase in which the heater is to be used in the winter and therefore with a rising load (heater shutdown, normally in operation), the application in tests takes place in the summer. In this case, a downward load was considered, thus resulting in the ignition, during the tests, of the normally off heater. The nominal power of the heater made available from the flexibility analysis was 1 MW. From the execution of the tests, it is noted that the operating point instead involves a variable consumption from about 380 to 500 kW. Therefore, an average value of 450 kW was chosen as the basis for the offers.

The activation of the ignition command is performed manually with a warning time initially equal to at least 120 minutes and then reduced to 60 minutes.

Steel Mill

The company's activity is focused on the production of metal core of exchange devices placed along the railway lines. The initial energy flexibility analysis involved all plant types and showed many available resources. Some of these were excluded because of infrastructural constraints and related costs of connection to the command network.

The following resources participated in the experimentation:

- Screw air compressor, normally off and available from the event of a call, with "no-load" operation. The nominal power of the compressor made available is 150 kW and it is assumed that the available no-load power is 30% for a total of 45 kW. From the execution of the first tests, the no-load operating point instead entails a flat consumption of about 30 kW which therefore becomes the basis of the offer. The shutdown command is implemented manually with a necessary notice time of at least 30 minutes.

- Automatic camera shot blasting machine. The plant is used for the cleaning of semi-finished products and is assumed to be available to switch off in the event of a call. The nominal power of the plant is 90 kW not equipped with an inverter and therefore not modular. It was initially assumed that all the power could be made available. From the execution of the first tests, it is noted that the nominal operating point instead involves a withdrawal of about 70 kW which therefore becomes the basis of the offer. During the load characterization phase, it was noted that the power adjustment could be performed also with a step adjustment, initially disconnecting only the turbines for the propulsion of the abrasive material for about 35 kW, and at a later time the dust extraction and filtration system for another 35 kW. Although this did not affect the maximum potential made available to the experiment, it provided a potential possibility of control in the aggregation of loads. The shutdown command is implemented manually with a necessary notice time of at least 30 minutes.

- The de-embossing system used to clean, downstream of the de-stamping, the solidified castings from the foundry earth. The system is activated following the unsetting of a minimum number of jets, in order to ensure continuous operation for a certain period of time. The system is made up of various sections for a total nominal power of 73 kW, the drive of its components and motors is not driven by an inverter, resulting in that the load is therefore not modulable. It was initially assumed that all the rated power could be made available. From the execution of the first tests, it was noted that the low contemporaneity of absorption of the loads making up the system involves a withdrawal of 20 kW, which therefore becomes the basis for the offer. The shutdown command is implemented manually with a necessary notice time of at least 30 minutes.

b) Aggregation platform and data acquisition

Compendia has been supported by HITACHI-ABB in the implementation of a Virtual Power Plant infrastructure, where all the industrial site's resources described above has been aggregated. Upon this aggregation the Virtual Power Plant has been operated as a Service Balance Provider. Moreover, the typical SCADA main features which Real-Time data Acquisition and monitoring and automation controls, has been deployed technology that help to manage the entire flow within the DEMO. Starting to the Baseline distinct and summation of all resources, total and punctual active power flexibility upward and downward, dispatching algorithm where locate the proper resources to call in reduction or power increasing and also parsing and managing of the Balancing Command customized for those tests.

Below some pictures to show some typical view of the Virtual Power Plant implementation.

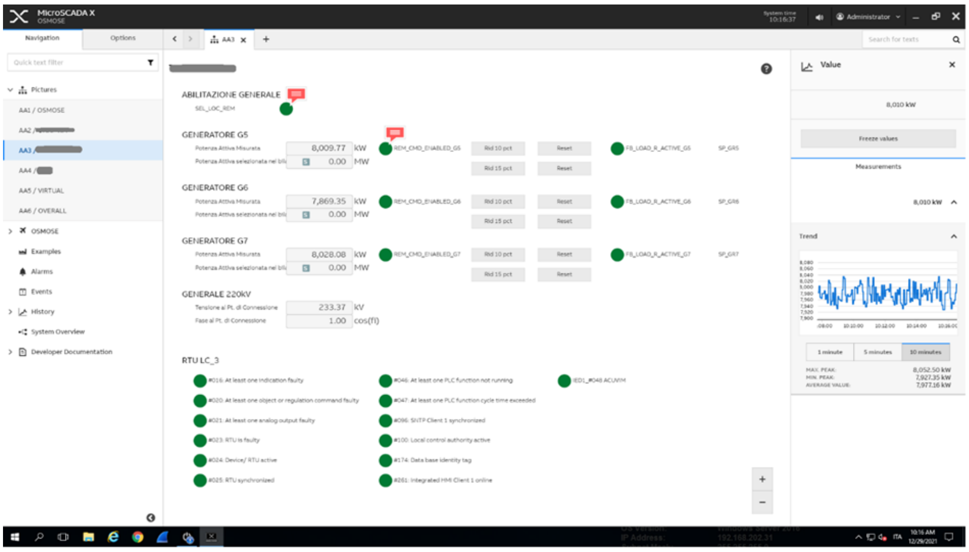

Figure 3-3: Overview of Compendia platform

There was possible monitoring, through the real-time data acquisition, the actual status of plant and get a sum of Power consumption and input defined as a Virtual Point of Interconnection.

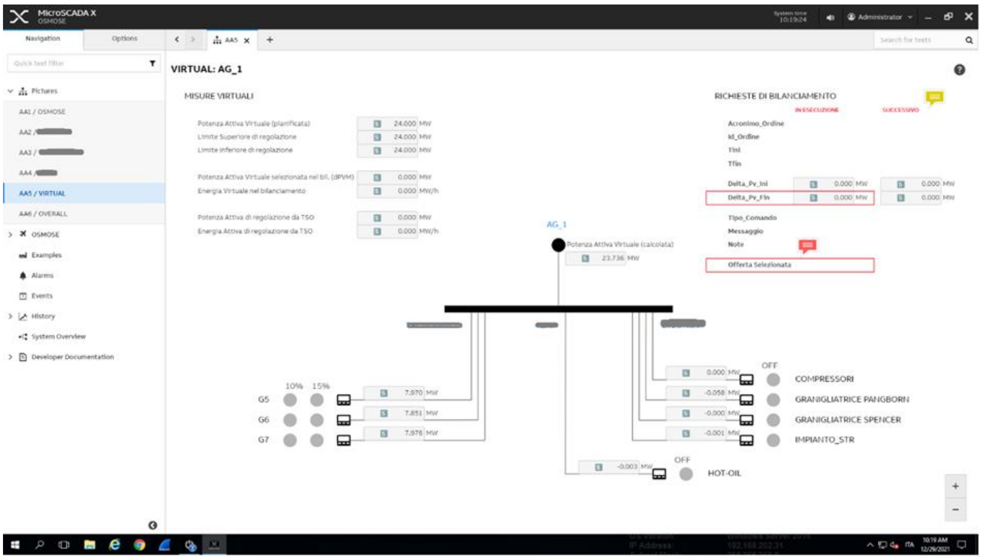

Figure 3-4: Virtual point of Interaction of Compendia platform

A set of Dashboard has been prepared to publish and overlapping Baseline, Realtime and calls for a reduction (or increasing) of Active Power demanded for the Congestion Management Use Case.

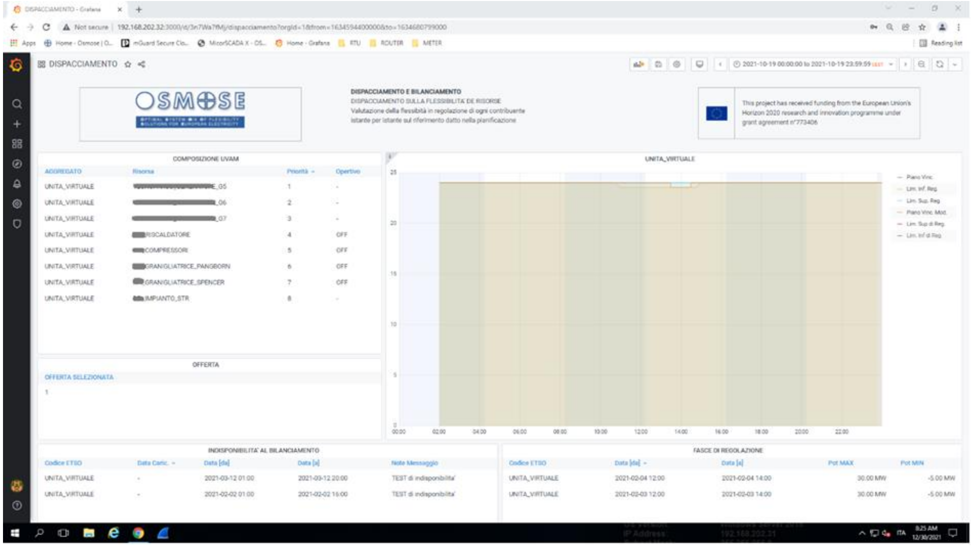

Figure 3-5: Example of data representation

For each of the resources available from the flexibility analysis, the theoretical flexible power of each resource was compared with the real situation occurred during the tests. The data used for the analysis are obtained from a database containing the results of the various tests carried out, each recorded every four seconds.

It is analysed the difference between the switching on (and switching off) times from the model and the real situation, also focusing on the duration of the actual test compared to the duration foreseen by the model. Once this difference has been evaluated, the time with which the load has reached the reference threshold value (ramp) was observed and, subsequently, was calculated the average value within the reference time range (limited respectively by the first value to reach the established load and from the last value to hold the established load). This data represents the average load that the resource offered during the test. Finally, KPI1 and KPI1* are evaluated as described in chapter 3.2.1.

c) Results

The details of all the executed tests are reported in Annex 2 (Chapter 7.2.1). Here the main evidence.

<u>Aggregate tests</u>

The aggregate tests were performed considering two different pairs of loads: the compressor of the Steel Mill with the hot oil heater of the Oil Refinery and the shot blasting machines with the STR of the Steel Mill. Unfortunately, in this last case, the results of the tests were unsatisfactory.

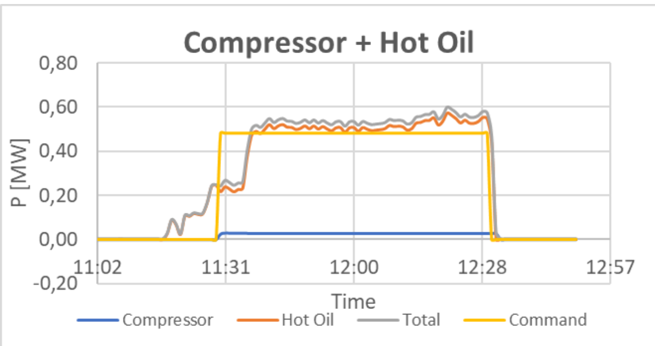

Figure 3-6: Example of resources aggregation of two different industrial plants (Oil Refinery + Steel Mill)

The results that emerged are the follows:

- The called P [MW] is composed by the sum of the single loads. The first one (0.035 MW) supplied by the compressor and the second part (0.45 MW) guaranteed by the hot oil heater.
- From the analysis of the aggregate loads, an average variable power value emerges from a minimum of 0,485 MW to a maximum of 0,596 MW, recording an average load modulated on the overall tests equal to 0,538 MW.
- The switch on times changes a lot depending on the load showing a progressive improvement with the succession of tests.
- Finally, KPI1 values varying from a minimum of 103% to a maximum of 324% while the KPI1* varies from 84% to a maximum of 164%.

Hot-oil heater (Oil Refinery)

The availability times of this plant have been much more flexible than the various resources made available by other sites. Therefore, it was possible to carry out the tests in a variable availability range typically from 10:30 to 12:30. Generally, the hot oil heater needs a predetermined time during which the load gradually increases up to the value indicated by the model. This time frame is defined as the "ramp". It is observed a progressive improvement, with the tests, of the timing in completing the ramp, passing from a maximum of 32 minutes to a minimum of about 4 minutes. Regarding the average power value measured once the predetermined threshold has been reached, this varies from 0,464 to 0,546 MW with an average value of 0,51 MW. These values should be compared with the power initially offered and called (0,45 MW).

As regards the KPI parameter, KPI1* values varying from 16% (in one test, due to some problem that occurred in the plant) to 127%, with a total average of 102%.

Considering the KPI1, the extreme values, observed in one test each, are much higher, with a minimum of 4% up to a maximum of 315%, showing an average value of 133%.

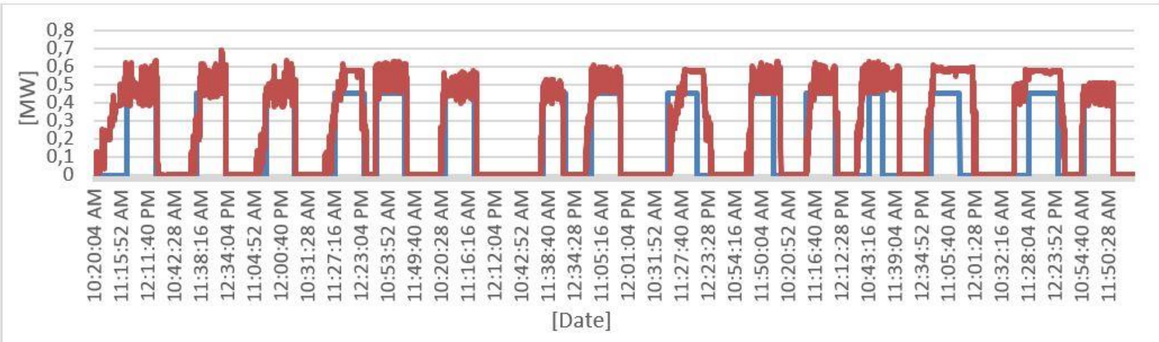

Figure 3-7: Summary of the hot oil heater results

As can be seen from the Figure 3-7, the real situation roughly reflects the model. In principle, future tests will have to try to regulate the load once fully operational, trying to maintain the value set by the model (0,450 MW) for the entire duration of the test.

STR plant (Steel Mill)

The tests involving the STR system always went from 10:45 to 11:00 for organizational reasons of the site. This resource was turned off during the tests. A problem encountered regards the re-ignition time (end of the regulation), which is a function of the daily working needs of the site. Therefore, it has not always been possible to maintain a profile similar to the model and, consequently, the analysis will focus on the first part of the test related to the shutdown (start of the regulation). As the analysis shows, the system needs a few minutes before shutting down. The measured shutdown ramp varies from a maximum of 6 minutes to a minimum of approximately 2 minutes.

As regards the KPI1* parameter values ranging from a minimum of 82% to 117%, with a total average of 101%. While, considering KPI1, it was not possible to evaluate the values as the system wasn't switched on again after the test.

Figure 3-7: Summary of the STR results

<u>Pangborn Shot Blast Machine (Steel Mill)</u>

The tests that involved this system all took place exclusively from 10:45 to 11:00 for organizational reasons of the site.

Similarly to the STR plant, the re-ignition time following the test depends on the daily working needs of the site. Therefore, it has not always been possible to maintain a similar profile of the model in the period after the test and, consequently, the analysis was mainly focused on the first part related to the shutdown (start of the regulation). As far as the shutdown ramp the timing varies from 4 minutes to 12 seconds.

Due to the manual operations, in most cases the resource was not turned on, so it was not possible to define a real duration. This means that KPI1 parameter could not be always evaluated. In the times when it was possible, it changes from 146 % to 388 %, with a total average of 263 %. While, considering the KPI1*, the values vary from a minimum of 0 % to a maximum of 105 %, showing an average value of 70%.

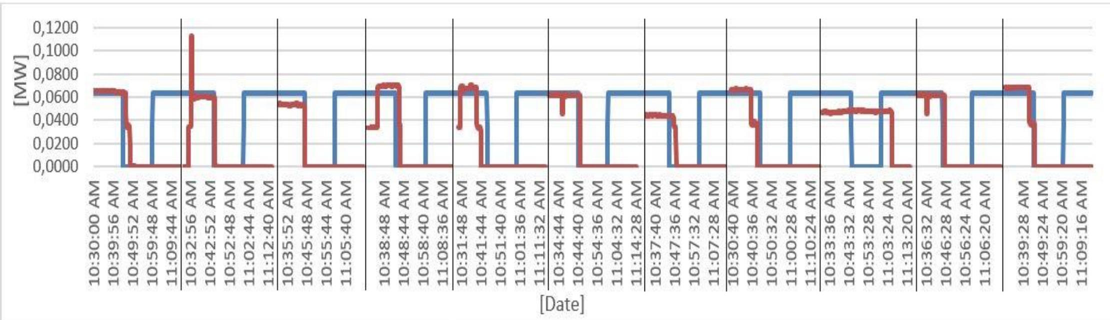

Figure 3-8: Summary of the Shot Blast Machine results

<u>Compressor (Steel Mill)</u>

The last utilities analysed for the Steel Mill is the compressor. The availability of this resource is much more flexible than the STR plant and shot blasting machines. In fact, it was possible to carry out the tests at different times. Generally, the guaranteed availability bands ranged from 10:30 am to 12:30

pm. It is important to point out that this resource, being a compressor, is characterized by a short duration ramp (4s). Once the load is switched on, it reaches the present limit almost instantly.

The average power values measured in the various tests vary from 0,0253 to 0,0270 MW with an average value equal to 0,0260 MW. These absorption values are almost constant once the maximum threshold is reached (although it never reaches the offered value of 0,03 MW).

As regards the KPI1 parameter, values ranging from 15% to 390% are highlighted with a total average of 77%. While, considering the Kpi1*, the values vary from a minimum of 0% to a maximum of 87%, showing an average value of 69%. The limit values of the KPIs were recorded on two occasions, in which manual operations showed their limits.

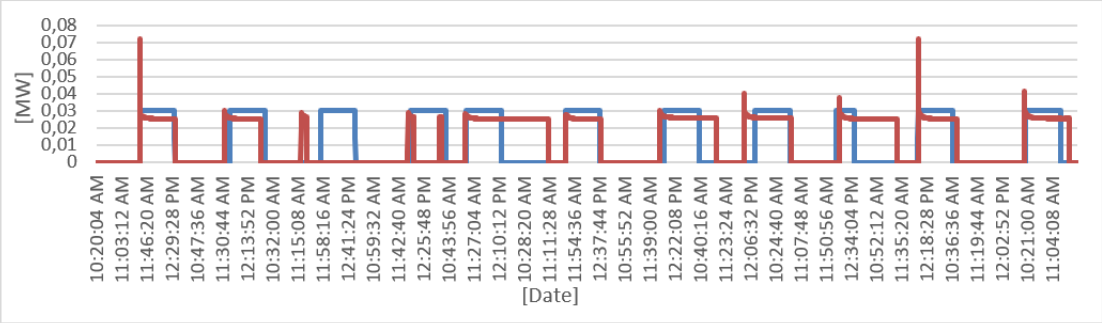

Figure 3-9: Summary of the Compressor results

Generators (Industrial Park)

The generators made available by the industrial park were tested exclusively in two sessions due to the effects (of the pandemic) on the costs of raw materials and electricity.

The first test regards the generator G5. During the test it needed 1 minute to reach the load envisaged by the model and once reached, it maintained an average value of 7,18 MW, thus yielding 0,8 MW on the grid as guaranteed by the preliminary analysis. Finally, as regards the shutdown and re-ignition timing, the test deviates a maximum of 2 minutes from what the model is.

The second test performed regards the generator G6, this user also took 1 minute to reach the load envisaged by the model and once reached, maintained an average value of 7,18 MW, thus yielding 0,8 MW into the grid as guaranteed by the preliminary analysis. Finally, as regards the shutdown and re-ignition timing, the test differs only by 1 minutes from the model.

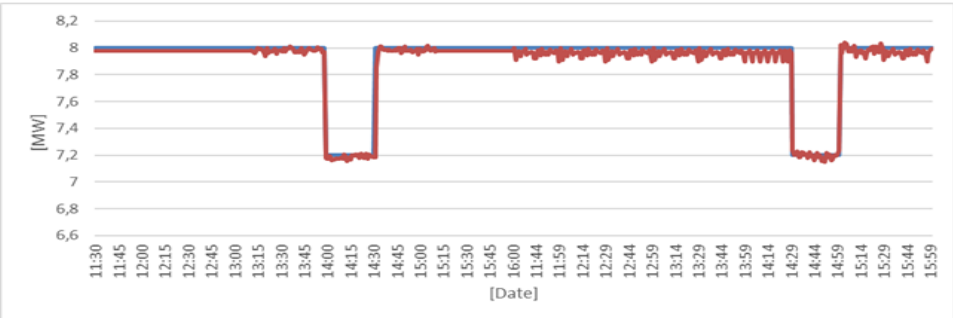

Figure 3-10: Summary of the Generators results

d) Recommendations

During the test sessions some critical issues related to the plants considered emerged. In particular, the main problem was related to the prediction of the baseline of the plants. This gap is essentially related to the low incidence of the loads used on the total consumption of the site. Therefore, predicting total consumption with the required levels of detail turns out to be too complex. The loads made available are too small compared to the total consumption within the site. For this reason, it is advisable to use loads already defined and characterized, dividing the specific consumption and the impact of these within the total consumption of the site.

Similarly, it was not possible to carry out a statistical analysis on the history to predict the absorption / injection curve since there is no cyclicality in the consumption data.

Tests carried out on the oil refinery showed that it is possible to modulate the load of an electric heater typically used for the chemical processes of the industry. However, attention should be paid to ramp times - variable and sometimes higher than the standards – and to the flexibility provided, often higher than required.

In plants such as the Steel Mill, except for the compressor, it has been demonstrated that a manual actuation of the commands is not possible to satisfy the service requirement. Therefore an automation system compatible with normal plant processes, must be implemented to enable this type of resources.

Plants as the industrial park, are theoretically ready to join the market for this kind of services, with the two tested generators. Nevertheless, it will be necessary to focus the attention on the real availability of the plant.

3.2.2.2 Enel X

a) Plant overview

In the period from August to October the modulation tests started. The tests involved one main EAF (Electric Arc Furnace) of the foundry with around 60 MW power that is monitored and controlled inside OSMOSE. The monitoring is entrusted to ABB RTU able to send to Enel X aggregator system (EXAG) active power measurements. EAF are deemed as a not flexible load for several reasons:

- Electrical energy is used to liquify metals by immersing electro[i]des inside scraps, that metal is part of the electrical circuit, the quality of scraps the phase transition and several other factors have impact on the power absorbed the adoption of power converters at grid interface strongly reduce these effects;
- Batch loading is still frequently used in this industrial sector and that imply a relevant amount of scraps inserted at the same time, with strong change of the furnace content and, therefore, of the absorbed power the continuous feeding is an emerging practice that strongly reduce these effects;
- Electrical energy is a key factor for the furnace, insufficient power may create local metal solidification and other dangerous factors, or simply a delay in the production chain, because most part of the EAF are only a step;
- Interoperability with the aggregator is not generally offered by the EAF manufacturer and actions by third parties may invalidate the conformity.

EAF power consumption is intermittent by nature since it is characterized by 40-50 min of full power with strong ripple due to the inherent status of the steel that is part of the electrical circuit (this ripple increase without the continuous steel feeding) followed by 7-15 minute of no power due to the furnace emptying.

b) Aggregation platform and data acquisition

In order to allow ENEL X to participate in the OSMOSE project, Tecnowatt has created a Hardware /Software infrastructure capable of satisfying the various aspects of the project. The project involves the implementation of a congestion resolution service for the foundry plant. Figure 3-11 shows the general layout of the network architecture. It can be noticed that at the datacenter two lines of communication to Terna are installed and an OSMOSE concentrator with the Exergy application has been installed. Connectivity with the systems takes place via a VPN over Internet tunnel on a 4G network between a firewall installed at the datacenter and a router appropriately preconfigured and installed by ABB:

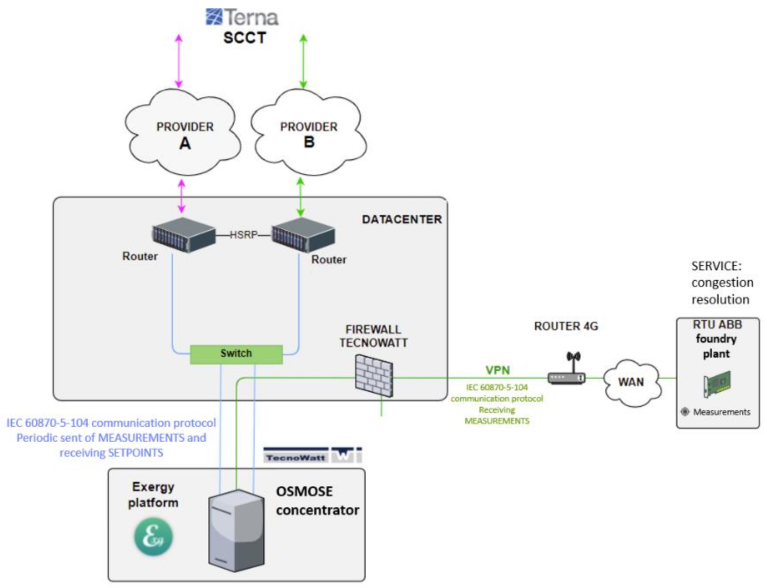

Figure 3-11: Communication scheme Terna-Platform

Enel X users have access to the Exergy platform and software provided by Terna has been used to exchange information related to offers via BDE files, see Figure 3-12. The software uses an exchange protocol called MFT. In order to manage the sending of offer files to Terna in Excel format, a form has been provided that allows to upload the file containing information relating to offers from the user's PC.

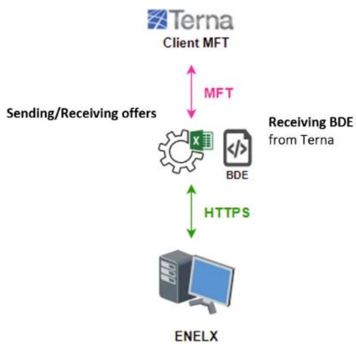

Figure 3-12: Protocol for Sending/Receiving offers and BDE

To monitor the sending of the offer file, a special section has been created within the portal. The command files received and processed by the Exergy system are visible in the specially created BDE command management interface. A section is also visible that allows the user to view the operating status of the MFT Client by viewing a logs file generated by the client itself which presents the latest operations performed by the software. Furthermore, by clicking on the specific file it is possible to view its contents to verify the modulation information received, see Figure 3-13:

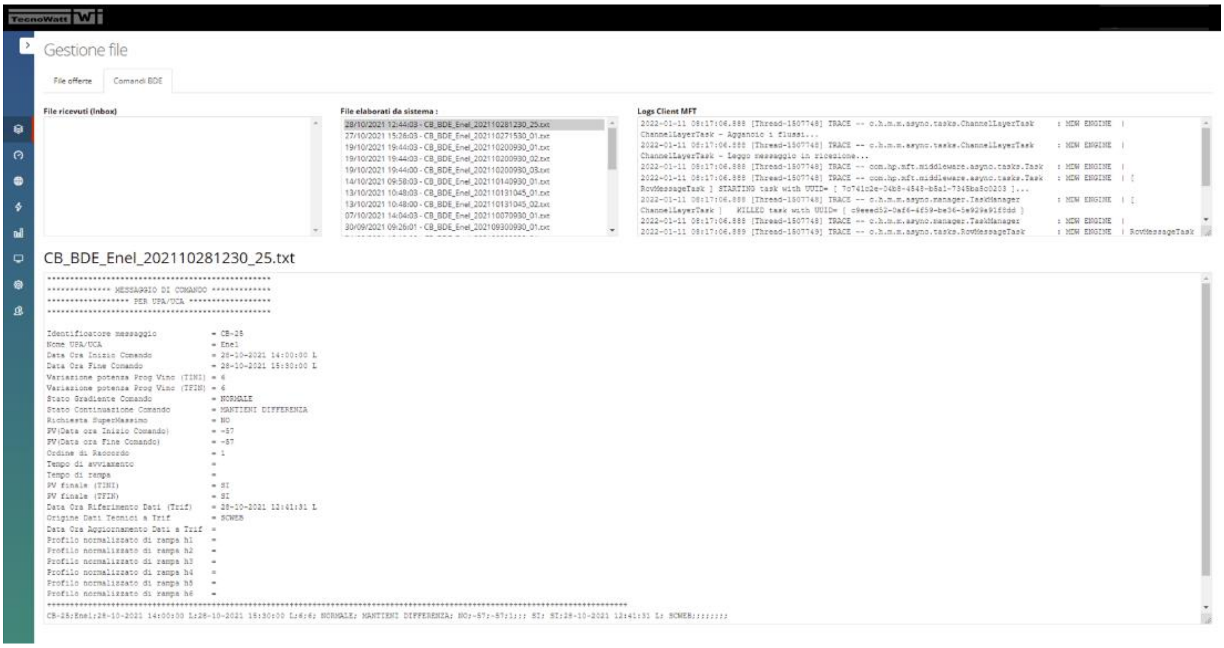

Figure 3-13: Overview of Enel X platform

The BDE files once processed by Exergy generate events that are forwarded via EMAIL and SMS appropriately parameterized with the references of the Enel X staff who will be responsible for carrying out the modulations. The measurement information and the sending of the set-points was defined in agreement with ABB using the IEC 60870-5-104 communication protocol required by Terna.

c) Results

<u>Forecasting Model of the baseline</u>

As a first step, a forecasting model has been tried to setup in order to provide a reasonable prediction of the daily trend of the loads of the steel furnace. Data are collected from the platform as daily files with 4 seconds timestep samples. In order to level the smaller load oscillations, firstly, the files have been sampled at 15 minutes intervals (that is also the forecast interval required by Terna). For this phase, days have been considered in which the modulation has not been applied yet. File have been used referred to days lying in the period between May and July. As a matter of facts, the chosen period is quite reliable as far as the operation of the furnace is concerned and, within it, only Wednesdays and Thursdays have been taken into account since these days are those in which the operation of the furnace is assured. In order to try to build a forecasting model, days have been selected in which the casting is well observable, since any model for prediction is strongly dependent from input data (Figure 3-14).

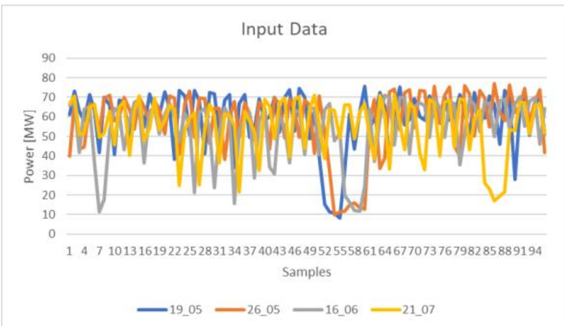

Figure 3-14: Input Data fed into the forecasting model.

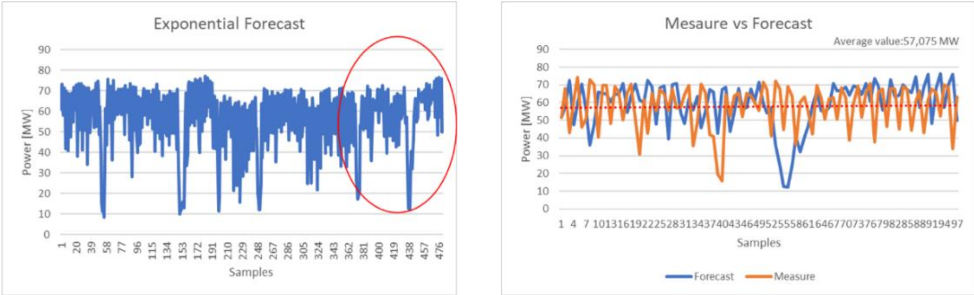

a) **b)**

Figure 3-15: a) Prediction for July 28th (red circled) based on data of May 19th and 26th, June 6th and July 21st.

b) Comparison between forecast and measure for July 28th**.**

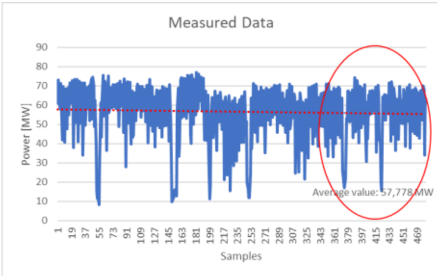

Figure 3-16: Measured data: May 19th and 26th, June 6th and July 21st and 28th

The first attempt of prediction saw the application of the exponential damping algorithm. Such method is based on the evaluation of past data that are weighed through an exponential rule so that the more recent observations have a deeper impact on the forecasted data. The results of the prediction are shown in the red circle in Figure 3-15a. It is evident that the irregularity of data does not allow an accurate prediction performed via-forecasting models. As a matter of facts, to have a precise prediction that is able to forecast the entire daily trend, including the casting, this should occur every day at the same time; that is because of the intrinsic dependence of prediction models from past data.

The addition of further days to the input data could be a reasonable solution to the problem, but at the moment we do not dispose of those additional data. Moreover, this could be a benefit only in the case castings occur, in most cases, in the same time interval. If not, the inclusion of more days would not be useful. As a proof of what anticipated, it is evident from Figures 3-15b that the model is not able to predict correctly the casting relative to July 28th. The most precise prediction in this case is the average value calculated on the last days: as evident from Figures 3-15b and 3-16 the value of 57 MW can correctly approximate the trend of the plant load both for July 28th and for the days used as input to the model.

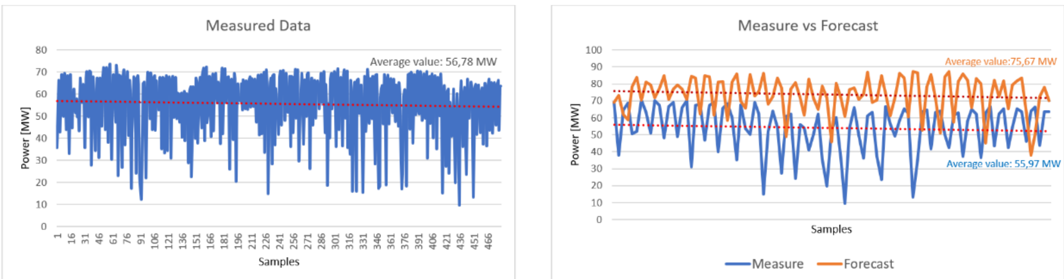

a) **b)**

Figure 3-17: a) Measured data for the week before July 19. b) Comparison between forecast and measure for July 19.

As a further proof of this, a continuous set of days has been used as input data for the model trying to give the construct a reasonable and coherent time series. Once again, the results highlight that the average value should be preferred to the prediction given by the exponential forecasting method. It is well noticeable if we calculate the average value of the prediction of the exponential algorithm: the value obtained is 20 MW higher than the average of the whole week (about 75 MW vs 56 MW), with an error of 41%, see Figure 3-17.

Modulation Tests

In the following section, results concerning modulation tests are shown and analysed. ΔP and KPI1* values are calculated with respect to average daily power. Moreover, samples have been discarded with power values lower than 30 MW that indicate the presence of casting. Due to the particular power absorption profile of the foundry, it has not been possible to calculate KPI1 and only KPI1* has been evaluated. The indication n.a. referring to the Switch Off Ramp for test IDs 10 and 11 indicates not available data. Lastly, AC means that the command has been implemented after the casting. Hereafter, the results on modulations (available for consultation in Chapter 8.2.2 in the Annex 2) are presented and commented:

Response Time – *Switch On Ramp* refers to the time intervals between the time of modulation start and that of effective execution of the command. The time interval has been calculated and it is possible to notice that, with respect to the first tests, in the latest ones it has been possible to obtain response times of a few seconds.

Concerning *Switch Off Ramp* a maximum value of 27’28’’ can be found for the first modulation test, while the latest tests report a precision in the respect of modulation end time of a few seconds: in particular, 28’’ for October 27th and 1’32’’ for October 28th.

Duration of the Modulation - With respect to the Real Duration of the modulation phase, in the first tests it is evident that the duration established by the call has not been respected with precision: with regard to test ID 1 (August 5th), let us notice that the modulation phase lasts 1h56’58’’ instead of the requested 1 hour. As a matter of facts, the response time of the modulation is of 11’4’’ and the service stopped almost half an hour later with respect to the command. This discrepancy has been solved in the last modulations, where the deviation between ideal and real duration reached the order of minutes or, in some cases, seconds. As a proof of that, the deviation is of 1’6’’ and 32’’, respectively for test IDs 19 and 20.

Forewarning – The tenth column of Table 8-10 (Annex 2) reports information concerning sent and received BDE commands: the time interval between the two events is indicated as ΔT1. It is possible to notice that in the first tests time interval between sent and effected command was up to 7 hours; in the last modulations reached forewarning is of 1 hour.

Continuous Modulation – ΔT2 stands for the hours of continuous modulation. The table shows that maximum time interval of continuous modulation is of 3 hours, in particular it concerns the interval from 1 p.m. to 4 p.m. of October 20th.

Flexibility – ΔP represents the difference between the power of the call and the effective one measured. Maximum power called is of 6 MW; looking at the results it can be noticed that maximum tested flexibility is of 10.28 MW corresponding to the total furnace load for test ID 19.

KPI1* - With reference to KPI1* and focalizing on the results about the whole foundry plant, the maximum value reached is of 171%, but in some cases, it approximates 100%, e.g., 99% and 98% for test IDs 12 and 13, respectively. In general, its value lies in the interval 52% - 171%, with a medium value of 119%.

Precision – The stability of the load with respect to the set point has been evaluated by means of two different KPIs:

- Squared Error (SE), see Table 7-10 (Chapter 8.2.2 in Annex 2).
- Percentage Error (PE), see table 7-11 (Chapter 8.2.2 in Annex 2).

The afore mentioned errors are calculated as:

$$SE = (x_i - X_i)^2$$

$$PE = \left(\frac{x_i - X_i}{X_i}\right)^2$$

where x_i is the current sample value and X_i the theoretical value calculated on the basis of the modulation request. Both are evaluated regarding their mean, maximum and minimum values. The two main loads are evaluated separately, e.g., EAF and whole plant load. MSE (Mean Squared Error) and MPE (Mean Percentage Error) are evaluated with respect to mean power of the day under exam.

CONCLUSIONS

Tests have been performed of the main EAF involved in OSMOSE Project. The furnace is considered an intrinsically intermittent load characterized by 40-50 minutes of full power with strong ripple caused by the fusion of steel in the furnace, followed by 7-15 minutes of zero power due to the furnace emptying. A first activity saw the attempt to develop a forecasting model for the daily trend of the EAF; the method has encountered the difficulty to catch the precise moment of the castings since they occur at different moments in the various days; moreover, the ripple of during the fusion is another issue. As a result of this it has been preferred to construct an easier method, that does not take into account the castings, but that is able to guarantee a greater precision. It has been noticed that the average value is the quantity that better approximates the trend of the furnace load. The greater is the size of the dataset on which the value is calculated, the more accurate is the prediction for the following day.

In the period between August and October modulation tests started. The modulations have allowed to test the power flexibility of the EAF. As a matter of facts, EAF are considered not flexible loads for various reasons: several factors influence the absorbed power in the metals liquefaction phase and batch loading causes strong changes in power absorption; moreover, insufficient power may create metal solidification and problems in the production chain. As a consequence, EAF manufacturers do not generally offer interoperability with the aggregator.

The executed tests have allowed to evaluate various characteristics of the EAF. Firstly, response time with respect to the sending of the command has been evaluated. In the first tests in particular, the service started after the casting, while in the latest ones (in October) it has been possible to obtain times of a few seconds, in some cases below 10 seconds.

In the first modulations, maximum flexibility has been declared to be 3MW; in the latest tests flexibility reached around 10 MW. With respect to forewarning time, the time interval between the sent and the execution of the BDE has gone from 7 hours to just over 1 hour.

Precision with respect to the set point has been evaluated. Both in the total load and in EAF load PE is below 10%. Finally, in the last tests periods of continuous modulation up to 3 hours have been tested.

Figure 3-18 shows the deviation between the real and the ideal trend for the test day October 27th. The ideal trend reports the trend given by the average prediction model explained at the beginning of the Results section and coincides with an average value of 67,6 MW, except for the modulation interval for which the ideal trend has an average value of 61,7 MW (P call= 6 MW).

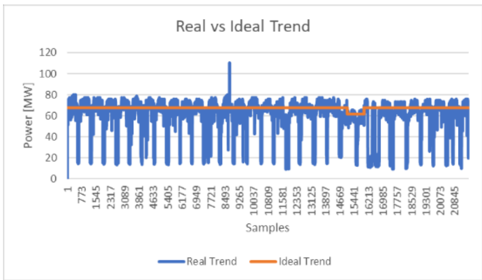

Figure 3-18: Comparison between real and ideal power trend of the plant load for October 27th.

d) Recommendations

As discussed in the previous section the flexibilization results were reached without any additional technology at the plant side (up to the overmentioned RTU). The flexibility products tested was only in scheduled mode, that means that all the power modulation were sent by the BSP to the plant with a forewarning and, at the plant level, the setting was made directly by operators; power regulation was possible acting on EAF electrodes distance.

EAFs are deemed as not flexible loads, nevertheless important results were reached without any strong investments on site. Unfortunately, this flexibility level is frequently insufficient for the TSO needs in most part of Europe. In all the EU countries, EAFs are still GWs of intermitted, disturbed and inflexible power that is managed by the TSO thanks to the flexibility offered by other actors (mainly rotating generation), but in the future energy systems these paradigms will change and flexibility should come from all possible sites (generations and loads), also because of the expected reduction of the rotating generation and the need to avoid green energy curtailment. Therefore, additional experimentations should be dedicated on this field in order to validate the possibility to extract all the possible flexibility from these plants with the desired characteristics.

In order to unlock additional flexibility, the following on site plant upgrades can be proposed:

- Power converter to control arc current and voltage.
- Electrical Energy Storage System (EESS).

Power converter plus EESS is still young for this application, several topics should be better indagated, for example:

- Power converter systems at this level of power, voltage/current disturbances, desired reliability etc. are not very frequent on the market.
- EESS with this level of daily cycles (and desired performances in general), are generally very expensive and bulky.
- Power converter systems with a DC link for EESS are even more infrequent and that may require AC integration (again more expensive and bulkier).

In other hands, all the technological bricks are still present and the benefits are expected to cover completely the overmentioned gaps. The inclusion in the EU research and innovation funding programmes could be a good option.

3.2.2.3 Edison

a) Plant overview

The test involved only one of the three investigated sites initially involved in the project, that is the Powertrain Industry.

The society supplies components for passenger cars and commercial vehicles, and the tested industrial site in particular produces two different powertrain systems that are customized according to the need, changing the size of the sprockets and consequently the transmission ratio. The production counts about 2000 transmission systems per day, obtained through four daily shifts of 6 hours each from Monday to Saturday, for a total of 280 working days per year.

The electricity requirements are entirely met through a HV grid connection; consumption at the meter is approximately 7-8 MW during working hours and 2-3 MW on Sundays, with a further variability linked to the two longest shutdowns in August and December, as can be seen in the figure below.

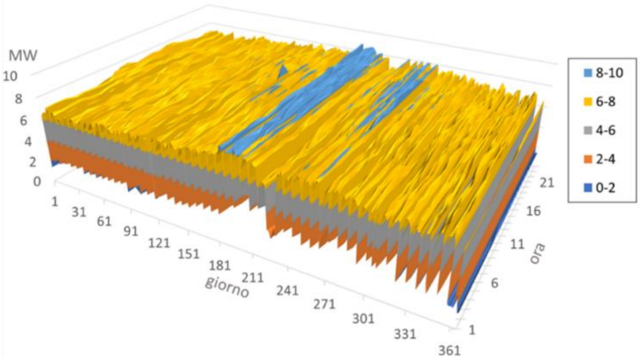

Figure 3-19: hourly consumption profile (site meter data)

The production process is very complex and highly integrated, with a bottleneck in the production of the mechanical parts that, when assembled, make up the drivetrain. The different machine tools are organized into production lines, and because of the customization options involving the need to produce a wide variety of parts, it is difficult to create appropriate buffers to make the operations of one line independent of the rest of the process in terms of offering flexibility services.

Both sheds of the plant are served by dedicated air conditioning systems, consisting of a chiller that supplies cooled water to multiple Air Handling Units (AHUs) providing ventilation and maintaining internal temperature within a certain range; such temperature control is required both for the comfort of the staff working in the halls and for the need to ensure very tight tolerances on the parts produced, thus becoming an important process parameter.

The shed's cooling system operates constantly at full load during summer, being modulated during the rest of the year, thus constituting a valid source of flexibility for the OSMOSE project: it is a matter of exploiting the thermal inertia of the shed to anticipate/delay the turning on of the chiller according to the need for flexibility, while maintaining the internal temperature of the shed within a suitable range.

In terms of available measurement and regulation points, only the overall absorption data of the chiller section is available, while this system is made up of three different units; the chiller feeds four different AHSs, each one adjustable with a temperature setpoint and equipped with a sensor providing ambient temperature data. The load variations to perform following Terna orders have been managed through AHSs temperature setpoint modifications, an indirect quantity: this adds a further source of uncertainty to the test, as it will be better shown in the next paragraphs.

b) Aggregation platform and data acquisition

Edison decided to manage the aggregation of the industrial loads by means of the commercial Exergy Platform of the company Tecnowatt. In order to satisfy OSMOSE project specification, Tecnowatt has developed the existing Software infrastructure to meet project requirements both for the TSO side (Terna systems connection) and the industrial side (connection with on-site ABB RTU).

The OSMOSE test has involved the implementation of a congestion resolution service an industry in the automotive sector, enabling the flexibility and the remote control of the chillers of the cooling system. The connection to the second site (car manufacturer) was put in place, even if at the end no test was performed. Figure 3-21 shows the general layout of the network architecture. It can be noticed that at the Aruba datacenter two lines of communication to Terna are installed and an OSMOSE concentrator with the Exergy application has been installed. Connectivity with the systems takes place via a VPN over Internet tunnel on a 4G network between a firewall installed at the Aruba datacenter and a Teltonika router appropriately preconfigured and installed by ABB:

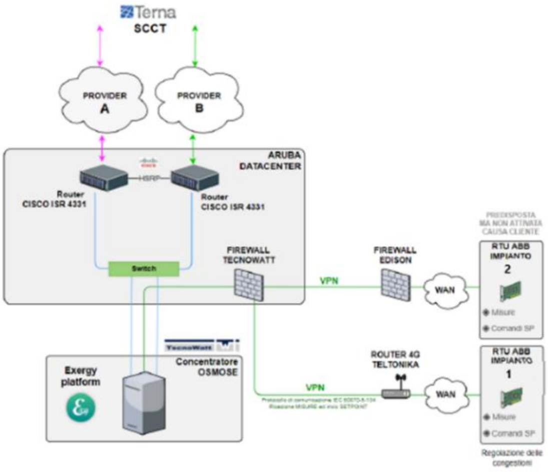

Figure 3-20: Communication scheme Terna-Platform

The platform has been set in the Powertrain industry, in order to collect all the data available for the flexibility resources (cooling unit); the possibility to remotely set different temperature set points for the system was also enabled, within the limits imposed by the client and the characteristics of the cooling system control.

The Exergy platform can be managed by Edison by a web application, and the MFT exchange protocol, provided by Terna in order to exchange Offer and BDE file, was implemented in the platform.

In order to manage the sending of offer files to Terna in Excel format, a form has been provided that allows to upload the file containing information relating to offers from the user's PC. To monitor the sending of the offer file, a special section has been created within the portal. The command files received and processed by the Exergy system are visible in the specially created BDE command management interface. A section is also visible that allows the user to view the operating status of the MFT Client by viewing a logs file generated by the client itself which presents the latest operations performed by the software:

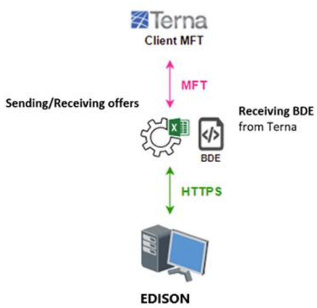

Figure 3-21: Protocol for Sending/Receiving offers and BDE

Furthermore, by clicking on the specific file it is possible to view its contents to verify the modulation information received:

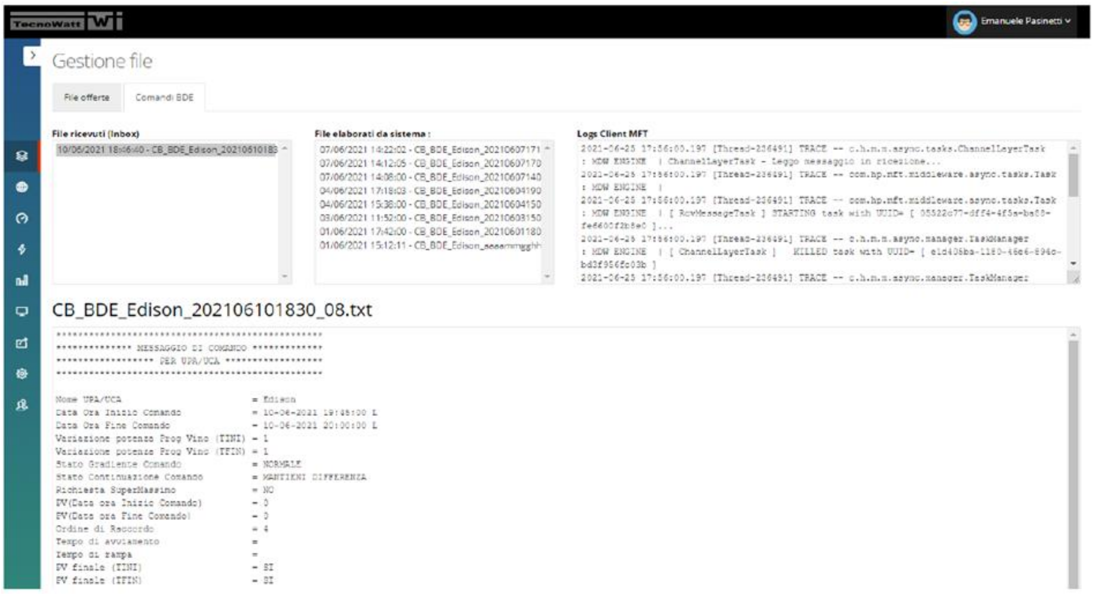

Figure 3-22: Overview of Edison platform

The BDE files once processed by Exergy generate events that are forwarded via EMAIL and SMS appropriately parameterized with the references of the Edison team who will be responsible for carrying out the modulations. The measurement information and the sending of the set-points was defined in agreement with ABB using the IEC 60870-5-104 communication protocol.

c) Results

First of all, a brief explication of how the test was performed based on the data acquired by the system; Figure 3-24 shows the profile of the main parameters of the test setup: the main one is power consumption (Orange line).

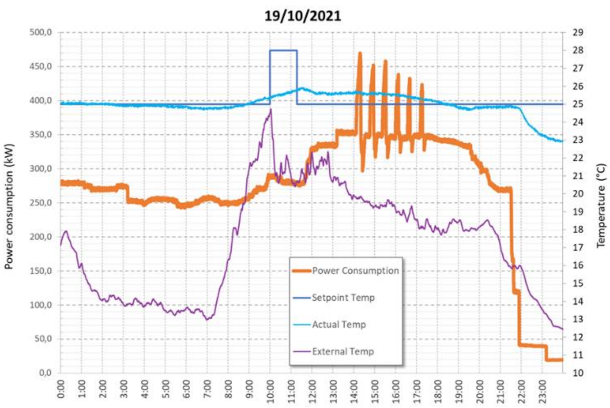

Figure 3-23: Test setup main parameters

This parameter is to be regulated, as anticipated in the previous paragraphs, by means of AHSs temperature setpoint (dark blue line in the graph); the effect of the regulation (in the example between 10:00 and 11:20) can be seen in the variation in the shed actual temperature (light blue line). The purple line shows the profile of external temperature, which is one of the two main driving forces impacting on the cooling system control, the other one being the thermal loads due to industry's process (mainly ovens and machine tools).

Such complex balance between the contribution of non-predictable thermal loads (related to the site production process) and hardly predictable external temperature made it impossible to forecast the chiller's power consumption profile, based on which operate the resource for OSMOSE purposes. On top of that, the chiller itself shows some power oscillations (between 14:00 and 17:00, in the graph), which are impossible to relate to specific operating points, thus adding uncertainty on any power absorption forecast. These oscillations can be explained by the lack of a storage system in the cooling unit, but they cannot be related to any specific operating conditions. A check on the local control system will be done by the client and the controller supplier in order to solve this system instability. It was therefore decided to assess the energy increases/decreases of the tests as a difference between the actual consumption and a baseline consumption curve created “ex-post” in the test post-processing phase. Figure 3-25 shows such baseline, in green, which is calculated as the interpolation of the actual consumption curve just before and after the test.

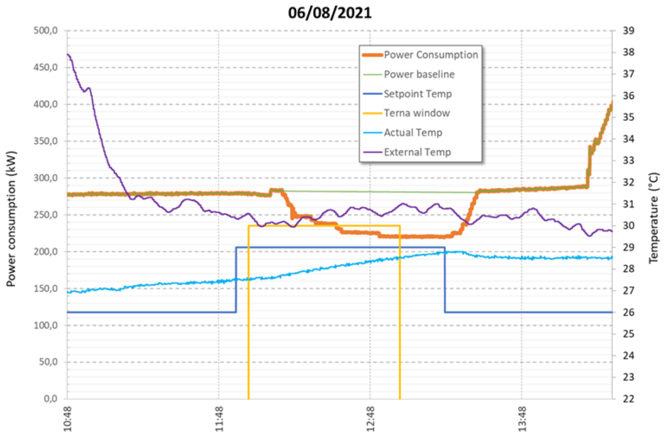

Figure 3-24*:* main parameters variations during the test of August 6

The last consideration before analysing the results is relevant to the power variations that the investigated resource could offer: as it will be clear from the wrap-up table, all tests were in the range of 50-100kW, too small figures, almost invisible at the site meter where exchanges with the grid are at MW level. Therefore, the consumption variations were calculated on the resource power connection, and the results basically represent a characterization of the resource itself rather than the site overall consumption.

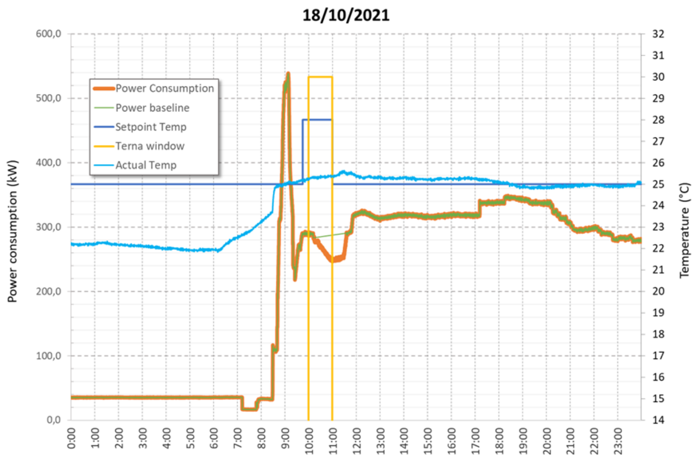

Figure 3-25: main parameters variations during the test of October 10

With respect to the tests, Figure 3-26 shows a downward call from Terna, as it can be seen from the orange curve of actual consumption, lower than the green power baseline around the so called “Terna window”, the actual test timeframe.

It can be noted that the setpoint variation is anticipated with respect to Terna’s window, to consider the system inertia and try to optimize the potential of the resource. Given the complexity of the system, it was difficult to determine the optimal anticipation duration, this being subject both to external parameters (ambient temperature, outside weather) and internal ones (additional thermal loads caused by the number of active machine tools in that moment). This uncertainty has an influence on the quantitative results of the tests, as shown in Chapter 7.2.3 in the Annex 2: the time difference between Switch on Ramp and Switch On time varies from 10 to more than 20 minutes, according to the specificities of the test day; the final impact of this parameter is visible on the KPIs, both 1 and 1*, which range from very low (25%, even a 6%) to super high figures (300%).

d) Recommendations

The tests carried out, as described, proved useful to characterize the flexibility resource represented by the chillers and the modality with which the regulation was carried out. Being the flexibility really small (50 kW) and the grid exchange measures unavailable, it has been not possible to evaluate any modulation from the grid perspective.

In general, it can be observed that it is very complex (or even impossible) to predict the behavior of the resource and its absorption profile: this is mainly due to the fact that the control logics of the refrigeration system were not known, and that different factors affect its behavior, such as the external temperature and the presence of thermal loads in the controlled environment. In addition, the regulation was also very complex, as it was obtained starting from an indirect quantity (ambient temperature set point) and not by means of a set point directly on the electrical absorption.

The unpredictability of the chiller behavior and the regulation through indirect quantities meant that it was not easy to uniquely characterize the response times of the resource, nor to correlate the contribution in terms of flexibility to a certain delta T set as a set point. However, the tests show that the response is never immediate but subject to a delay due to the inertia of the system and to the operating set up at the time of regulation.

In order to develop a better control of the chiller resources for the purposes of the DSM, there is a need to implement the temperature-electrical absorption conversion logic within the local BEMS. In this way, the complexity of resource management can be implemented by the providers who developed the system and the control logics so that it is possible to obtain a better response to the regulation requests.

From the dialogue with the technology supplier, it emerged that this type of implementation could be carried out on plant control systems, but most of the time (as in the case studied), this evolution should be natively implemented by the OEM (Original Equipment Manufacturer) of the chillers, making available control interfaces for the set point of absorbed electric power (control function that is not foreseen by current machines). Working with OEM to make products “ready” to be regulated in terms of electrical absorption is essential to enable effective control of these resources, and could provide a “natively enabled” flexibility for the electrical system in the future.

At the level of the BEMS, for the sole downward flexibility (load reduction), it would be possible to implement a control mode based on the existing load limiting functionality (already present on the machines) to obtain a finer regulation through the control of a direct set up, even if implemented for a different purpose. This mode, intervening at the inverter level, should obtain a quick response on the electrical absorption of the order of a few seconds. To obtain this type of regulation, however, a more complex and important intervention is required on the existing control system on the plant, which must be managed in a non-standard manner for each control system.

Another upgrade to more effectively manage the flexibility provided by the chillers is to insert a refrigeration energy storage system, in order to make it more independent with respect to the plant and external conditions and to be able to decouple the production of refrigeration energy from the request of the plant.

A reflection should also be made on the chiller resource itself: on the one hand it must be considered that in a high voltage connected plant the flexibility made available by the chillers was only 50 kW; on the other hand, the chillers (both for air conditioning and industrial use) are an equipment present in every plant and also in the tertiary sector, and are therefore very a very diffused asset. An optimized management of the flexibility given by these equipments, even if very distributed, fragmented and complex to implement, could constitute an interesting resource of flexibility in the long term. However, in order to enable it and be able to use it effectively, it will be necessary that the enabling costs will be shifted to a development by manufacturers (OEM), while it is not economically feasible to carry out ad hoc developments on individual sites, given the reduced flexibility made available.

An evolution of the chillers as described and a control with direct absorption variables could in the future also enable the provision of other flexibility services such as secondary frequency regulation.

3.2.3 Conclusions on congestion management from DSR

Tests conducted in the experimental congestion resolutions campaign have shown that many industrial plants, connected directly to the high voltage grid, could be a potential source of flexibility for the electrical system, even though the flexibilities enabled were sometimes small compared with the total power consumption of the sites. With some improvements, most of the tested resources could be integrated in the market, for example through the pilot projects that Terna is carrying out (e.g. UVAM project). Nevertheless, some general technical limitations have been highlighted:

- The main problem, common to all BSPs, concerns the baseline forecast. The total consumption of an industrial plant is a function of many internal processes, which are almost always unpredictable. Therefore, even if only a part of the industrial plants participates to the regulation, BSPs should still have a monitoring of all the systems.

- Resources without a direct control of the power required an evolution of the control system towards a standard which should allowed for the BSPs, the same management in case of aggregation. Industrial plants should be therefore equipped with appropriate technologies. To allow this, the system will have to make these investments cost-effective for the plants.

- The activation time (time between the reception of the command and the execution) has often been too long. With the integration of a predictive algorithm as Z-EMS or with some technological improvement of the plants, this limitation could be overcome.

- The duration of the modulation and the continuity of the offers were lower than the market requirements. However, the approach used in the project which considers both availability and maximum duration, could allow to integrate more resources in the market.

Other specific constraints related to each tested resources, described in the recommendation paragraphs of each BSP, will have to be taken into account in order to gradually allow the integration of the industrial resources.

In future, if no sufficient remuneration will be provided for the service, the useful modular electric power could be only a very small percentage of the total achievable power. At the same time, it will be necessary to quantify: costs related to the adaptation of the plants, to fully comply with the technical TSO regulations, and the economic losses related to the power modulations. Since all these factors can vary a lot depending on the plant, a detailed cost-benefit analysis should be the next step to understand whether if it is really possible and useful to enable industrial plants to the ancillary grid services.

3.3 Automatic Voltage Control (AVC)

3.3.1 Test planning and execution

Automatic Voltage Control (AVC) tests was performed with local test sessions in the industrial park (High Voltage level: 220 kV) through the variation (increase or decrease) of the power factor cos φ reference of the three generators (Medium Voltage level:15 kV) in order to evaluate the voltage variations on the transmission grid.

Initially the tests had to be carried out also with the sending either V or Q setpoints directly from Terna control application to the BSP Gateway via IEC-870-5-104. For this reason, Terna and Compendia have developed all the configuration needed to perform remote tests, as described in chapter 2.3 of D5.3 and correctly connected the RTU and executed some communication tests.

Unfortunately, several technical constraints have emerged from the plant:

- The three generators are intended to provide electricity to different users connected in low voltage with the plant. This means that the site has the obligation to guarantee to its customers a certain quality of the service. For this reason, medium voltage level must be kept always in the range 14,4 – 14,9 kV to ensure for users that the final voltage level remains within the boundary provided by the reference standards. Thus, limiting the effect of the regulation on the high voltage site.
- If the medium voltage level is taken out of the range 14,4-14,9 kV, automatically the 15-220 kV transformer variators would bring the voltage back to an intermediate value (around 14.6 kV), cancelling the effect of regulation.
- Power factor cos φ shall not be less than 0,89. This means that, depending on the real-time boundary conditions of the plant (HV and MV value, load required by customers), the theoretical band could be further reduced, in case the cos φ already reached its technical limit.
- For each single generator, the power factor can only be adjusted by a maximum of two percentage point at a time, so as not to prejudice the operation of the generators and the medium-low voltage grid stability.
- Once inserted the OSMOSE setting in the control system for remote regulation, plant operators could no longer modify parameters until before deactivating the OSMOSE cabinet.

In addition, deadlines of the project and availability issues of the plant did not allow to develop a logic of conversion from a set point value in V or Q (from Terna to the BSP) to cos φ (from the BSP gateway to the plant). Moreover, ABB LCU did not provide to the BSP the real time medium voltage value of the plant.

All these reasons have prevented the execution of AVC remote tests and allowed to perform only tests from the control room of the plant without a direct interaction with the Compendia gateway and then with Terna. Therefore, after a first preliminary test, Terna has defined two types of tests to be carried out locally with the goal to identify the maximum potential of the three generators, considering all the technical constraints explained.

The evaluation parameters of these tests were:

- Voltage drops on the two voltage levels (MV and HV).
- Amount of reactive power provided by the generators.
- Response time after inserting a new command.

3.3.2 Main results

3.3.2.1 Local tests results

a) Preliminary test

A preliminary test was performed with the aim to assess a first characterization of the generators, considering all the constraints previously explained. On the day of this test, the industrial park had active 2 out of 3 generators, further limiting the availability to regulate the cos φ. Nevertheless, manually an operator of the plant has changed the cos φ of the two generators, before from an initial condition of 0,94 to 0,9 (injection of reactive power and increase of the voltage level), then from 0,9 to 0,98 (absorption of reactive power and decrease of the voltage level) before reporting the cos φ to its initial value. Below the main evidence of this test:

- On the medium voltage side of the plant, it was observed a total voltage jump of 200 V in the range 14,6 – 14,8 kV, as shown in Figure 3-28 (these data were acquired by the Scada systems of the plant).
- From Terna systems, on the high voltage side (Figure 3-28), it has been observed a variation from 227 kV to 228 kV, during the reduction phase of the cos φ, and from 228 kV to 225,7 kV during the increasing phase of the cos φ.
- The effects of the regulation were observed at the timestamp immediately after the insertion of a new value of cos φ

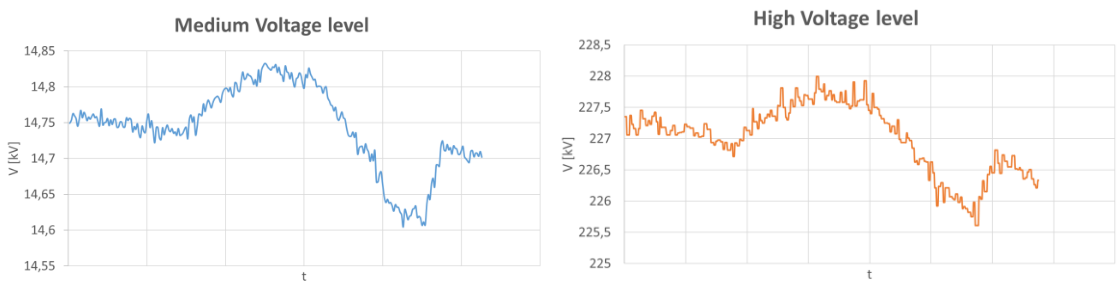

Figure 3-26: Medium and High Voltage variation observed during the preliminary AVC test performed on the Industrial Park

Figure 3-29 represents the % voltage deviation on the medium and high voltage sides, considering as a reference value, to evaluate the deviation, the average of all the data measured before the test.

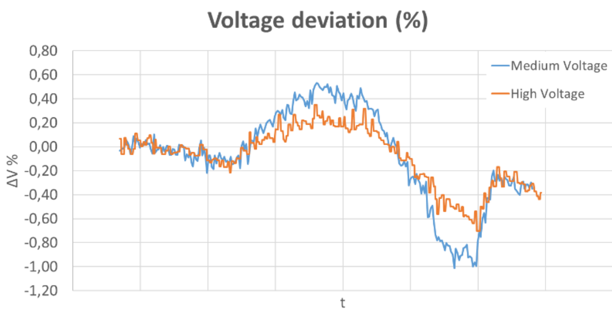

Figure 3-27: Medium and High Voltage Deviation observed during the preliminary AVC test

As expected, the deviation is more significant on the medium voltage level, due to internal reactive power absorption between the generators and the 15-220 kV power transformer. Nevertheless, it has been interesting to notice that the trend of the two curves is almost the same.

b) Local tests

Two local test sessions have been carried out in coordination with the plant operators. In both tests were present all three generators and they have been tested to the limits imposed by the plant. Manually it has been changed the cos φ of the generators with different ramp times starting from an initial value of 0,96. Below the structure and the main evidence of these tests.

<u>TEST 1</u>

Phase 1:

- The cos φ has been changed from the initial condition of 0,96 to 0,92 increasing the voltage level with a variation R1 of 0,01 point per minute. It was observed a voltage drop of about 0,13 kV on the medium voltage level and 0,9 kV on the high voltage level with a reactive power drop of around 3 MVAr.
- cos φ has been changed from 0,92 to 0,99 with the same variation R1. It was observed a voltage drop of about 0,3 kV on the medium voltage level and 2,5 kV on the high voltage level with a reactive power drop of around 6,5 MVAr.
- cos φ value was restored to the initial value of 0,96.

Phase 2:

- The cos φ has been changed from 0,96 to 0,92 with a variation R2 of 0,01 point each 30 seconds. It was observed the same voltage drop of the phase 1.
- cos φ has been changed from 0,92 to 0,99 with the same variation R2. Even in this case the variations were the same of the phase 1.
- cos φ value was restored to the initial value of 0,96.

Phase 3:

- The cos φ has been changed from 0,96 to 0,94 with a variation R3 of 0,02 point each 30 seconds. It was observed a voltage drop of about 0,1 kV on the medium voltage level and 0,5 kV on the high voltage level with a reactive power drop of around 1 MVAr.
- cos φ has been changed from 0,94 to 0,98 with the same variation R3. It was observed a voltage drop of about 0,2 kV on the medium voltage level and 1,5 kV on the high voltage level with a reactive power drop of around 3 MVAr.
- cos φ value was restored to the initial value of 0,96.

In all the phases the variations were observed in the timestamp immediately after the command's insertion.

The results of this test are represented in the following figures:

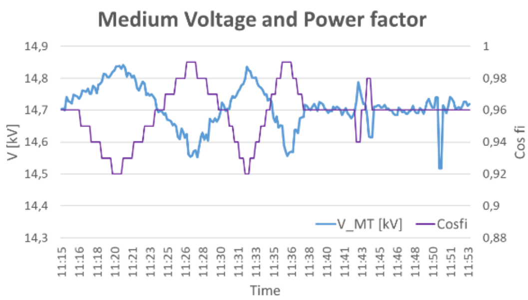

Figure 3-28: Medium Voltage observed after the variation of the Power Factor of the plant

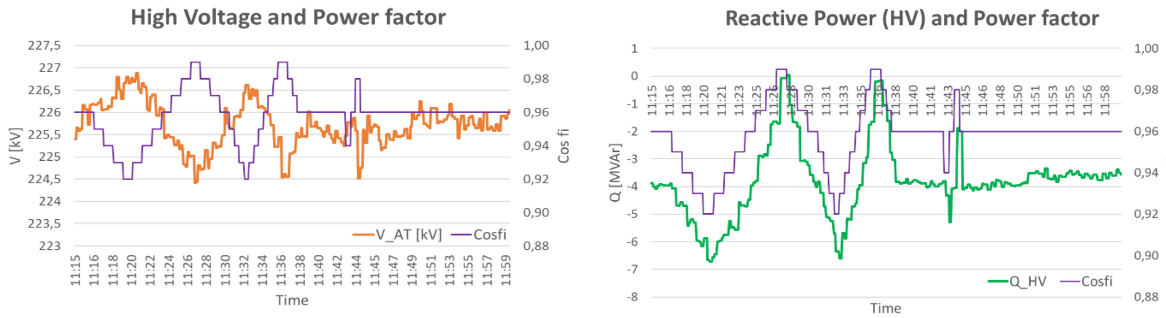

Figure 3-29: High Voltage and Reactive Power observed after the variation of the Power Factor of the plant

<u>TEST 2</u>

Phase 1:

- The cos φ has been changed from the initial condition of 0,96 to 0,99 decreasing the voltage level with a variation R1 of 0,01 point per minute. It was observed a voltage drop of about 0,2 kV on the medium voltage level and 1,5 kV on the high voltage level with a reactive power drop of around 4 MVAr.
  In this first variation the medium voltage level reached the limit of 14,4 kV. Therefore, automatically, the 15-220 kV transformer variators brought the voltage back to the intermediate value (around 14.6 kV), cancelling the effect of the regulation on the medium voltage side. The new configuration of the transformer variators affected the medium voltage level of the successive phases (Fig. 3-32).
  High voltage level and reactive power seemed unaffected by the intervention of the transformer variators.
- cos φ has been changed from 0,99 to 0,92 with the same variation R1. It was observed a voltage drop of about 0,3 kV (from 14,6 kV to 14,9 kV) on the medium voltage level and 1,8 kV on the high voltage level with a reactive power drop of around 5,5 MVAr.
- cos φ value was restored to the initial value of 0,96.

Phase 2:

- The cos φ has been changed from 0,96 to 0,99 with a variation R2 of 0,01 point each 30 seconds. It was observed the same voltage drops of the phase 1, but since it was changed the asset of the transformer variators, no limits were reached during this phase.
- cos φ has been changed from 0,99 to 0,92 with the same variation R2. Even in this case the drops in voltage and reactive power were the same of the phase 1.
- cos φ value was restored to the initial value of 0,96.

Phase 3:

- The cos φ has been changed from 0,96 to 0,98 with a variation R3 of 0,02 point each 30 seconds. It was observed a voltage drop of about 0,1 kV on the medium voltage level and 0,5 kV on the high voltage level with a reactive power drop of around 1 MVAr.
- cos φ has been changed from 0,94 to 0,98 with the same variation R3. It was observed a voltage drop of about 0,2 kV on the medium voltage level and 1,5 kV on the high voltage level with a reactive power drop of around 3 MVAr.
- cos φ value was restored to the initial value of 0,96.

Even in this test the variations were observed in the timestamp immediately after the command's insertion.

The results are represented in the following figures (in this test the reactive power supplied by the generators on the medium voltage side was also acquired and saved):

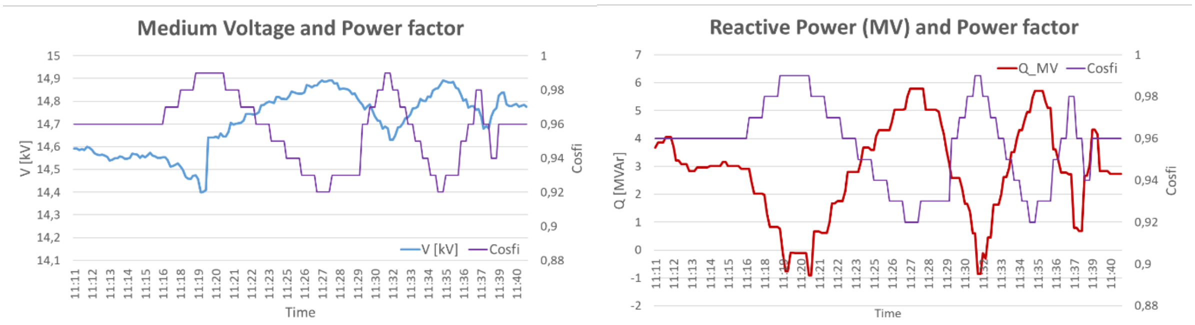

Figure 3-30: Medium Voltage and Reactive Power observed after the variation of the Power Factor of the plant

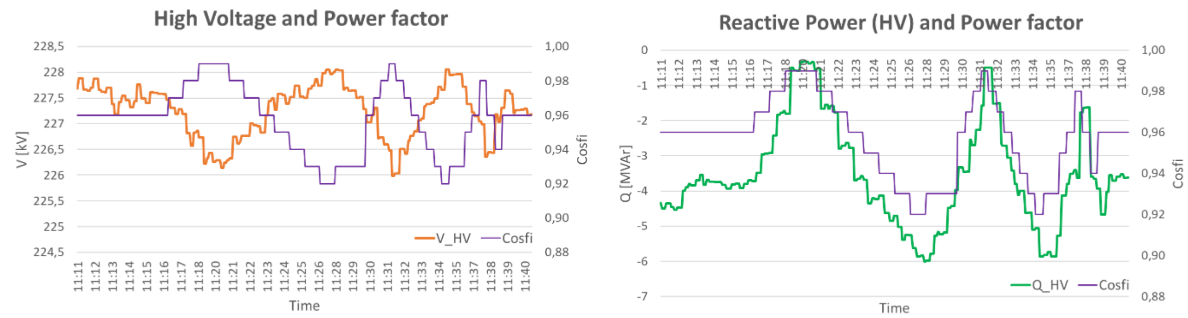

Figure 3-31: High Voltage and Reactive Power observed after the variation of the Power Factor of the plant

3.3.3 Conclusions on voltage regulation from DSR

The types of tests carried out are very different from what was initially defined by Terna, in accordance with the Italian grid code currently in force. The several constraints imposed by the plant strongly limited the test campaign.

Although it was not possible to test concretely, the crucial point was the availability of the plants to allow a remote and automatic control of their facilities, which is a necessary condition for the so-called fast regulation (such as voltage regulation), that cannot be performed manually. Nevertheless, it has been demonstrated that potentially these resources, located in medium voltage and used for the internal processes of the plant, are able to regulate the voltage level (HV) of the grid.

The main conclusion is that to enable this type of resources to the voltage regulation it would be necessary to optimize the HV / MV distribution and transformation electricity grid of the plant and develop a logic for converting the set point (from V or Q to cos φ) in order to overcome the numerous constraints currently present. Finally, it will be necessary to investigate with the TSO the current regulation methods implemented in HV as they are not adequate to the potential contribution offered by these medium-sized resources (generators connected on MV grid)

4 Dynamic Thermal Rating (DTR)

4.1 Test planning and execution

4.1.1 Overview

For both Sensor Based and Weather Based methods, starting from meteo data (measured for the first case and forecasted for the latter) .csv files containing the theoretical ampacity values of the considered line where taken as result of the Algorithm elaboration. These values represent the dynamic loadability curve of each line, refreshed at each 15’ time step of the day, namely the dynamic limits of ampacity.

The comparison of the dynamic loadability curves with the static limits of each tested line shows the increase of its possible maximum ampacity and how long it can be held without exceeding the conductor’s ground clearance.

Hereinafter the comparison charts will be showed.

4.2 Main Results

4.2.1 Sensor-based DTR

In order to assess the effectiveness of the cooperative sensor network in the task of assessing the dynamic thermal rating of the 11 spans of the 7 monitored lines, a preliminary analysis on the accuracy of the conductor temperature estimated by the master nodes has been performed. To this aim, the following KPI has been considered:

$$E(t) = |Tm (t) - Ts (t)|$$

where $E(t)$ is the absolute prediction error for the sample time t, while $T_m(t)$ and $T_e(t)$ are the conductor temperature measured by the conventional sensor and the corresponding estimation computed by the cooperative sensor network for the same time sample, respectively.

This KPI has been computed for all the 11 spans of the 7 monitored lines for a 8 months-time period, ranging from April to November 2021. The corresponding results are summarized in Table 4-1, which reports the statistical features of the considered KPI for all the monitored spans.

Table 4-1-1 - Absolute Prediction Error

Line ID	Span ID	Average [°C]	Standard Deviation [°C]
701	99	0.4840	0.5441
701	100	0.5984	0.6583
702	95	0.6574	0.7510
729	97	0.8992	0.8155
729	98	0.5731	0.6407
705	101	0.6741	0.6710
705	102	0.6722	0.6788
938	103	0.6735	0.8164

938	104	1.0485	2.2216
934	109	0.8945	1.0358
769	96	0.8278	0.6938

By analysing these data, it is worth noting the excellent prediction accuracy characterizing the cooperative sensor network, which by integrating advance thermal modelling techniques with environmental variables measured at about 5 meters from the ground allows accurately estimating the conductor temperature without requiring complex and expensive temperature sensors directly connected to the line conductors. This conclusion has been also confirmed by the analysis of the histogram of the considered KPI for all the monitored span, which are reported in Fig.4-1.

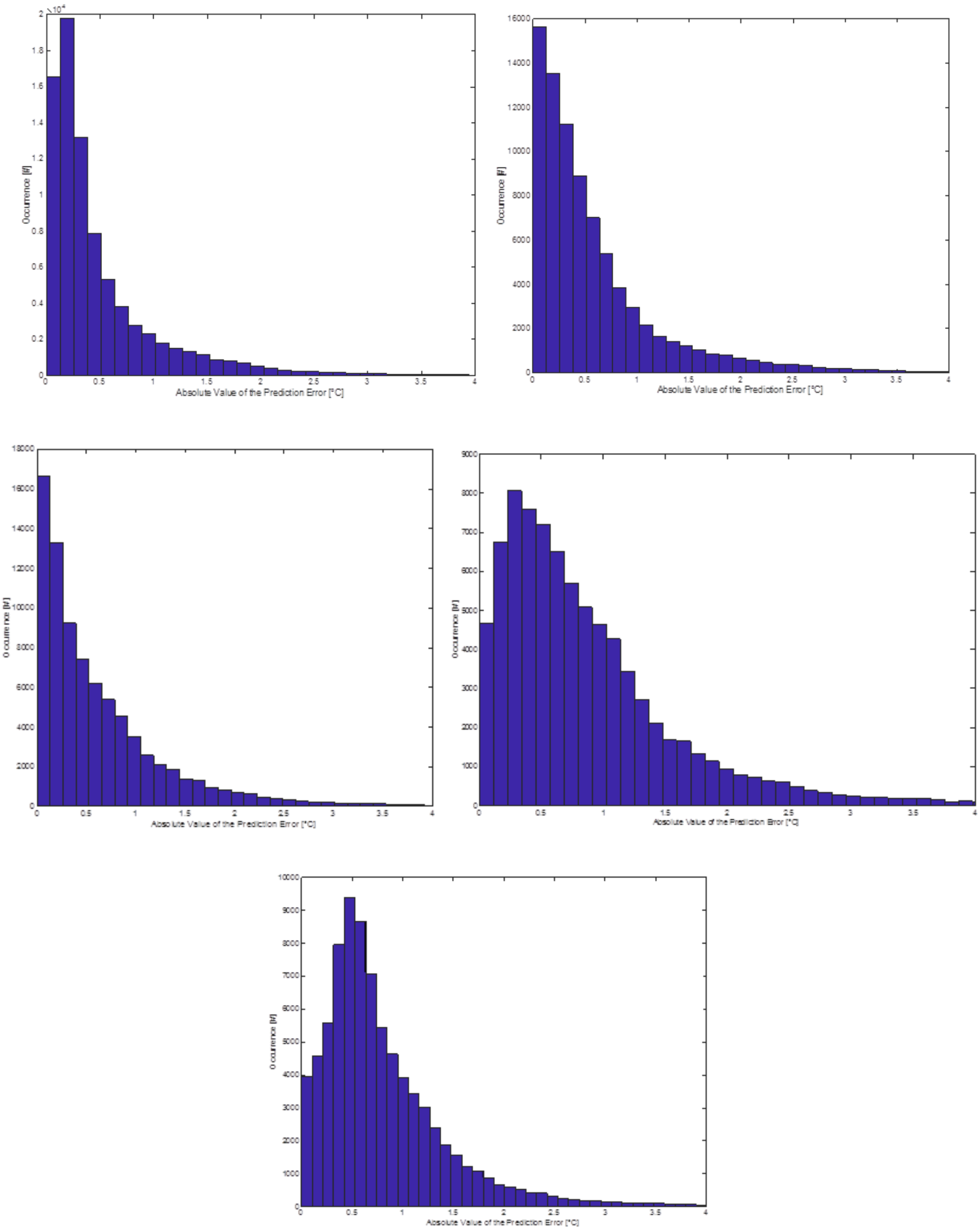

Figure 4-1: Histogram of the absolute prediction error for the monitored line spans

After assessing the accuracy of the sensor network in the task of estimating the conductor temperature, its effectiveness in computing the dynamic thermal ratings has been analysed. To this aim two KPIs characterizing the improvements deriving by the adoption of the computed thermal ratings compared to the conventional (static) ones has been considered. To this aim the duration curve of the dynamic thermal rating by the sensor network at 15 and 180 min, and the corresponding % increase of line rating have been computed. The obtained results for all the monitored lines span are reported in Fig. 4-2.

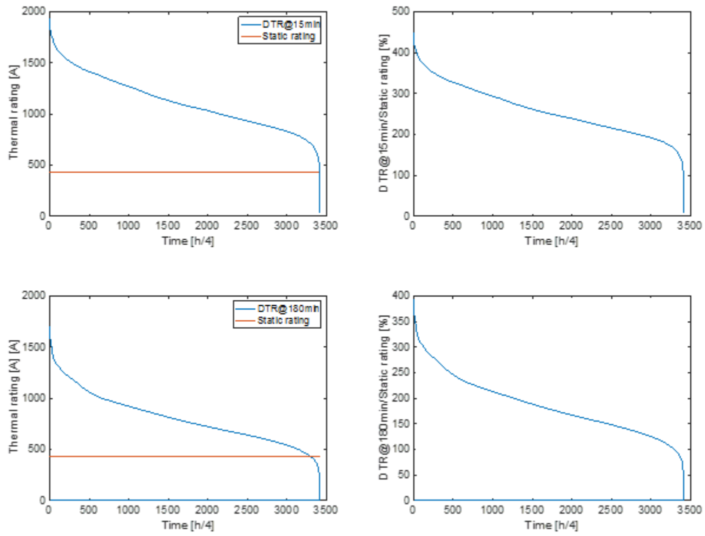

Figure 4-2 :KPI for the monitored line spans: a) Duration curve of DTR @15min VS static rating; b) Duration curve of KPI "% increase of line rating@15min"; c) Duration curve of DTR @180min VS static rating; d) Duration curve of KPI "% increase of line rating@180min";

The analysis of these KPIs confirmed the benefits deriving by the application of the cooperative sensor networks in accurately and reliably assessing the real load capability curves of the monitored overhead lines.

4.2.2 Weather-based DTR

The weather-based DTR algorithm developed in OSMOSE has been implemented and tested on two 150-kV sub-transmission lines located in Southern Italy. The path section monitored in one of the lines, equipped with standard ACSR conductors with a diameter of 31.5 mm, was composed by 20 spans placed between two dead-end towers. Conversely, the section under test on the other line, equipped with standard ACSR conductors with a diameter of 22.8 mm, was composed by 30 spans.

Each quarter of an hour, the weather conditions expected for the following 3 hours along the line path have been forecasted. Starting from the present conductor's temperature, estimated span by span based on recent weather and loading conditions, the maximum current that can be sustained for the next α minutes has been then calculated. The maximum allowed temperature of conductors is 55°C, while the parameter α was varied iteratively from 15 minutes to 3 hours, with steps of 15 minutes. This procedure allowed calculating, every 15 minutes, an overloading curve that was provided to the TSO Optimum Power Flow. All the different rolling-horizon routines were automized and interfaced.

The following figures report the results obtained in a test campaign carried out between February and November 2021. The main KPIs addressed by this analysis regard the comparison between Static and Dynamic Thermal Rating. STR has been assumed equal to 560 A and 370 A, respectively for the 31.5-mm and the 22.8-mm conductor, according to Terna operational procedures. Only the thermal limit of the conductor (55°C) was considered, while mechanical constraints like maximum sags or minimum clearance-to-ground were not activated.

In terms of dynamic rating, the 15-min DTR and the 180-min DTR, i.e., the two extremes of the loadability curve (α =15’ and α =180’), have been analyzed. In fact, DTR is usually higher than STR due to main reasons:

1. STR assumes extreme and very conservative weather conditions that stress the temperature of conductors: high ambient temperature, maximum solar radiation and absence of wind; conversely, DTR is based on weather short forecasting, which means on realistic ambient, solar and wind conditions that usually correspond to higher conductor cooling than supposed in STR;
2. DTR properly captures the real thermal behavior of the conductor, which basically corresponds to a 1st-order dynamic system; this means that the response to a step of current do not correspond to a step of conductor’s temperature, rather to an exponential function that reaches its steady-state conditions in 4-5 time constants τ, where τ is around 7-10 minutes; this is why 15-min DTR is higher than 30-min DTR, while all the time horizons α beyond 45 minutes can be considered already corresponding to the same steady-state conditions.

It is important to notice that comparing 180-min DTR and STR provides information regarding the first phenomenon (i.e. realistic weather instead of conservative meteorological conditions), while 15-min DTR gives evidence to the effect of thermal transients. The impact of transient effects depends on the α/ τ ratio, on the difference between the two steady-state conductor’s temperatures (for t=0- and t=∞), and on the temperature of the conductor itself (the higher the temperature, the lower tau, due to non-linearities of the thermal model).

The two next figures show the time course and the duration curve of the comparison between 180-min DTR and STR, for the line n.1, the one with the larger conductor (diameter of 31.5 mm).

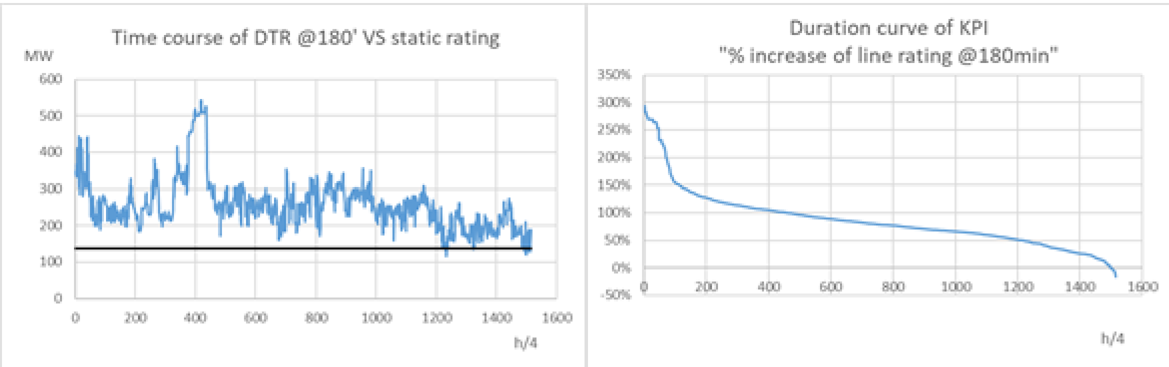

Figure 4-3: Time course and duration curve of 180-min DTR VS STR. Line #1.

These figures clearly show that exploiting short-term weather forecasting, instead of using conservative meteorological parameters, already increases the rating of the line up to a peak of +294%. This peak value must not surprise: according to the CIGRE thermal model of a 31.5-mm conductor, in case of 8-m/s wind, no solar radiation (night) and 10°C of ambient temperature, the steady state temperature of the conductor reaches its limit of 55°C only with a current of around 2300 A (around 4 times STR). Most interesting is the observation that, for approximately 30% of the testing campaign, DTR at least doubles the steady-state thermal rating. Only in 1% of conditions, DTR180’ is lower than STR. The average value of the ratio (DTR180’-STR)/STR is 86%.

The two next figures show the time course and the duration curve of the comparison between 15-min DTR and STR, for the same 150-kV line. As evident, in short time horizons the thermal transient phenomena enhance the added value of DTR with respect to STR, by a markup that varies from +20% (in working points where 180-min DTR was already at its maximum performance) to around +40% (when 180-min DTR was only slightly over-performing STR). For approximately two thirds of the considered quarters of an hour, 15-min DTR at least doubles STR. Only in 0.2% of conditions DTR15’ is lower than STR. The average value of the ratio (DTR15’-STR)/STR is 125%.

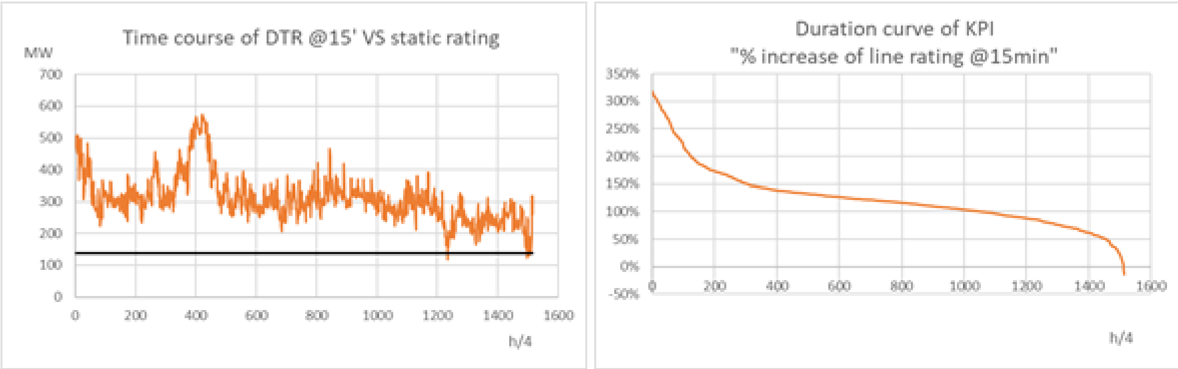

Figure 4**-4: Time course and duration curve of 15-min DTR VS STR. Line #1.**

Very similar results have been obtained for the second line, the one with the smaller conductor (diameter of 22.8 mm) and focused by a longer test campaign, as reported in the next figures.

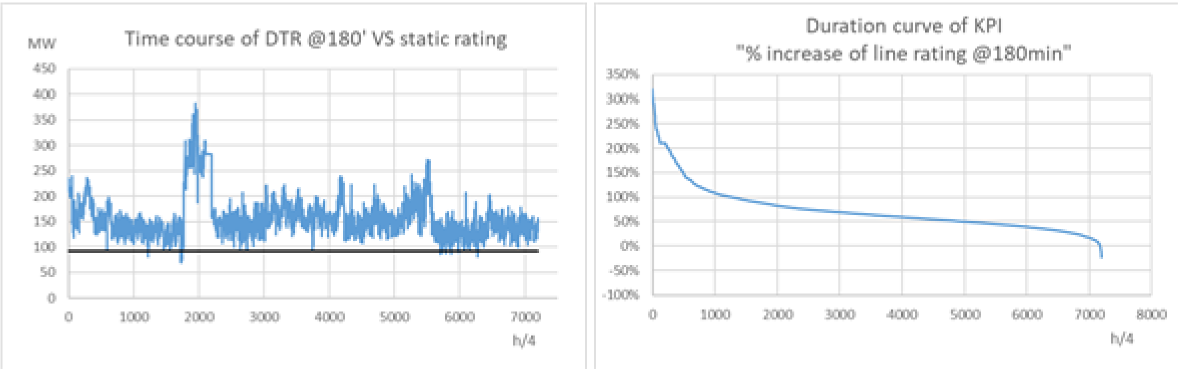

Figure 4**-5: Time course and duration curve of 180-min DTR VS STR. Line #2.**

It is very clear, above on the left, the peak of DTR during the very windy days occurred in late February 2021 (quarters 1850-2100). Also in this line, as shown above on the right, DTR180’ increases the rating of the line up to a peak of +320% w.r.t STR. The average value of the ratio (DTR180’-STR)/STR is 73% and its most probable value is 210%.

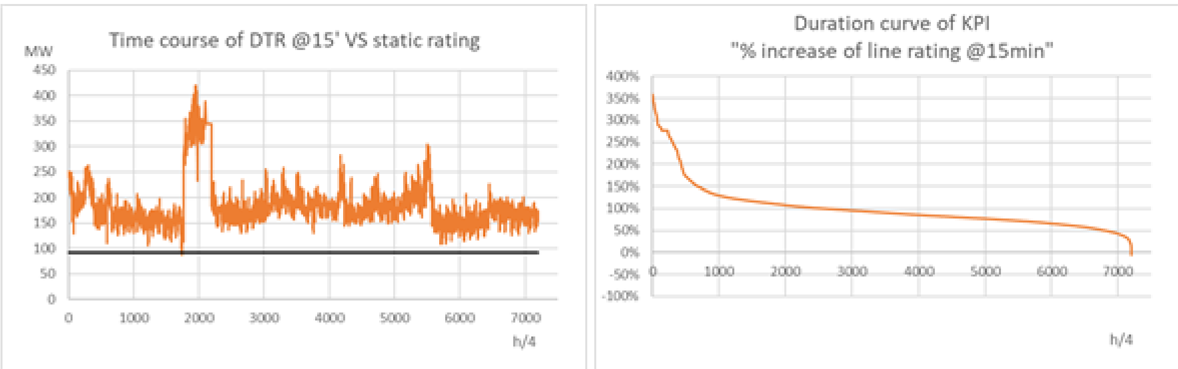

Figure 4**-6: Time course and duration curve of 15-min DTR VS STR. Line #2.**

Due to the thinner conductor, in line #2 the time constant of thermal heating is slightly lower (around 7 minutes instead of 10). This implies that the transient thermal phenomena have a smaller impact than in the first line, because at the end of the first 15 minutes the conductor has already experienced almost two-time constants. The added value of 15-min DTR with respect to 180-min DTR, assuming STR as the base reference, consequently slightly decreases to the range [+10; +30%]. In any case, DTR180’ is lower than STR only in 0.3% of conditions, while DTR15’ is lower than STR only in one quarter of an hour, over more than 7200 analysed.

To better understand the performance of DTR in the different seasons, for line #2 the data previously reported for the entire test campaign have been analysed also separately for winter (October-March) and summer (April-September) conditions, obtaining the following results.

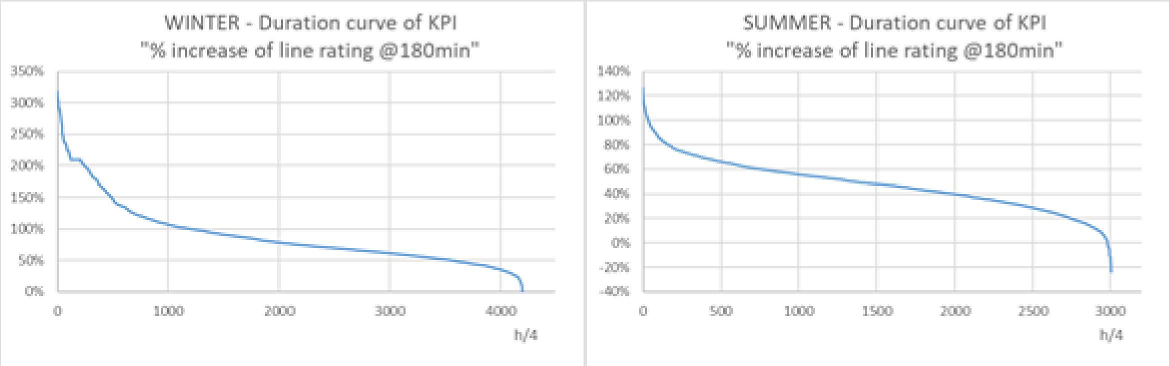

Figure 4-7: Duration curve of 180-min DTR VS STR, in winter (left) and summer (right). Line #2.

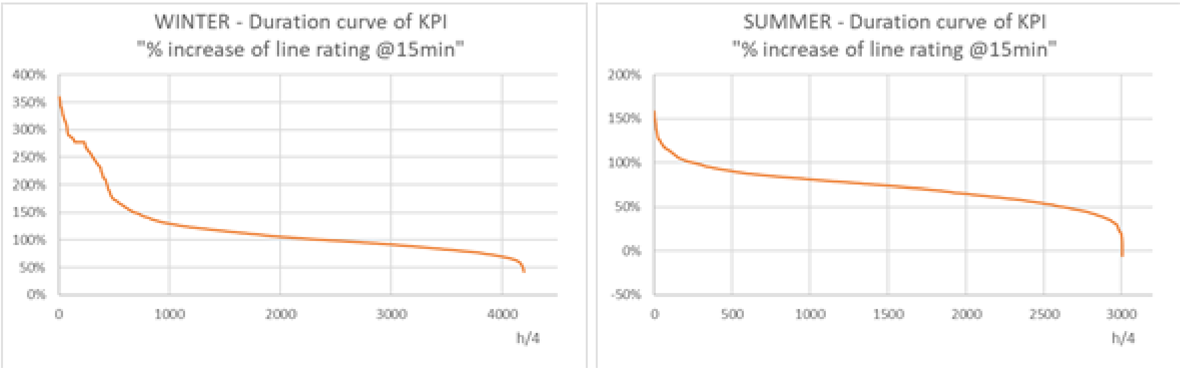

Figure 4-8: Duration curve of 15-min DTR VS STR, in winter (left) and summer (right). Line #2.

It is clear, both for α=180min and α=15min, that winter circumstances enhance the performance of Dynamic Thermal Rating, since DTR properly captures the real cooling conditions of the conductor in any season. In winter, the lower ambient temperature and the higher wind speed strongly increase the rating of the line and DTR is always higher than conservative STR. In summer, DTR is able to capture the fact that, even if very sporadically, the real weather conditions can be windless and even hotter than supposed by the static approach: in 0.8% of summer conditions, DTR180’ is lower than STR; only in one quarter of an hour over 3000 under analysis, DTR15’ is lower than STR.

The following tables report, for α=180min and α=15min, the main parameters of the comparison between DTR and STR.

Table 4-3 - Analysis of the KPI “(DTR180’ – STR)/STR”

150-kV line	Season	Max KPI	Average KPI	Mode of KPI	Hours with DTR>2STR	Hours with DTR<STR
#1 (diameter 31.5 mm)	Year	294%	86%	+269%	30%	1%
	Winter	294%	116%	269%	45%	----
	Summer	158%	72%	101%	20%	1.8%

#2 (diameter 22.8 mm)	Year	319%	73%	210%	17%	0.3%
	Winter	319%	91%	210%	28%	------
	Summer	126%	48%	49%	1.2%	0.8%

Table 4-4 - Analysis of the KPI "(DTR15' – STR)/STR"

150-kV line	Season	Max KPI	Average KPI	Mode of KPI	Hours with DTR>2STR	Hours with DTR<STR
#1 (diameter 31.5 mm)	Year	318%	125%	132%	66%	0.2%
	Winter	318%	165%	118%	95%	----
	Summer	239%	105%	122%	54%	0.3%
#2 (diameter 22.8 mm)	Year	359%	102%	277%	37%	0.01%
	Winter	359%	122%	277%	57%	-----
	Summer	158%	73%	81%	8.6%	0.03%

4.2.3 Conclusions Sensor-based DTR

On the basis of the obtained experimental results, it can be said that the adoption of the cooperative sensor networks allows reliably improving the thermal rating assessment, without requiring the deployment of complex and expensive sensors for the direct measurement of the conductor temperature. This benefit is mainly due to the effectiveness of the built-in thermal modelling techniques, which allow estimating the conductor temperature on the basis of easily measured environmental variables. Moreover, the adoption of a wireless-based cooperative communication system allows increasing the sensors pervasion and, consequently, the effectiveness of the sensor network in reliably estimating the critical span location.

4.2.4 Conclusions Weather-based DTR

The test campaign performed since February 2021 clearly shows the effective operation of the weather-based tool developed within the Osmose project and implemented on two 150-kV sub-transmission lines in Southern Italy. In winter, the excellent performance obtained for the dynamic thermal rating compared to the traditional static ampacity is certainly related to the fresh and extremely windy weather conditions experienced all along the monitored lines during the cold season. Indeed, this has significantly boosted conductor's cooling with respect to the conservative meteorological conditions assumed by STR. It is also worth observing that this aspect resulted much more effective than the transient thermal aspects that are properly captured by DTR procedures when the overloading window is shorter than 4-5 thermal time constants of the conductor.

In summer, the markup of DTR with respect to STR remains substantial (on average, +70-100% depending on the considered line), but compared with winter windy conditions is roughly halved. In any case, weather based DTR has proven to be able to capture the fact that, even if very sporadically, in summer the real weather conditions can be totally windless and even hotter than supposed by the static approach.

5 Renewable Energy Systems (RES)

5.1 Introduction

The OSMOSE project experimentation related to innovative services provided by RES plants involves one plant owned by Enel Green Power (EGP) and located in Pietragalla and two other owned by Edison (ERIN) and located in Vaglio (both refer to the same point of connection). The Pietragalla EGP plant is an integrated RES + Storage power plant and is made of a 18 MW wind power plant (9 x 2 MW turbines) and a 2MW/MWh Battery Energy Storage System. The Edison power plants considered are the "Vaglio" and "Vaglio IR" wind farms for a total 35 MW power (20MW + 15 MW plant, 14*2.5 MW turbines); from now on they will be referred to uniquely as "Vaglio" power plant. The core of the experimentation is to test automatic voltage regulation (AVC) and Synthetic Inertia. In the previous months, the Pietragalla and Vaglio plants have been updated to allow for the provision of Automatic Voltage Regulation (AVC) following a reactive power or voltage set-point. As far as Synthetic Inertia is concerned for the Pietragalla plant, a Synthetic Inertia controller has been developed and installed in the plant premise and its action tested during the experimental phase. As for Synthetic Inertia developments in the Vaglio plant, the activity was structured in order to develop and validate in Vaglio the firmware/software upgrades on the turbine necessary to test the inertial response. Laboratory bench and full-scale tests of these upgrades were tested at SGRE laboratories but its validation in Vaglio could not be performed due to lack of time (during laboratories activities more tests were needed than forecast).

5.2 Automatic Voltage Regulation

5.2.1 Test Planning and Overview

The experimental campaign aimed to test the technical capabilities of the Pietragalla and Vaglio plant to provide reactive power regulation.

The tests were planned in order to match different factors, among which the favourable wind forecasts and no planned maintenance or activities on the transmission lines in the area or on the plants themselves. For both the Pietragalla and Vaglio plant the approach adopted for the experimentation consisted in:

- Sharing of the test specification.
- "Local" execution of the test: the set-points are sent from the own Plant control room/control system.
- "Remote" execution of the test: the set-points are sent from the TSO premises, involving the personnel who usually deals with tele-control of the plants connected to the HV grid who would manually insert the required set-points to be received from the plant.

Since remote tests are more complex to set and organize, this approach allowed us to reduce the number of possible issues that would happen during these tests. The execution of remote tests was preceded by communication tests between plant and TSO in order to verify that all the new data objects necessary for the AVC test were correctly exchanged.

The main reference used for the tests to be performed during local and remote experimentation was the technical document related to the Voltage Regulation Pilot Project (2020) promoted by Terna in the framework of Delibera 300/17 along with the Allegato 17 of the Italian Grid Code. Main purpose of the tests is to address both the static and dynamic response of the single plants after a V or Q set-point is received.

Test Q

During these tests, the plant control systems need to elaborate a percentual Q set-point. The tests proposed are similar to those which can be seen in Figure 5-1 a) and Figure 5-1 b).

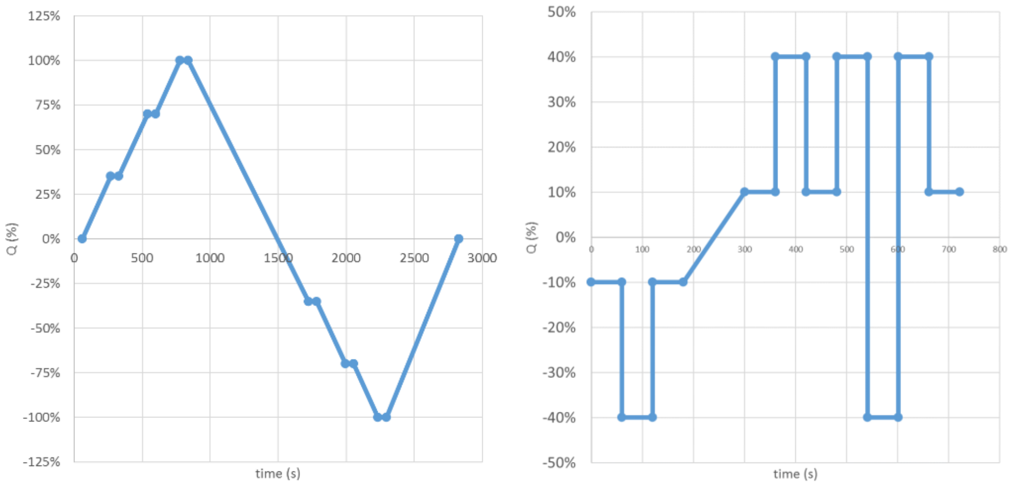

Figure 5-1 a) Test Q – static response b) Test Q dynamic Response

The graph shown in Figure 5-1a depicts a slow variation (10%/min) of the reactive power set-point: the main purpose of this test typology is to assess the P-Q capability of the plant to reach the demanded set-point and its precision. The reactive power set-point is not an absolute value but a percentage given by the ratio of the desired reactive power value and the available Q capability. So, for instance, when the plant is asked for a 100% set-point it has to provide the maximum available Q. In the proposed test, the plant is asked to linearly increase its Q provision from 0% to 35% to 70% and to 100% and then decrease, following a similar path but contemplating also a sign change in Q. The linear part of the curve has a 10%/min slope - usually, such slope has been reproduced by sending 30s apart set-points. On the other hand, when one of the “main” set-points (for instance: 35%, 70%, 100%, in the first rising part of Figure 5-1a is sent the controller waits 60s before sending the next one. The second test shown in Figure 5-1b, depicts step variations of the reactive power-set point: the scope is to test and evaluate the dynamic response of the plant (in this sense, it is an evolution on the first test). Step variations are asked to the plant controller both in the inductive and capacitive regions of the capability curves, and also a sign change of the Q set-point is contemplated, from a 40% to -40% Q level.

Test V

During these tests, the plant control systems need to elaborate a V set-point, which represents the desired tension at the HV level of the transformer. The plant will adjust its reactive power insertion/absorption accordingly to the requested V set-point. The test shown in Figure 5-2 depicts a reference V set point variation: analogously to what seen for the other two test typologies, both static and dynamic responses are analysed, but in one single session, while ideally asking the plant to modify the HV voltage between 95% and 105% of the nominal value. In the first part of the test the plant is asked to slowly vary the HV voltage, by sending set-points with a 2%/min slope and reaching both the 95% and 105% limit. The plant is then asked to respond to some increasing step set-points. When a V set-point is sent, the plant systems need to calculate the Q value according to the implemented Q=f(ΔV) curve. With the purpose of assessing the impact of the Q=f(ΔV) slope on the regulation and actually see if the plant follows and how, three different Q=f(ΔV) curves were tested for the Vaglio plant (see Figure 9-3 in Annex 9)

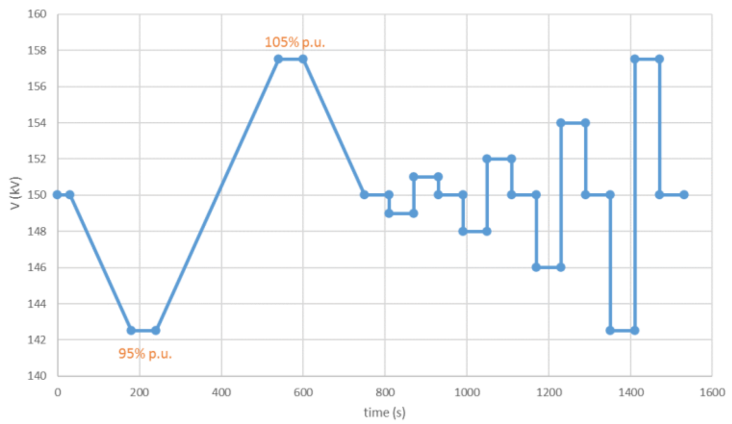

Figure 5-2 Test V

5.2.2 Main Results

The KPI aims to identify the effectiveness of RES plants (and relative communication/technology chain) in providing AVC by considering the reactive power actually provided by the plant and the TSO's reactive power request in the experimentation timeframe. For each quarter hour long interval, the real time differences between the requested and supplied reactive power values are calculated, referring to a certain sampling time. A final KPI value for the whole quarter hour is calculated as an average of all the values:

$$KPI_{DQ_{qdo}} = \sum_{1}^{900/\Delta tc} (KPI_{DQ} * (1 - Limit)) * \Delta tc/900.$$

Where:

KPI_DQ is the value of KPI for each Δtc of the testing session, evaluated as:

KPI_DQ = $0.5 * \left|\frac{Q_{th} - Q\_PdC\_mis}{Qlim\_PdC}\right|$

Q_{th} is the amount of reactive power required to the plant; Q_PdC_mis is the reactive power measured at the Point Of Connection (PoC); $Qlim\_PdC$ is the real-time reactive power limit at the PoC; Δtc is the sampling time (usually equal to 1 s); $Limit$ is equal to 1 when the voltage limit has been reached, 0 otherwise. In case KPI_DQ is >1, its value is set equal to 1 when calculating KPI_DQ_qdo. The more the KPI is closer to 0, the better the performance of the plant. The KPIs were calculated separately for the remote tests performed with the two plants. In the following the notation "KP" and "KV" will be used to denote if the KPI was calculated for tests in the Pietragalla plant or Vaglio plant respectively; the numerical notation, following "KP" or "KV" indicates the order of the test and the reference quarter hour in which the KPI was calculated. For example: "KV2.3" means this KPI was calculated for remote test #2 in Vaglio during the third quarter hour of the test. In Annex 9 one can find graphs of both local and remote tests performed.

As for the Pietragalla plant the main KPIs calculated during remote tests, corresponding to Figure 5-3 in the Annex, are shown below:

	Type of test	Duration	KPI
KP1.1	Q	15 min	0,0323
KP1.2	Q	15 min	0,0134

Table 5-1 AVC KPI Pietragalla remote tests

Due to well know storage performances, in Pietragalla “dynamic response” tests were directly performed.

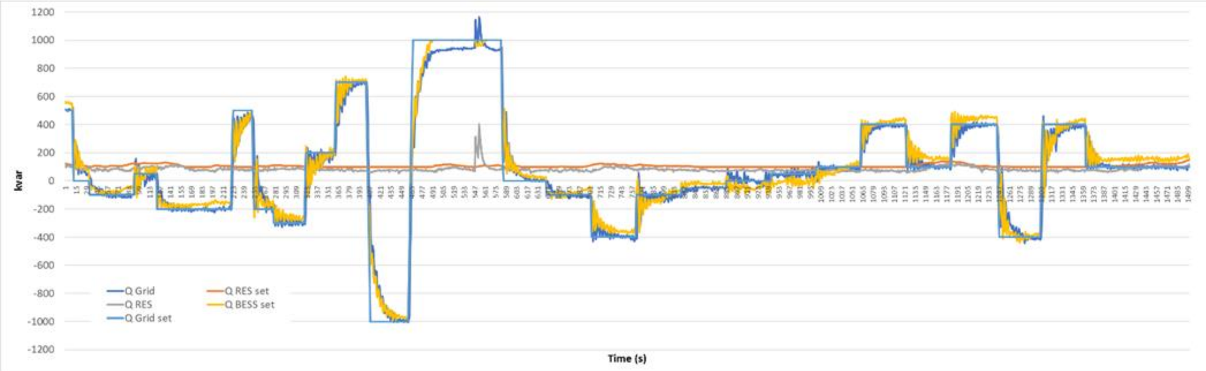

Figure 5-3 Remote test (Pietragalla) – Q set points. The light blue curve indicates the TSO requested Q, while the blue curve the grid measurement. More detail in Section 9.2.

Indeed, to push further, it was decided to test the plant for setpoints which were more challenging than those initially foreseen (a -100%, + 100% reactive power jump was asked to the plant, besides the foreseen -40%, 40%, as can be seen from Figure 5-3). As one can observe directly from Table 5-1, KP1.1 is worse than KP1.2. In the first part of the test, where KP1.1 is calculated, the plant is indeed asked to provide its maximum reactive power output and does not fully reach it. This is linked to how regulation is performed in this plant. The wind plant is responsible for the compensation of internal reactive losses and acts following the plant internal reactive losses variation due to Q flows, while BESS is mainly responsible for power provision at the connection point. In case of low active power production, as was during the tests, the wind power plant has a lower Q capability to compensate internal reactive losses – in this case, the storage plant has to provide both services: losses compensation and set-point tracking at the connection point. This is the main cause for some of the set-points not being fully reached and therefore the difference between KP1.1 and KP1.2. The wind plant is the main responsible for losses compensation and, in doing so, it follows its own dynamics– in general, this dynamics, which depend on the turbines control systems, is slower than that of the storage system: while providing power, the storage has to adapt to this dynamics with the effect of a slow-down in the reactive power contribution at the point of connection and with effects also on accuracy and oscillations. Not considering the specific case described above, in average, about 20 s are needed for the full provision. The KPI is calculated considering a ±1 Mvar maximum theoretical reactive power provision: indeed, as one can observe from Figure 5-3, when the plant is asked for a 100% Q insertion the set-point generated corresponds to 1000 kvar. If one also considered the wind plant contribution, the maximum theoretical reactive power provision would be higher (up to 7 Mvar) and therefore the KPI lower.

As for the Vaglio Plant, the tests were both of the “static response” and “dynamic response” type as one can observe from graphs reported in Annex 9. The main KPIs calculated during remote tests, corresponding to Figure 5-4 and Figure 5-5, are shown below:

	Type of test	Duration	KPI
KV1.1	V (Parametrization # 3)	15 min	0,076943806
KV1.2	V (Parametrization # 3)	15 min	0,183671198
KV1.3	V (Parametrization # 3)	15 min	0,250801726
KV2.1	Q	15 min	0,040913753
KV2.2	Q	15 min	0,015866754
KV2.3	Q	13 min	0,047757759

Table 5-2 AVC KPI Vaglio remote tests

For a detail on parametrization one can refer to Figure 9-3 in Annex 9. Some of the KPIs, here and afterwards, are to be considered less reliable since they were calculated on a shorter period than 15 minutes. The overall KPI performance was influenced by the fact that after a certain Q threshold the wind turbines would not vary their Q output anymore.

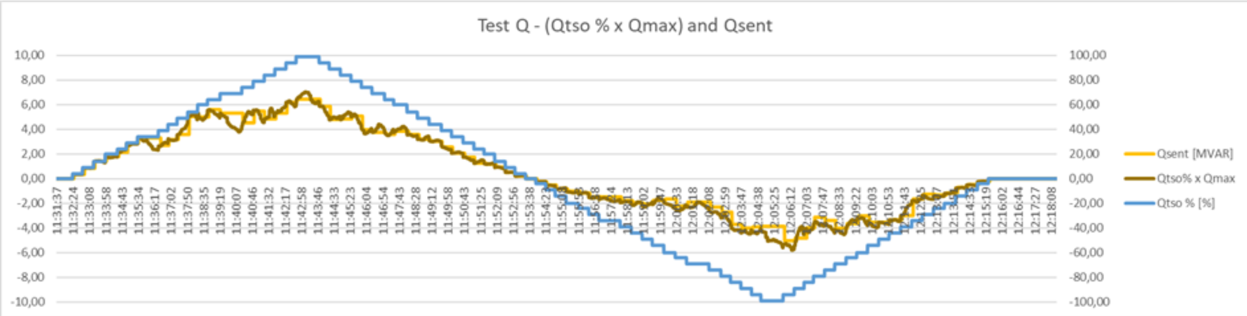

Figure 5-4 Remote test (Vaglio) – Q set-points. "Qtso%" is the percentual set-point sent from the TSO control room, "Q sent" is the actual Mvar set-point sent from the local SCADA, while the brown curve is the measured Q at the POC. More detail in Section 9.1.

This anomaly, showing a sort of unexpected capability saturation, which was finally explained after a deeper analysis by the WTG manufacturer and highlighted the need of a first level SCADA upgrade to solve a bug in one of the wind farms connected the point of connection, can be clearly seen through the KPI and looking at Figure 5-4 in the annex: KV2.1 (and KV2.3) refer to part of the test where the reactive power request is increasing (decreasing) above (under) the said threshold, while KV2.2 refer to the central part of the test, where no capability issue arise, hence the higher KV2.1 and KV2.3 values and the lower KV2.2 value.

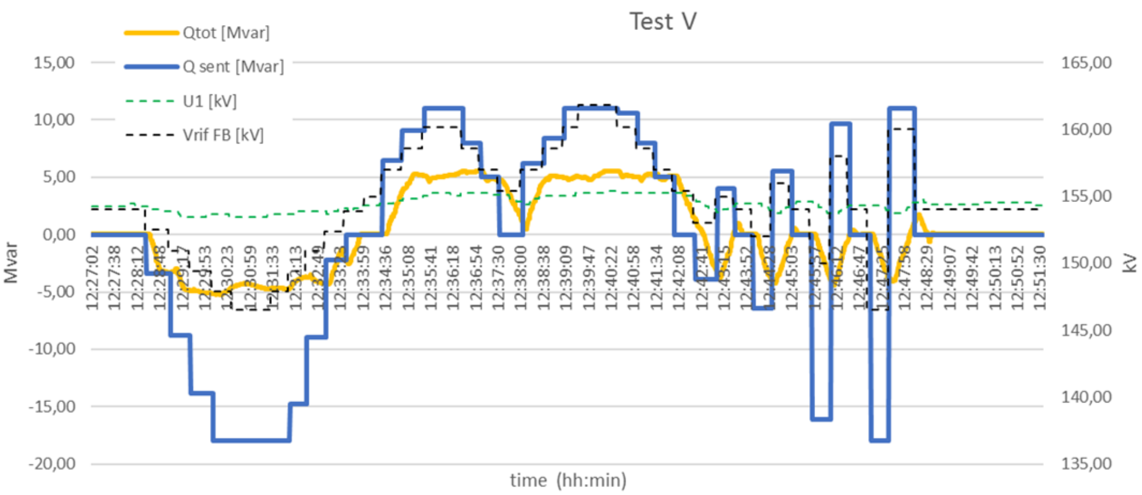

Figure 5-5 Remote test (Vaglio) – V set-points. Black dotted line represents the sent V set-points, while the blue line the corresponding Q set-points. Yellow line represents the measured Q at the POC. More detail in Section 9.1.

One can also notice the KPI being higher for the tests with Q set-point with respect to the tests with V set-point: indeed, the test with V-set-point (Figure 5-5) required the plant higher reactive power variations and, since a maximum power reactive variation (Mvar/s) setting is active and the saturation anomaly previously described exists, the plant provides the requested Q with more difficulty, hence the worse KPI. KPIs were calculated also for the local tests with V set-point where all the three parameter configurations were tested (Figure 9-4, 9-5, 9-6 in the annex), with final KPI values analogous to those seen above:

	Type of test	Duration	KPI
KV3.1	V (Parametrization # 1)	15 min	0,1709
KV3.2	V (Parametrization # 1)	11 min	0,1627
KV4.1	V (Parametrization # 2)	15 min	0,2200
KV4.2	V (Parametrization # 2)	14 min	0,1446
KV5.1	V (Parametrization # 3)	15 min	0,2553
KV5.3	V (Parametrization # 3)	13 min	0,1702

Table 5-3 AVC KPI Vaglio local tests (V set-points)

Overall, approximately 10-11 s are needed to reach a 0.5 Mvar reactive power delta, with times increasing with power output request. For the highest jumps that could be requested (and could be reached) during the tests (about 9 Mvar as can be observed from Figure 9-2 and Figure 9-3) approximately 45-50 s were needed.

The cause for the registered response times is mainly imputable to the components of the overall control system architecture, mainly constituted by a local embedded and first level Scada, which manages the V and Q regulations: this part of the architecture is a bit slow due to OPC protocol in sending the set-point to the power plant controller which is responsible to communicate to each WTG the set-point it has to manage – it introduces delays in terms of seconds. Both the local embedded and the first level SCADA operate carrying out a multitude of operations besides AVC regulation. A potential solution could be the adoption of a dedicated local embedded which elaborates remote requests of regulation and transfers them directly to the power plant controller supplied by the WTG manufacturer. This embedded would be only responsible for regulations and able to directly connect and control the WTG. The presence of machine limitations on the Q variations due to the anomalous behavior described before also contributed to slower response time.

5.2.3 Conclusions on voltage regulation from wind power plants

In conclusion, the experimentation showed that both a single wind power plant and an integrated wind and storage plant are technically capable of providing reactive power regulation, although they could not do it in the times requested by the Italian Grid Code, i.e. 5 seconds for the 100% Q provision. It was observed that the full time to reach the requested set-point increases with the magnitude of the requested Q variation and this is due to various factors. Both the plants' response is obviously influenced by the active power present at the moment of the tests, as it directly influences the wind power plant Q capability and, in general, the presence of the storage plant allows more confidence in the provision of the service. The response delays can also be linked to control system architecture that are not originally thought for this type of regulation and therefore their improvement, as suggested, could reduce activation times. The other limitations and anomalies that showed up during the tests and reduced the overall performance are linked to the specific technology and it is believed they can be overcome with future developments.

5.3 Synthetic Inertia

5.3.1 Test Planning and Overview

As the synthetic inertia experimentation in Pietragalla is concerned, planning of the tests took into account various factors, among which primarily the availability of the 2 MW/MWh storage system installed in the plant premise and responsible for the service provision. During experimental activities, indeed, the storage system was entirely devoted to synthetic inertia testing. Usually the device would be activated in the morning and let run for the whole day, with data analysis being made ex-post. The

Synthetic Inertia Control Device (SICD) was developed in order to command the storage system active power provision as soon as a rocof event is detected. Detection of such event and the consequent power response can be adjusted on the SICD by setting different modifiable parameters such as:

- Minimum and maximum State of Charge above which/ under which the service provision is active;
- Objective-SOC i.e. the SOC value at which the storage system heads back to after service provision
- Dead bands, droop, hysteresis. The power contribution to be injected can be adjusted by setting a proper ROCOF and Frequency dead band: the work done during the development phase revealed indeed that injecting power following only a rocof indication would be too hectic and could also be linked to other factors not related to a grid event; for this reason, the power injection is activated only when both frequency and rocof thresholds are exceeded. The power injection then follows a linear curve, dependent on ROCOF, with a specific droop and hysteresis. A holding time can be set for the contribution, in order to avoid intermittent operation, as well as a “ramp down gradient” representing the speed at which the power injection reduces after the persistence time has passed.

The device is also capable of performing a hybrid “rocof + frequency dependent” regulation, meaning that the power set-point sent to the BESS is the sum of a power contribution depending on ROCOF and a power contribution depending on frequency. In the reminder of the experimentation only the purely rocof dependent modality was tested.

Regarding experimentation in Vaglio, activity was structured in two main items:

i. Development of an upgraded firmware/software respectively (i) on the converter on the WTG nacelle and (ii) on the control system of the WTG, including a laboratory bench and full-scale tests of the upgrade

ii. Validation of the above mentioned firmware/software upgrade on a wind turbine at Vaglio plants.

On the basis of the initial technical specification the wind turbine supplier Siemens Gamesa (SGRE) undetook the activity through software modeling and simulations in order to find parameter ranges in terms of gain and intervention thresholds to properly configure the service with the aim to avoid fatigue issue in WTG lifetime. As a result, new converter firmware and PLC software were developed. SGRE needed more time than forecast to optimize firmware and software. In fact, the laboratory test phase (both at bench scale and full-scale level) as reported by the WTG supplier was more difficult than foreseen at the beginning. SGRE carried out a second laboratory test in August 2021 due to difficulties in understanding unexpected behaviors. More time will be necessary to allow to finalize the last firmware/software development before installing them in a real WTG. Due to lack of time to end the OSMOSE test, ERIN decided not to proceed with the validation on a WTG in Vaglio wind farms. Results analysis coming from laboratory bench tests will be shown in the following.

5.3.2 Main results

Details and results on the Pietragalla experimentation are given first, followed by the results of experimental activity on wind turbines.

Starting from HV voltage measurements, the SICD continuously calculates frequency and rocof and elaborates an active power set-point which is sent to the PCS of the storage system for activation; the parameters that guide the setpoint generation are summarised in Table 9-1 in Annex 9. During the 60 hours ca. experimentation, the SICD generated a set-point when a simultaneous frequency and rocof variation was overcome (±20mHz above or below the nominal 50 Hz value and ±30mHz/s for the ROCOF). After the set-point is generated and sent to the PCS, the SICD asks for this value for the following 10 seconds as holding time; after this time, there is a ramp down period during which power insertion reduces to zero. As a matter of example, a typical activation is shown in Figure 5-6. The power insertion was commanded since both frequency and rocof thresholds were exceeded (-36,17 mHz, -36,58 mHz/s) – the set-point generation required in this case about 200 ms. The power request, which corresponds to the maximum available to the storage system (800 kW) was kept for the following 10 s, a power de-ramp period then followed as expected. During the plateau period the SICD is not expected to generate further power set-points, in case an event is detected.

All parameters reported in Table 9-1 in Annex 9 (thresholds, ramp-rate, holding time, ramp-down, etc.) are settable in order to change the behaviour/performance of service provision.

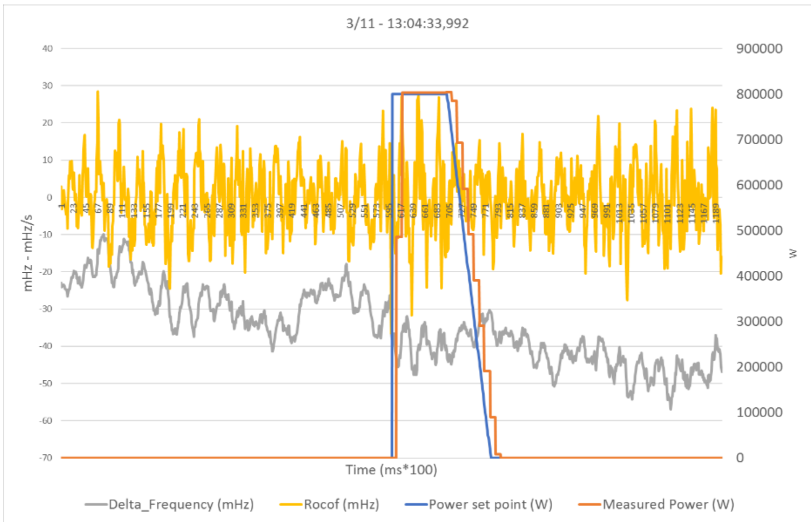

Figure 5-6 SICD activation (3/11, 13:04:33)

The KPI chosen to analyse synthetic inertia provision focuses on the availability of the implemented chain:

$$KPI_{IS} = \frac{n_{av}}{n_{ex}}$$

Where :

$$n_{av} = number\ of\ hours\ in\ which\ synthetic\ inertia\ supply\ is\ available$$

$$n_{ex} = experimentation\ hours$$

Availability is strictly connected to the plant SICD and battery conditions – since during the tests the battery was never in fault conditions, never showed issues regarding low/high SOC values that would make the provision unfeasible, and the power insertion was always managed to remain in the plant power limits at the Point Of Connection this KPI can be considered of unitary value, denoting optimal availability of the system.

During the whole experimentation the device activated for 174 times. These activations are the result of about 288 event detections (passing of rocof and frequency thresholds): the activations number is lower than the event detections mostly due to the 10s plateau period during which the device can still recognize an event but does not send a set-point. Out of all the 174 activations, 115 of them were characterized by a response time (time between the event and the set-point send to the storage system) lower than 300 ms (average 250 ms); the other 59 activations were characterized by a response time higher than 1 s. This could be caused by particular bugs in the log file more than the real SICD reactivity, since these slow-reaction events are all absorption events while the fast-reaction ones are all insertion events. On top of the 250 ms ca, one can add about 100/200 ms which are needed by the PCS+BESS control to elaborate the set-point and actually provide the requested active power. Although the measurement system employed during the tests on the BESS has slow refresh times (in the order of 1 s) and could not easily catch this very fast reaction on this part of the chain, these 100-200 ms response times (power provision after activation) are typical for lithium storage systems and measured also in Pietragalla. Overall, times in the range of 400 ms are then needed from HV voltage measurements to power insertions.

Some anomalies were noticed on the results and will be the object of upgrades and further analysis on the device, as for example, in few cases the device commanded an activation to an event detection during a de-ramp phase, when it was not supposed to, or some of the events were the result of the detection of very high frequency and rocof values which are usually not detected on the grid.

As far as the developments regarding the firmware/software upgrades performed by Siemens Gamesa on Vaglio-like turbines, the testing activities that could be performed are described in the following. After an initial modeling simulation, two different testing typologies were set up as described in Figures 5-7 and Figure 5-8 here below.

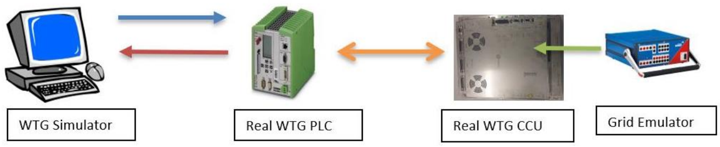

Figure 5-7 Reduced scale laboratory test bench

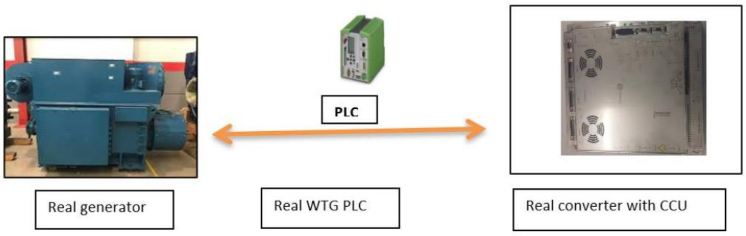

Figure 5-8 Full scale test bench

Both reduced scale laboratory test bench and full scale test bench involved the use of a grid emulator (not pictured in Figure 5-8) and full scale test also included a load simulator. The generator, Programmable Logic Control (PLC) and Converter Control Unit (CCU) are all real WTG components. The CCU measures frequency and its firmware has been updated with functionalities to calculate and filter ROCOF; this data is communicated to the PLC whose software has been updated in order to generate a rocof-proportional active power set-point when certain ROCOF thresholds are overcome. The set-point is then communicated to the CCU which finally adjusts the rotor voltage, frequency and current in order to reach the balance point sent by the PLC.

Tests and analysis carried out at SGRE labs suggest that a maximum 10% delta power (with respect to the nominal 2.6 MW turbine power) can be requested to the turbine because (i) mechanical and electrical constrains due to design (maximum torque parameter which could not be overpassed) do not allow higher values and (ii) to avoid a stand-by risk behavior of a WTG after tenth second during a frequency event due to rotor speed decreasing up to critical values that could stop WTG power production. For over-frequency events the delta power (decreasing) value could be a value higher than 10%. Starting from this consideration, thresholds were calculated and then tested accordingly.

ΔP/Pn	df/dt (mHz/s)	K (% s/ mHz)
0.1	5	2
0.1	12	0.833
0.1	80	0.125
0.1	…	…

Table 5-4 Example of tested K – rocof thresholds combinations.

From Table 5-4 one can infer that the power contribution is proportional with df/dt until the df/dt value in Table 5-4 is reached; after that it saturates to the 10% of the nominal power (Pn) value. In Figure 5-9 one of the tests from the reduced scale laboratory test bench can be analyzed. In this case, the wind turbine was working at 20% of its nominal power; being the ΔP/Pn=0,1 and K=4, the detected 80 mHz/s rocof event (one can see the green curve representing frequency) required the full 10% nominal power insertion which would then be reached in few seconds. After a certain holding time, there is a ramp down period during which power returns to its previous level.

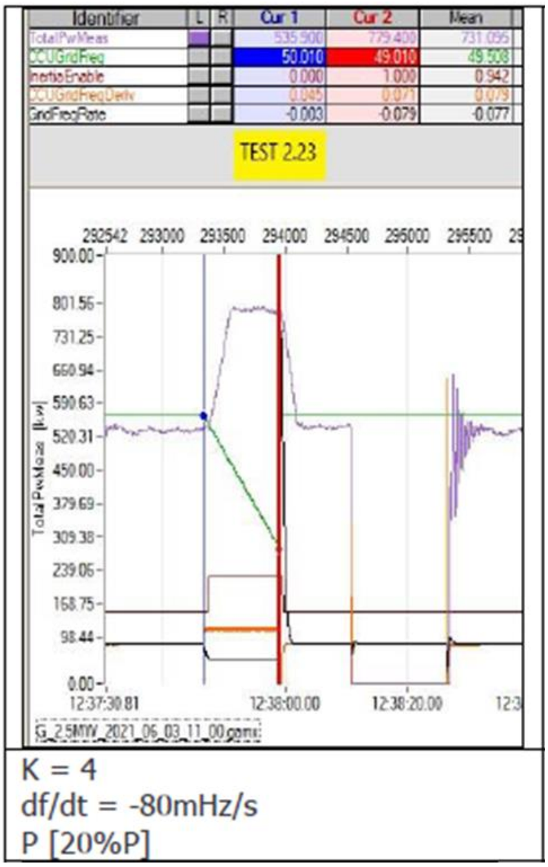

Figure 5-9 Reduced scale laboratory test bench experimental result example

Simulations gave an insight on the maximum times the rocof-proportional insertion can be held (considering a 10% ΔP/Pn): i) In case of low winds, when active power oscillates between 10% up to 25% of the nominal power, the maximum allowable time is 3 seconds; ii) In case of high winds: above 25% Pn, the maximum time tested, at least in simulations, has been 30 seconds. These times should guarantee no risks (mechanical, electrical, standby) are undertaken by the turbine. Besides the turbine own dynamics in reaching the set-point the reaction time will comprehend i) few milliseconds (ms) necessary for filtering calculation. This will depend on the window defined for taking measurements, the lower df/dt value the bigger should be the window (more noise), but this will imply to have a lower reaction time ii) 8 ms communication between CCU-PLC to communicate df/dt iii) 20 ms for PLC calculus with the received df/dt value. At this point ΔP will be calculated and this reference value will be sent to the CCU (converter).

Activity results should be deepened in a further step of development in the future with a validation on a real installed and operating WTG. Focus should be put on increasing the power variation boost up to the maximum WTG nominal power so to study if this can reduce the risk to send WTG in a stand-by mode after the frequency event intervention. It is also to be better understood how this type of intervention would impact expected operating WTG lifetime and if appropriate tresholds could be defined. Additional focus would be needed also on the rocof calculation methodology and the adopted filtering techniques.

5.3.3 Conclusions on inertia from wind power plants

As for the experimentation conducted in Pietragalla, the innovative device showed response times lower than 300 ms, denoting its strong capability in quickly performing all the operations that range from real-time frequency and rocof calculation to set-point generation. Besides some further analysis on specific points of the performed tests, a more thorough analysis that could complement the results of the Osmose experimentation should have to focus on a more advanced definition of the events to which the power insertion has to follow.

As for the experimentation conducted on the wind turbines test bench, simulations on turbine components showed that a 10% nominal power contribution, result of the use of the turbine inertia, can be safely provided by the turbine in a matter of seconds following a rocof detection and be held for times depending on the running active power. Field experimentation on a real turbine could provide validation to these considerations, as well as further analysis on lifetime impacts of such power insertions and rocof calculation methodology and event definition.

6 Overall conclusion from WP5 demonstrator

Finally, all the relevant evidence collected in the demonstrator have been illustrated. Given the complexity and the heterogeneity of the contents, a summary of all the conclusions drawn for each technology/service is reported in this final chapter, with a perspective at system level. From this point of view, three main key learnings can be summarized:

1) **How to unlock existing flexibility from the grid: a combination of advance dispatching technique and “capital light” investments**

KPI values shown in Chapter 2.2 demonstrated that an algorithm for congestion detection can forecast the real behaviour of the grid, detecting when there are going to be congestions and when not, with an accuracy that can reach up to 80%. Precision levels, i.e. when the forecast detect a false congestion, instead of a true one, showed reduced values around 50%. This is mostly due to the fact that some detected congestion will be solved by Terna EMS: running in parallel the Z-EMS, which was necessary due to the nature of the experiment, is not an optimal configuration. However, the studies demonstrated that such precision increase up to 88% when a larger portion of the area is involved. Combining the good accuracy from the Z-EMS, which exploits effective load and generation forecast techniques and a more accurate rating of the lines thanks to DTR (from 2 to 4 times higher than the standard rating currently considered), it has been demonstrated that residual flexibility from existing assets can be exploited. This shows that the planning of new grid infrastructures – which will always be needed in order to increase efficiency and security of supply – can also benefit from a combined approach with capital light investments, such as the one tested, in order to maximize grid flexibility and minimize costs for the system.

2) **Relying on wind power plants for system flexibility: what are the next developments?**

The experimentation clearly showed that both a single wind power plant and an integrated wind and storage plant are technically capable of providing reactive power regulation. The test results were not fully compliant with the timing of delivery requested by the Italian Grid Code, i.e. 5 seconds for the 100% Q provision. The main cause was identified mainly due to the plants control system architecture that, although upgraded for the experimentation, have not been originally developed for this type of regulation. Therefore, more effort should be devoted into the definition of control logic standards that allow to exploit the full potential of the wind resource in terms of voltage regulation. Coupling storage with such non-programmable resources has shown to improve their performance.

As far as frequency stability is concerned, the provision of synthetic inertia proved to be quite reliable in terms of activations, when requested from a storage integrated plant. However, more effort should be dedicated to the identification of the control parameters that allows a useful effect of the resources. One of the most important areas to explore in the future is the correct identification of a “grid event” that requires the activation of the resource. Simulations performed in laboratory tests on wind turbines underlined a potential in deploying also the kinetical energy of wind turbines, about 10% of nominal power contribution, in order to support grid frequency. On-field experimental activities should allow to validate these considerations on a real wind turbine.

3) **Expectations on Demand Side Responde from industrial sites**

Industrial sites proved to be reliable resources when it comes to slow services such as balancing and congestion management, considering the amount of energy extracted during the tests (about 114 MWh) and the high availability of the offers provided with respect to the TSO needs. A full real time test procedure, with bidding and control from the aggregators, resulted possible with some relevant upgrades to the site, that should be justified by a proper remuneration. The only technical open point remained the possibility to know the baseline of the single loads within each plant, given their small size with respect to the whole plant installed capacity. This can affect the controllability of the loads, that resulted nevertheless reliable.

When it comes to faster regulation, such as a-FRR, one of the plants retired from the project. The other possible load, a HVAC system, proved difficult to be controlled, as the inertia of such large industrial buildings is high and a direct correlation between regulating temperature and power input was difficult to be found. As far as voltage regulation is concerned, many obstacles have been found in the upgrades of industrial sites, which are very far from being able to provide this system remotely without a proper upgrade. Furthermore, the regulation on the MV side of the plants in order to obtain an useful effect on the HV side requires control systems based on complex logics. Generally speaking, the medium voltage generators of the industrial park involved in the experimentation proved to be reliable resources, but their capability was very limited by constraints on the medium voltage side, given the fact that the industrial site's main focus is to guarantee a steady production, which is their primary object. For these reasons, faster regulation services do not yet seem to be reliable from a system point of view.

What are the next steps?

Work Package 5 tackled a huge variety of possibilities for future system flexibility, and its results will help a better understanding of new resources. These insights can for sure be beneficial to the update of grid codes and the ancillary services market evolution. That being said, WP5 work is not concluded yet: with task 5.6 and corresponding D5.6, all the above findings will be analysed in a scalability and replicability analysis, to give some answer on whether the tested flexibility resources can be feasible from a techno-economic point of view at a wider scale level.

7 Annex 1 – Zonal – Energy Management System

7.1 Dashboard

The Dashboard is a software tool, a nodejs web application, developed in the context of the OSMOSE project. It is put at disposal of TERNA operator in order to exploit the following main features:

1. addressing the Z-EMS congestion management (detection and resolution): the TERNA operator can see the detected congestions, manage the proposed solutions (DTR and available resources) and have a clear understanding of the residual congestions. As it is shown in Figure 2-1, clicking on the “Create BDE” button, TERNA Operator, can choose one or more offers selected by the Z-EMS in order to solve the congestion through the availability of BSP: He can therefore create and submit a BDE that is the regulation command sent by Terna operator to Balancing Service Provider (BSP). The process of BDE creation and submission is applied in case it is not possible to solve the detected congestions by means of DTR activation Figure 7-1;

2. monitoring the overall process of data retrieving and orchestration (Input Z-EMS) and the main outcome of Z-EMS processing (Output Z-EMS status: REF _Ref93311866 \h * MERGEFORMAT ￼￼Data ￼Figure 13￼￼, the “Data check” tab allows to know if relevant inputs for the Z-EMS execution (e.g., the admittance matrix of the grid for current quarter of hour) are available for each run of Z-EMS execution and at the same time provides information about the Z-EMS status showing which optimization model (M1 M2, M3 and M4) is provided in real time. Moreover, the “View history” button allows the TERNA Operator to select one specific data from the Calendar in order to show information about a specific Z-EMS execution done in the past;

3. seeing the graphical representation of DTR loadability curves and the line current measures: the Figure 7-3 shows the “DTR” Tab; the Terna Operator can select the date, the interval time and the monitored line related to the loadability curve and the line current measure he would like to know. The same information is provided in real time by clicking on the “Real time” button.

4. showing the BSPs offers and manage the interaction with each BSP through the regulation orders (BDE): as it is explained in section 3.2, some tests directly involving BSP have been done with the aid of the Dashboard. In particular, the “DSR” Tab allows the TERNA operator to see the BSPs offers and manly to select the offers and to send the regulation orders (BDE) to the correspondent BSP. This process is performed without the support of Z-EMS and therefore it doesn’t depend from Z-EMS outputs Figure 7-4

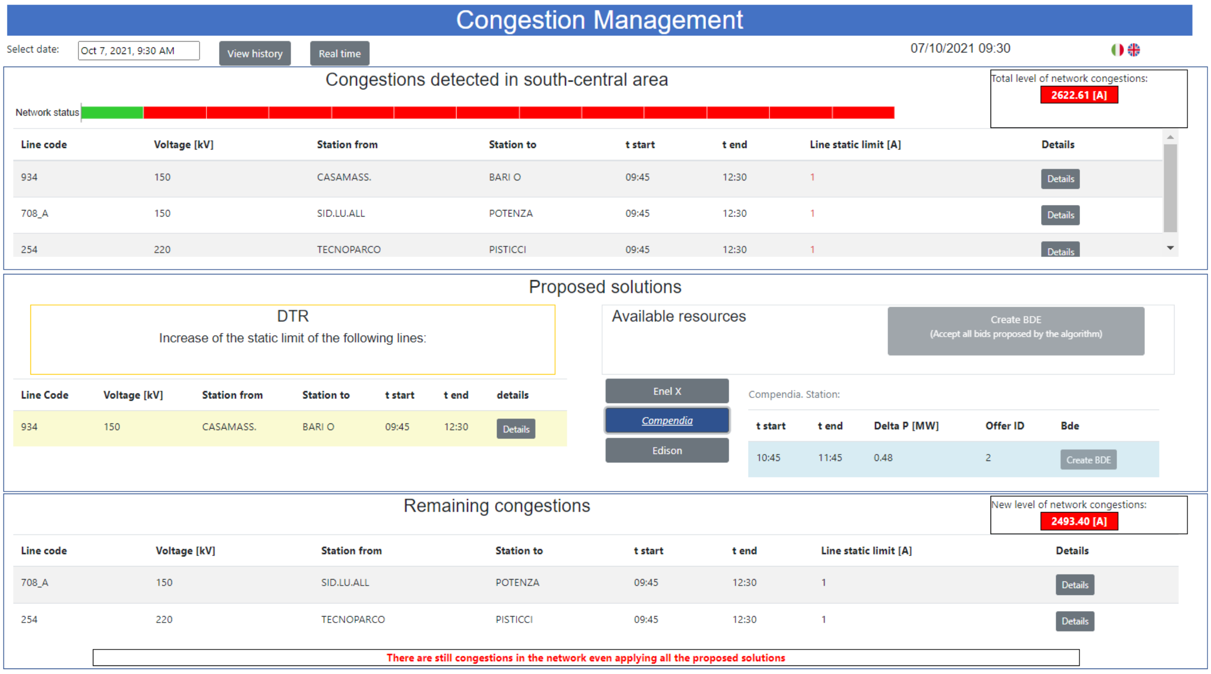

Figure 7-1 – Dashboard: Congestion Management Tab

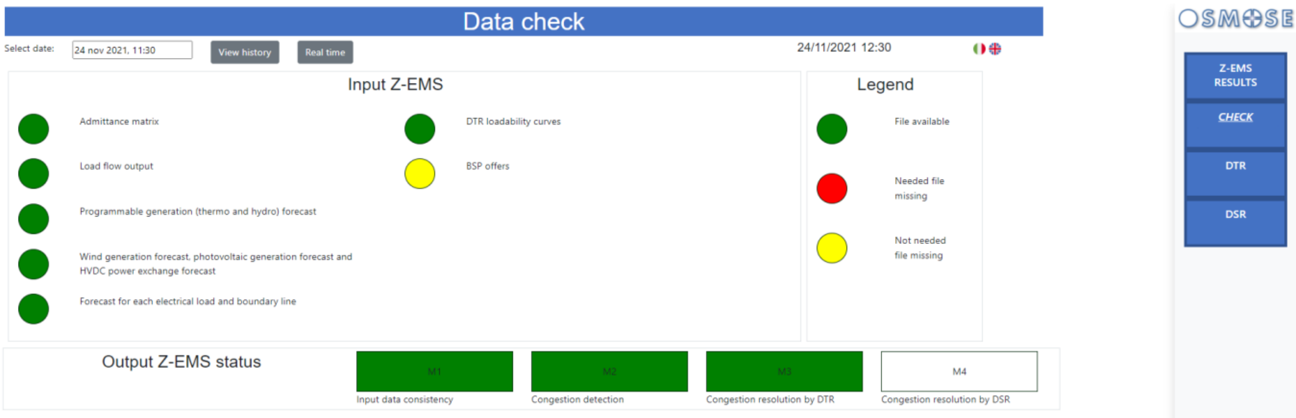

Figure 7-2 – Dashboard: Data check Tab

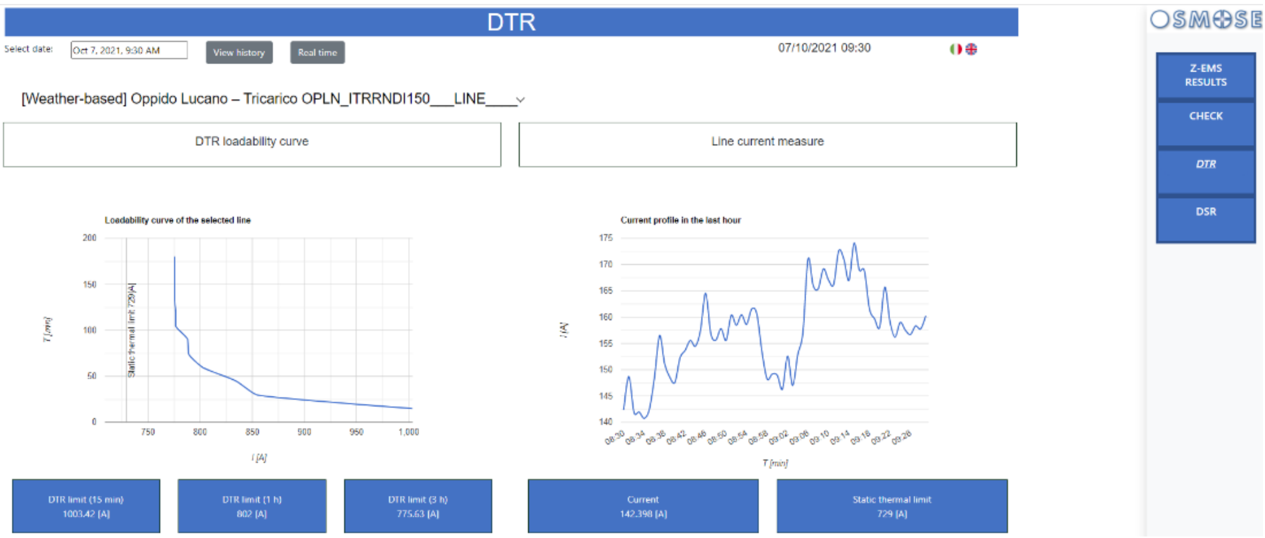

Figure 7-3 – Dashboard: DTR Tab

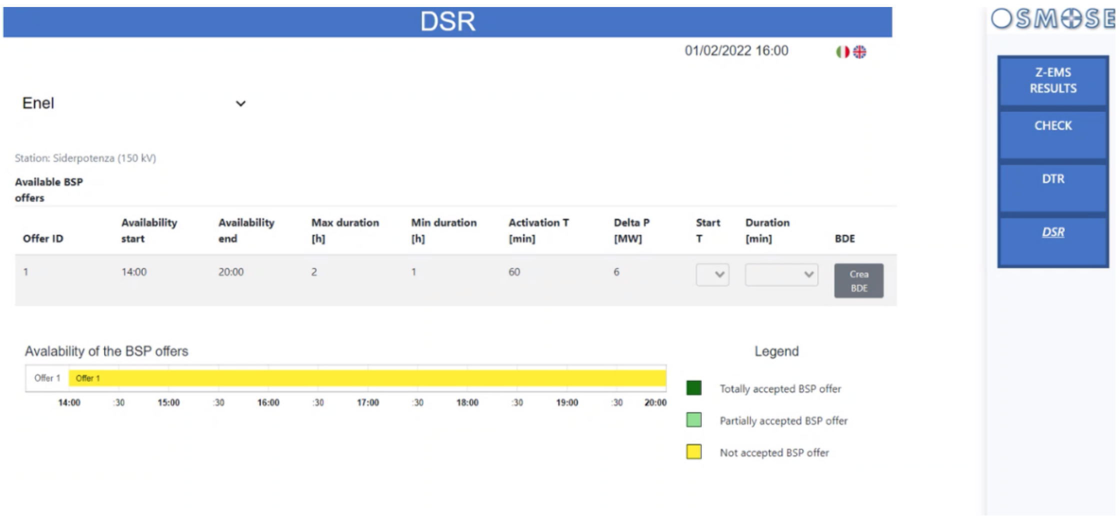

Figure 7-4 –Dashbord DSR Tab

7.2 Report of Z-EMS test sessions

Here the main characteristics of all sessions are reported. In particular, column "DTR" indicates which DTR algorithm has been used for the run, either the weather-based ("wb") or the sensor-based ("sb"). Column "DSR" indicates if DSR resources were available. Column "Add-on" explains the main characteristic of the run and the changes respect to previous sessions. Column "KPI" reports 79hether or not the KPI, that have been already saved, will be considered for ex-post analysis.

#	Session name	DTR	DSR	Notes	Start	End
1	**Preliminary tests**					
1.1	Preliminary test	none	N	-	15/02	15/02
1.2	Preliminary test with DTR	wb	N	Wb DTR integration (*Sviluppo*)	18/02	18/02
1.3	Preliminary test #2	wb	N	Full CPU and RAM requirements in Testing Environment (*Collau-*	03/03	10/03

				do)		
1.4	Long-run	wb	N	Micca and current measurements integration in Operational Environment (*Esercizio*)	19/03 11:45	30/03 13:45
2	**DTR-DSR integration tests**					
2.1	Short test DSR	none	Y	BSP offers integration in Testing Env. (*Collaudo*)	30/03 13:00	30/03 18:30
2.2	Short test DTR sensor-based	sb	N	Sb DTR integration, even with variation of line current limits	01/04 12:00	01/04 15:30
2.3	Long test DTR sensor-based #1	sb	N		01/04 16:00	04/04 18:00
2.4	Long test DTR sensor-based #2	sb	N		06/04 09:45	12/04 13:15
2.5	Long test DTR weather-based	wb	N		12/04 14:00	16/04 10:45
2.6	Long test DTR sensor-based #3	sb	N	One-month long test with some interruptions	17/04 00:00	15/05 12:25
2.7	Long test DTR weather-based	wb	N	Long test with many interruptions: software maintenance needed	05/06 17:45	22/06 01:30
2.8	Short test DSR with Dashboard	N	Y	First test in Collaudo environment	08/06 16:00	08/06 19:45
3	**In-vitro tests**					
3.1	Run #1 with Dashboard	wb	Y	Fake BSP offers used	18/06 09:30	18/06 19:45
3.2	Run #2 with Dashboard	wb	Y	Fake BSP offers used	21/06 10:30	21/06 16:30
3.3	Run #3 with Dashboard	wb	Y	Fake BSP offers used	22/06 10:15	22/06 19:45
3.4	Long-run with Dashboard	wb	Y	Real BSP offers used. Forced congestions changed during the days.	28/07 17:00	05/08 21:00
3.5	List of runs with Dashboard	wb	Y	Real BSP offers used, during BSP tests days [30/09 09:00 – 01/10 09:15]; [07/10 09:30 – 07/10 14:30]; [11/10 18:15 – 12/10 11:15]; [28/10 11:00 – 28/10 16:15];		
				Final Z-EMS deployment	**31/07**	
4	**Full tests**					
4.1	Long test #1	N	N		08/07 15:15	14/07 12:00
4.1	Long test #2	wb	N		24/07 00:30	28/07 16:00
4.3	Long test #3	wb	N	From now on, final Z-EMS version is used	06/08 00:00	13/08 00:00
4.4	Long test with DTR and	wb	Y	Some interruptions, due to in-	23/09	18/10

	DSR			vitro tests. BSP available on date: [13/10]; [14/10]	16:00	17:15
4.5	Long test with DTR and DSR	sb	Y	Interruption [30/10 00:00 – 02/11 16:15]	28/10 16:45	30/11 21:00

8 Annex 2 – Demand Side Response

8.1 DSR Congestion Resolution Test Calendar

Here the main characteristics of all DSR test sessions are reported for each BSP partner of the project.

Table 8-1: Overview of Compendia tests

Compendia								
ID test	**Plants involved**	**P call [MW]**	**Type**	**Availability hours**	**Callable hours**	**Called hours**	**Executed hours**	**Notes**
1	Industrial Park	0,8	Downward	0,5	0,5	0,5	0,5	
2	Industrial Park	0	Downward	0	0	0	0	Retired offer
3	Steel Mill	0,09	Upward	0,25	0,25	0,25	0,25	
4	Steel Mill	0,035	Upward	0,5	0,5	0,5	0,5	
5	Steel Mill	0,045	Downward	1	1	1	1	
6	Industrial Park	0,8	Downward	0,5	0,5	0,5	0,5	
7	Steel Mill	0,09	Upward	0,25	0,25	0,25	0,25	
8	Oil Refinery+Steel Mill*	0,48	Downward	8	2	2	2	
9	Steel Mill	0,09	Upward	0,25	0,25	0,25	0,25	
10	Oil Refinery+Steel Mill*	0,48	Downward	8	2	2	2	
11	Oil Refinery	0,45	Downward	4	1	1	0	Problems with data
12	Steel Mill	0,09	Upward	0,25	0,25	0,25	0,25	
13	Oil Refinery+Steel Mill*	0,48	Downward	8	2	2	2	
14	Oil Refinery	0,45	Downward	4	1	1	0	Problems with data
15	Steel Mill	0,09	Upward	0,25	0,25	0,25	0,25	
16	Oil Refinery+Steel Mill*	0,48	Downward	8	2	2	2	
17	Oil Refinery	0,45	Downward	4	1	1	0	Problems with data
18	Oil Refinery	0,45	Downward	4	1	1	1	
19	Steel Mill	0,09	Upward	0,25	0,25	0,25	0,25	
20	Oil Refinery+Steel Mill*	0,48	Downward	8	2	2	2	
21	Oil Refinery	0,45	Downward	4	1	0,75	0,75	
22	Steel Mill	0,09	Upward	0,25	0,25	0,25	0,25	
23	Oil Refinery+Steel Mill*	0,48	Downward	8	2	2	2	
24	Steel Mill	0,09	Upward	0,25	0,25	0,25	0,25	
25	Oil Refinery+Steel Mill*	0,48	Downward	8	2	2	2	
26	Oil Refinery	0,45	Downward	4	1	0,75	0,75	
27	Steel Mill	0,09	Upward	0,25	0,25	0,25	0,25	

28	Oil Refinery+Steel Mill*	0,48	Downward	8	2	2	2	
29	Steel Mill	0,07	Upward	0,25	0,25	0,25	0,25	
30	Oil Refinery+Steel Mill*	0,48	Downward	8	2	2	0	Not Executed
31	Steel Mill	0,09	Upward	0,25	0,25	0,25	0,25	
32	Oil Refinery+Steel Mill*	0,48	Downward	8	2	1	1	
33	Oil Refinery	0,45	Downward	4	1	1	0	Problems with data acquisition
34	Steel Mill	0,09	Upward	0,25	0,25	0,25	0,25	
35	Oil Refinery+Steel Mill*	0,48	Downward	6	2	2	2	
36	Oil Refinery	0,45	Downward	4	1	1	1	
37	Steel Mill	0,09	Upward	0,25	0,25	0,25	0,25	
38	Oil Refinery+Steel Mill*	0,48	Downward	6	2	2	2	

*When aggregate tests have been carried out, the columns "hours" are evaluated as the sum of the hours of each component involved

Table 8-2: Overview of Enel X tests

Enel X								
ID test	**Plants involved**	**P call [MW]**	**Type**	**Availability hours**	**Callable hours**	**Called hours**	**Executed hours**	**Notes**
1	Foundry	3	Upward	3	1	1	1	
2	Foundry	3	Upward	3	1	1	1	
3	Foundry	6	Upward	6	1	1	1	
4	Foundry	6	Upward	6	1	1	1	
5	Foundry	6	Upward	6	1	1	1	
6	Foundry	6	Upward	2	1	0,5	0,5	
7	Foundry	6	Upward	4	1	0,5	0,5	
8	Foundry	4,5	Upward	6	1	1	1	
9	Foundry	6	Upward	12	2	2	2	
10	Foundry	4,5	Upward	5	1	0,5	0,5	
11	Foundry	4,5	Upward	5	1	1	1	
12	Foundry	4,5	Upward	10	1,5	1,5	1,5	
13	Foundry	6	Upward	6	1	1	1	
14	Foundry	4,5	Upward	6	1	1	1	
15	Foundry	3	Upward	6	1	1	1	
16	Foundry	3	Upward	6	1	1	1	
17	Foundry	4,5	Upward	6	1	1	1	
18	Foundry	6	Upward	6	1	1	1	
19	Foundry	6	Upward	4	2	1	1	
20	Foundry	6	Upward	4	2	1,5	1,5	

Table 8-3: Overview of Edison tests

Edison								
ID test	**Plants involved**	**P call [MW]**	**Type**	**Availability hours**	**Callable hours**	**Called hours**	**Executed hours**	**Notes**
1	Powetrain industry	0,05	Downward	3,5	1	1	1	
2	Powetrain industry	0,05	Downward	3,5	1	1	1	
3	Powetrain industry	0,05	Downward	9	1	1	0	Not Executed
4	Powetrain industry	0,05	Downward	9	1	1	1	
5	Powetrain industry	0,05	Downward	9	1	1	1	
6	Powetrain industry	0,1	Downward	3	1	1	1	
7	Powetrain industry	0,1	Downward	9	1	1	1	
8	Powetrain industry	0,05	Downward	9	1	0,5	0,5	
9	Powetrain industry	0,04	Downward	9	1	0,75	0	Not Executed
10	Powetrain industry	0,04	Downward	9	1	1	0	Not Executed
11	Powetrain industry	0,04	Downward	9	1	1	1	
12	Powetrain industry	0,07	Upward	8	1	1	1	
13	Powetrain industry	0,07	Upward	9	1	1	1	

8.2 DSR Congestion Resolution Test Results

Here the results of all the tests performed in the experimental campaign, divided by BSP and by industrial plant.

8.2.1 Compendia

Aggregate test results (Oil Refinery + Steel Mill)

Table 8-4: Results of the aggregate tests (Hot Oil Heater + Compressor)

ID TEST	Date	Aggregate Theoretical duration [h]	P call [MW]	Switch On time	Switch Off time	Real duration [h]	Switch on Ramp	Switch off Ramp	P Average [MW]	Kpi1	Kpi1*
8	22 June 2021	1	0,48	10:42:16	12:34:00	01:51:44	00:32:16	00:01:48	0,501	127%	84%
10	24 June 2021	1	0,48	11:30:08	12:33:04	00:54:56	00:14:28	00:00:08	0,542	114%	108%
13	8 July 2021	1	0,48	10:56:32	12:32:32	01:01:40	00:08:04	00:00:36	0,518	115%	104%
16	15 July 2021	1	0,48	11:31:52	12:34:20	01:02:28	00:20:52	00:09:20	0,573	124%	111%
20	29 July 2021	1	0,48	10:26:48	11:35:24	01:08:36	00:09:44	00:00:12	0,51	128%	106%
23	5 August 2021	1	0,48	10:44:20	11:46:45	01:02:25	00:11:48	00:00:12	0,543	126%	113%
25	16 September 2021	1	0,48	10:51:40	12:30:40	01:27:00	00:19:08	00:13:16	0,568	138%	96%
28	23 September 2021	1	0,48	10:59:04	12:05:20	01:06:16	00:12:20	00:04:48	0,534	103%	97%
30	30 September	1	0,48	-	-	-	-	-	-	-	-

	2021										
32	7 October 2021	0,5	0,48	10:15:52	12:50:44	01:28:48	00:07:52	00:00:08	0,551	324%	164%
35	14 October 2021	1	0,48	10:20:44	12:05:16	01:44:32	00:09:24	00:02:06	0,596	191%	125%
38	21 October 2021	1	0,48	10:56:04	12:01:56	01:05:52	00:02:40	00:00:24	0,485	111%	100%

Oil Refinery results (hot oil heater)

Table 8-5: Results of the hot oil heater tests

ID TEST	Date	Theoretical duration [h]	P call [MW]	Switch On time	Switch Off time	Real duration [h]	Switch on Ramp	Switch off Ramp	P Average [MW]	Kpi1	Kpi1*
8	22 June 2021	1	0,45	10:42:16	12:34:00	01:19:28	00:32:16	00:01:48	0,475	136%	84%
10	24 June 2021	1	0,45	11:36:56	12:31:52	00:54:56	00:14:28	00:00:08	0,516	117%	109%
11	30 June 2021	1	0,45	-	-	-	-	-	-	-	-
13	8 July 2021	1	0,45	11:30:52	12:32:32	01:01:40	00:08:04	00:00:36	0,491	121%	110%
14	14 July 2021	1	0,45	-	-	-	-	-	-	-	-
16	15 July 2021	1	0,45	11:31:52	12:34:20	01:02:28	00:20:52	00:09:20	0,546	129%	116%
17	20 July 2021	1	0,45	-	-	-	-	-	-	-	-
18	22 July 2021	1	0,45	10:29:24	11:33:52	01:04:28	00:00:16	00:00:24	0,535	127%	119%
20	29 July 2021	1	0,45	10:26:48	11:35:24	01:08:36	00:09:44	00:00:12	0,485	126%	108%
21	3 August 2021	1	0,45	10:55:04	11:38:48	00:43:44	00:04:44	00:00:04	0,464	104%	97%
23	5 August 2021	1	0,45	10:44:20	11:46:45	01:02:25	00:11:48	00:00:12	0,518	124%	115%
25	16 September 2021	1	0,45	11:03:40	12:30:40	01:27:00	00:19:08	00:13:16	0,542	145%	96%

26	21 September 2021	1	0,45	11:18:40	12:31:16	01:12:36	00:12:20	00:00:08	0,525	161%	117%
28	23 September 2021	1	0,45	10:59:04	12:05:20	01:06:16	00:09:28	00:04:48	0,508	112%	104%
30	30 September 2021	1	0,45	-	-	-	-	-	-	-	-
32	7 October 2021	0,5	0,45	10:21:08	11:49:56	01:28:48	00:07:52	00:00:08	0,525	325%	117%
33	12 October 2021	1	0,45	-	-	-	-	-	-	-	-
35	14 October 2021	1	0,45	10:20:44	12:05:16	01:44:32	00:09:24	00:02:06	0,570	188%	127%
36	19 October 2021	1	0,45	10:59:56	12:46:16	01:46:20	00:00:04	00:07:52	0,579	4%	16%
38	21 October 2021	1	0,45	10:56:04	12:01:56	01:05:52	00:02:40	00:00:24	0,459	109%	102%

Steel Mill results (STR plant, Pangborn Shot blast machine, Compressor)

Table 8-6: Results of the STR tests

ID TEST	Date	Theoretical duration [h]	P call [MW]	Switch On time	Switch Off time	Real duration [h]	Switch on Ramp	Switch off Ramp	P Average [MW]	Kpi1	Kpi1*
3	9 June 2022	0,25	0,02	-	09:56:00	-	-	00:05:00		N.C.	95%
22	22 June 2021	0,25	0,02	-	10:41:48	-	-	00:06:48	0,023	N.C.	117%
24	24 June 2021	0,25	0,02	11:30:12	10:45:24	00:44:48	00:00:12	00:03:44	0,022	N.C.	109%
38	21 October 2021	0,25	0,02	-	10:35:24	-	-	00:01:28	0,021	N.C.	82%

Table 8-7: Results of the Pangborn Shot Blast Machine tests

ID TEST	Date	Theoretical duration [h]	P call [MW]	Switch On time	Switch Off time	Real duration [h]	Switch on Ramp	Switch off Ramp	P Average [MW]	Kpi1	Kpi1*

3	9 June 2021	0,25	0,07	22:55:00	09:56:00	12:59:00	00:05:00	00:01:00	0,074	234%	105%
5	9 June 2021	0,5	0,045	-	-	-	00:01:00	00:01:00	-	146%	80%
7	22 June 2021	0,25	0,07	-	10:48:36	-	-	00:04:40	0,064	N.C.	82%
9	24 June 2021	0,25	0,07	-	10:46:16	-	-	00:00:48	0,06	N.C.	83%
12	8 July 2021	0,25	0,07	-	10:45:00	-	-	00:00:12	0,053	N.C.	81%
15	15 July 2021	0,25	0,07	11:37:36	10:47:12	00:50:24	00:04:40	00:00:52	0,07	288%	71%
19	29 July 2021	0,25	0,07	12:00:24	10:41:44	01:18:40	00:01:28	00:02:10	0,068	338%	81%
22	5 August 2021	0,25	0,07	11:48:48	10:45:52	01:02:56	00:06:00	00:00:12	0,062	248%	66%
24	16 September 2021	0,25	0,07	-	10:48:24	-	-	00:00:12	0,044	N.C.	46%
27	23 September 2021	0,25	0,07	-	10:40:04	-	-	00:03:20	0,066	N.C.	55%
29	30 September 2021	0,25	0,07	-	10:42:16	-	-	00:00:12	0,048	N.C.	81%
31	7 October 2021	0,25	0,07	-	11:05:25	-	-	00:00:04	0,062	N.C.	0%
34	14 October 2021	0,25	0,07	-	10:45:54	-	-	00:00:08	0,064	N.C.	66%
37	21 October 2021	0,25	0,07	-	10:45:12	-	-	00:00:08	0,068	N.C.	96%

Table 8-8: Results of the Compressor tests

ID TEST	Date	Theoretical duration [h]	P call [MW]	Switch On time	Switch Off time	Real duration [h]	Switch on Ramp	Switch off Ramp	P Average [MW]	Kpi1	Kpi1*
4	9 June 2021	1	0,035	10:01:00	11:01:00	01:00:00	00:00:04	00:00:08	0,0262	60%	57%
8	22 June	1	0,035	11:29:56	12:30:16	01:00:20	00:00:04	00:00:08	0,0256	85%	85%

	2021										
10	24 June 2021	1	0,035	11:30:08	12:33:04	01:02:56	00:00:04	00:00:08	0,0256	89%	86%
13	8 July 2021	1	0,035	10:56:32	11:06:36	00:10:04	00:00:04	00:00:12	0,0270	18%	0%
16	15 July 2021	1	0,035	11:24:56/ 12:19:40	11:35:04/ 12:23:04	N.C.	00:00:04	00:00:08	0,0270	15%	12%
20	29 July 2021	1	0,035	10:28:04	X	N.C	00:00:04	00:00:08	0,0253	390%	86%
23	5 August 2021	1	0,035	10:45:44	11:46:32	01:00:48	00:00:04	00:00:08	0,0254	86%	84%
25	16 September 2021	1	0,035	10:51:40	12:29:52	01:38:12	00:00:04	00:00:08	0,0261	142%	87%
28	23 September 2021	1	0,035	11:42:16	12:02:04	00:19:48	00:00:04	00:00:04	0,0261	116%	86%
30	30 September 2021	1	0,035	-	-	-	-	-	-	-	-
32	7 October 2021	0,5	0,035	10:15:52	12:50:44	02:34:52	00:00:04	00:00:04	0,0263	285%	74%
35	14 October 2021	1	0,035	10:30:13	11:17:38	00:47:25	00:00:04	00:00:12	0,0258	96%	85%
38	21 October 2021	1	0,035	10:57:24	12:15:16	01:17:52	00:00:04	00:00:04	0,0259	112%	86%

Industrial Park results (Generators)

Table 8-9: Results of the generators tests

ID TEST	Date	Theoretical duration [h]	P call [MW]	Switch On time	Switch Off time	Real duration [h]	Switch on Ramp	Switch off Ramp	P Average [MW]	Kpi1	Kpi1 *
1	3 June 2021	0,5	0,8	13:59	14:32	00:33:00	00:01:00	00:02:00	0,78	98%	98%
2	9 June 2021	0	0	-	-	-	-	-	-	-	-
6	10 June 2021	0,5	0,8	14:30	15:01	00:31:00	00:01:00	00:01:00	0,81	96%	96%

8.2.2 Enel X

The following tables report the results regarding modulation tests performed on the foundry plant.

Table 8-10: Results of the furnace modulation tests.

ID	Date	P call [MW]	Theoretical Duration [h]	P Average furnace [MW]	P Average plant [MW]	Switch On Ramp [h]	Switch Off Ramp [h]	Real Duration [h]	ΔT1 [h]	ΔT2 [h]	ΔP plant [MW]	ΔP furnace [MW]	KPI1* Plant [MW]	KPI1* EAF [MW]
1	Aug. 5th	3	1	48,82	65,20	11’4’’	27’28’’	1h56’58’’	30’	1	4,93	4,34	164%	145%
2	Sep. 9th	3	1	48,17	63,14	AC	16’	1h1’	30’	1	3,20	4,40	107%	147%
3	Sep. 15th	6	1	49,75	66,68	AC	5’56’’	47’12’’	30’	1	6,67	7,96	111%	133%
4	Sep. 16th	6	1	48,55	65,96	3’4’’	5’56’’	1h9’	5h30’	1	7,87	6,40	131%	107%
5	Sep. 22nd	6	1	50,42	66,30	14’52’’	14’52’’	1h29’44’’	4h	1	6,31	5,71	105%	95%
6	Sep. 23rd	6	0,5	49,57	65,37	1’28’’	12’44’’	44’12’’	5h30’	1	7,82	8,64	130%	144%
7	Sep. 23rd	6	0,5			6’40’’	12’32’’	24’8’’	7h		8,09	9,39	135%	157%
8	Sep. 29rd	4,5	1	49,31	64,54	3’2’’	15’56’’	1h16’28’’	6h30’	1	2,64	5,03	59%	112%
9	Sep. 30th	6	2	49,17	66,11	3’16’’	2’32’’	2h5’48’’	4h30’	2	8,47	7,55	141%	126%
10	Oct. 6th	4,5	0,5	49,41	65,29	2’32’’	1’36’’	34’8’’	n.a.	1,5	7,06	4,09	157%	91%
11	Oct. 6th	4,5	1			AC	1’20’’	1h15’	n.a.		2,33	4,48	52%	99%
12	Oct. 7th	4,5	1,5	48,85	66,33	AC	6’44’’	1h23’12’’	5h30’	1,5	4,44	4,22	99%	94%
13	Oct. 13th	6	1	48,81	63,95	28’	12’24’’	1h12’52’’	4h15’	2	5,91	7,80	98%	130%
14	Oct. 13th	4,5	1			6’	6’8’’	1h6’16’’	5h15’		4,71	5,04	105%	112%
15	Oct. 14th	3	1	48,29	64,02	8’20’’	12’56’’	55’24’’	3h30’	1	-0,08	-0,10	-3%	-3%
16	Oct. 20th	3	1			4’’	2’20’’	57’36’’	3h30’		2,53	3,08	84%	103%

17	Oct. 20th	4,5	1	49,13	63,53	24’’	18’32’’	1h18’8’’	4h30’	3	5,67	6,98	126%	155%
18	Oct. 20th	6	1			AC	7’24’’	29’36’’	5h30’		8,88	8,49	148%	142%
19	Oct. 27th	6	1	49,84	67,60	48’’	28’’	1h1’16’’	1h15’	1	10,28	9,42	171%	157%
20	Oct. 28th	6	1,5	49,64	67,27	AC	1’32’’	1h30’32’’	1h30’	1,5	8,44	8,74	141%	146%

Table 8-11: Precision of the modulation evaluated by means of SE.

ID	Date	P call [MW]	MSE [MW2]		Min SE [MW2]		Max SE [MW2]	
			Total Load	EAF	Total Load	EAF	Total Load	EAF
1	Aug. 5th	3	20,691	6,083	0,176	4.7E-4	1031,823	213,137
2	Sep. 9th	3	25,846	8,207	0,003	0,001	740,114	226,351
3	Sep. 15th	6	18,696	126,652	0,002	2,106	537,089	173,020
4	Sep. 16th	6	15,122	59,184	0,001	0.001	460,935	862,303
5	Sep. 22nd	6	14,038	4,112	0,070	0,001	179,455	159,062
6	Sep. 23rd	6	19,915	10,322	0,040	0,010	263,462	134,777
7	Sep. 23rd	6	14,894	12,035	0,014	8.76E-5	605,332	180,643
8	Sep. 29th	4,5	21,034	4,398	1.61E-5	7.2E-7	580,329	122,084
9	Sep. 30th	6	21,126	6,265	0,001	0,003	122,25	77,394
10	Oct. 6th	4,5	47,186	10,323	0,002	0,001	721,256	179,738
11	Oct. 6th	4,5	20,741	7,598	6.08E-	0,003	813,516	184,678
12	Oct. 7th	4,5	15,812	3,297	5.04E-5	2.64E-5	832,559	112,103
13	Oct. 13th	6	25,79	6,632	1,180E-04	3,923E-04	418,074	118,357
14	Oct. 13th	4,5	13,131	2,229	0,002	0,002	809,622	53,878
15	Oct. 14th	3	21,188	11,099	0,001	0,001	228,366	97,726
16	Oct. 20th	3	19,572	3,788	0,001	3,481E-04	846,588	218,606
17	Oct. 20th	4,5	17,698	10,103	0,004	0,001	709,913	172,485
18	Oct. 20th	6	30,191	8,110	1,641E-04	5,490E-06	693,490	157,461

19	Oct. 27th	6	41,562	9,639	0,004	0,003	993,709	163,754
20	Oct. 28th	6	27,138	9,349	1,275E-06	2,425E-04	975,117	137,771

Table 8-12: **Precision of the modulation evaluated by means of PE.**

ID	Date	P call [MW]	MPE (%)		Min PE (%)		Max PE (%)	
			Total Load	EAF	Total Load	EAF	Total Load	EAF
1	Aug. 5th	3	6,113	4,055	0,673	0,047	51,640	31,857
2	Sep. 9th	3	6,598	4,032	0,091	0,017	45,234	31,754
3	Sep. 15th	6	5,626	25,423	0,068	3,317	38,195	30,065
4	Sep. 16th	6	5,476	29,843	0,063	20,866	35,805	48,098
5	Sep. 22nd	6	5,458	3,665	0,438	0,059	22,215	28,394
6	Sep. 23rd	6	6,444	6,357	0,336	0,230	27,342	26,646
7	Sep. 23rd	6	4,009	6,140	0,198	0,021	41,444	30,849
8	Sep. 29th	4,5	5,800	3,201	0,007	0,002	40,121	25,069
9	Sep. 30th	6	5,178	4,693	0,047	0,059	46,521	29,400
10	Oct. 6th	4,5	7,162	4,676	0,077	0,054	44,182	29,854
11	Oct. 6th	4,5	5,690	21,463	0,013	0,078	46,923	32,792
12	Oct. 7th	4,5	5,050	3,25	0,011	0,012	46,666	23,875
13	Oct. 13th	6	25,270	32,663	0,019	0,046	35,286	25,414
14	Oct. 13th	4,5	4,210	2,586	0,072	0,103	47,864	16,567
15	Oct. 14th	3	5,881	6,660	0,052	0,057	24,764	21,826
16	Oct. 20th	3	4,784	2,976	0,048	0,040	48,072	32,048
17	Oct. 20th	4,5	5,754	5,762	0,103	0,053	45,140	29,424
18	Oct. 20th	6	6,757	5,365	1,641E-04	5,490E-06	45,849	29,532
19	Oct. 27th	6	7,645	6,323	0,099	0,126	51,170	29,190
20	Oct. 28th	6	6,488	5,969	0,002	0,036	50,968	26,899

8.2.3 Edison

Powertrain industry results (Chiller)

Table 8-13: Results of the chiller tests

ID	Data	Theoretical duration [h]	P call [MW]	Switch On time	Switch Off time	Real duration [h]	Switch on Ramp	Switch off Ramp	P Average [MW]	Kpi1	Kpi1*
1	Aug. 5th	1	-0,05	13:51:58	15:00:50	01:08:52	14:31:38	15:50:50	-0,006	25%	6%
2	Aug. 6th	1	-0,05	11:54:59	13:17:43	01:22:44	12:13:03	13:30:23	-0,04	127%	106%
3	Oct. 7th	1	-0,05	11:21:25	12:30:00	01:08:35	n.a.	n.a	0	0%	0%
4	Oct. 8th	1	-0,05	15:47:04	17:00:56	01:13:52	16:22:48	17:33:40	-0,04	133%	95%
5	Oct. 18th	1	-0,05	09:45:12	11:00:20	01:15:08	10:11:52	11:35:36	-0,02	71%	31%
6	Oct. 19th	1	-0,01	10:00:35	11:17:55	01:17:20	10:32:47	11:47:31	-0,01	257%	111%
7	Nov. 2nd	1	-0,01	14:15:20	14:59:40	00:44:20	14:34:12	15:34:52	-0,02	302%	106%
8	Nov. 3rd	0,5	-0,05	10:16:04	12:19:48	02:03:44	10:26:40	13:02:56	-0,025	268%	57%
9	Nov. 8th	1	-0,04			00:00:00					
10	Nov. 9th	1	-0,04			00:00:00					
11	Nov. 16th	1	-0,04	09:29:47	10:46:55	01:17:08	09:50:27	11:03:19	-0,035	92%	39%
12	Nov. 17th	1	0,07	10:39:54	11:57:46	01:17:52	10:44:14	12:12:14	0,04	80%	56%
13	Nov.18th	1	0,07	10:21:39	11:53:11	01:31:32	10:25:51	11:57:35	0,02	37%	36%

9 Annex 3 - RES

9.1 AVC tests in Vaglio

- 27/01/2021 – Local test (Q set-points)

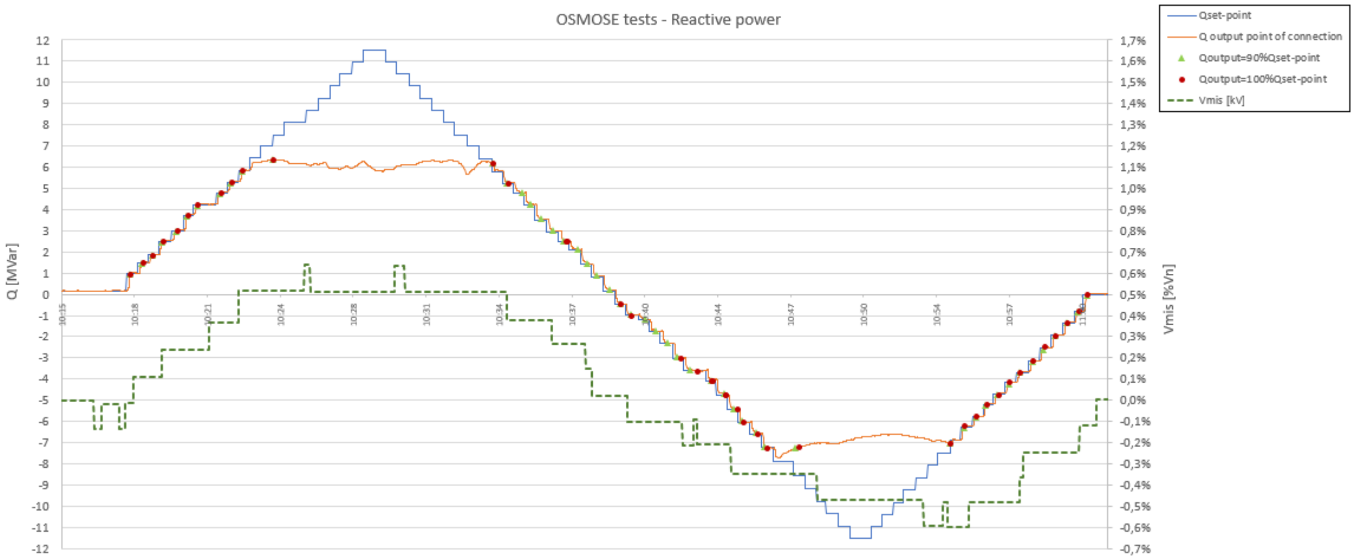

Figure 9-1 Local Test - Q set-point

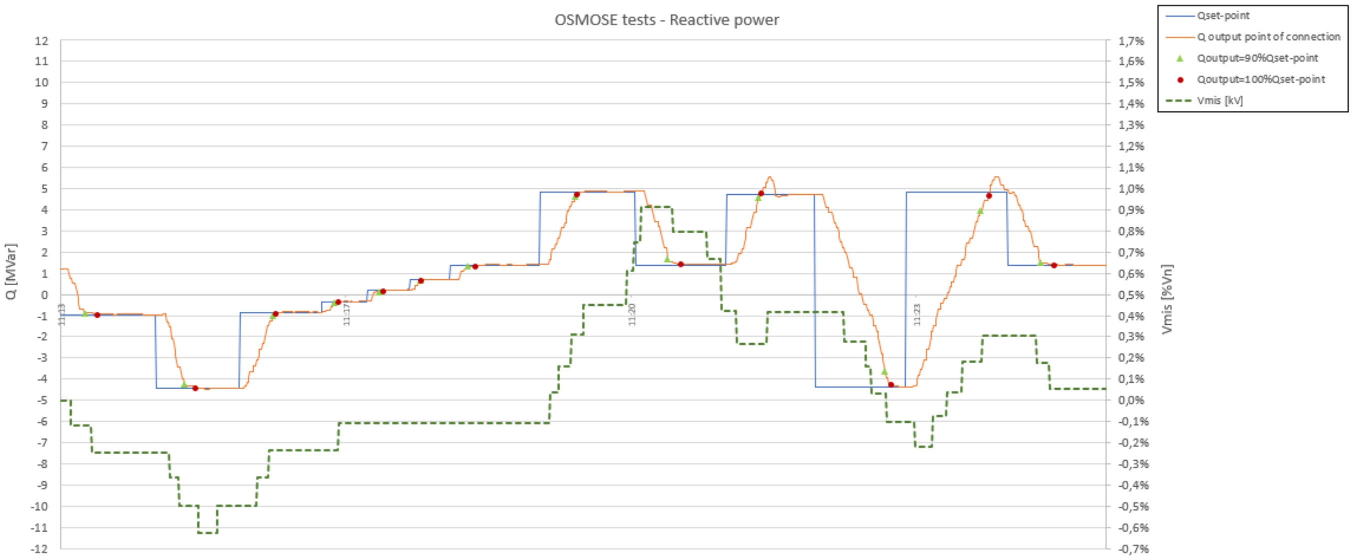

Figure 9-2 Local Test - Q set-point

In both fig 9.1 and 9.2 the orange curve corresponding to the total reactive power at Point of Connection (PoC) entailed to face an anomalous behavior on Siemens Gamesa (SGRE) plant regulator which seemed to cut the capability curve in terms of a cap to a max and min reactive power absorbed / injected to the grid (equal to approx. +6,4 MVAr / -7MVAr). On January 2022, SGRE confirmed after deepened analysis and tests, that the regulation tool did not properly work in sending the right reactive set-point to one of the two wind farms (in particular, Vaglio n. 6 WTGs). During Vaglio tests (both local and remote with Terna), this behavior was not solved and still persistent in graphs and results. In any case, although this anomalous behavior, high level voltage at the Point of Connection generally follows the Q behavior. For some of the set-points asked, especially those requiring the highest Q variations (see Fig. 9.2 when a Q inversion is asked) up to 45 s are needed to fully reach the requested set-point. The way and speed in voltage changes could depend on power grid features (antenna or strong power grid configuration).

- 25/06/2021 – Local tests (Voltage set-point)

The local tests in Vaglio following a locally sent voltage set-point highlighted similar features as those with Q set-points. In this case the local embedded Power Plant Controller with Sirius software simulated voltage set-points in order to verify the behavior of the plants in providing reactive power following a V set-point, according to a Q=f(ΔV) curve. This curve can be parametrized and three parameter families, below here summarized (Figure 9-3), were tested during these local tests (Figure 9-4, Figure 9-5, Figure 9-6).

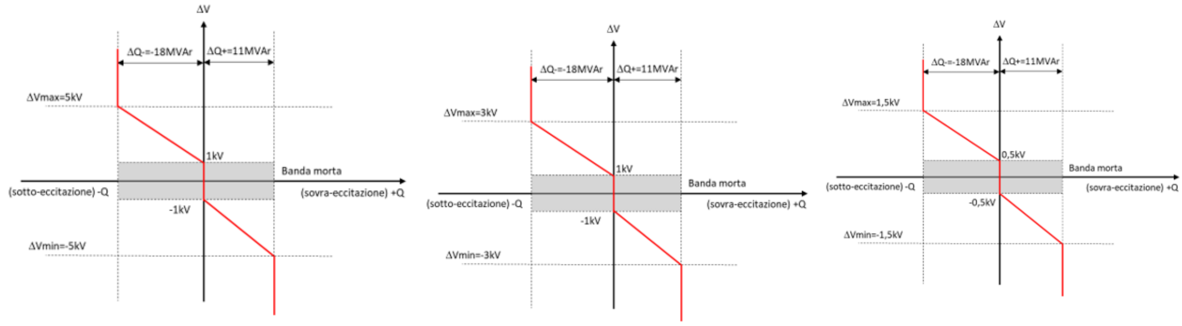

Banda Morta	±1 kV
ΔVmax	+5 kV
ΔVmin	-5 kV
ΔQ+	11 MVAr
ΔQ-	-18 MVAr

Banda Morta	±1 kV
ΔVmax	+3 kV
ΔVmin	-3 kV
ΔQ+	11 MVAr
ΔQ-	-18 MVAr

Banda Morta	±0,5 kV
ΔVmax	+1,5 kV
ΔVmin	-1,5 kV
ΔQ+	11 MVAr
ΔQ-	-18 MVAr

Figure 9-3 Q=f(ΔV) curves used for Vaglio plant. From left to right, parametrization #1, #2, #3

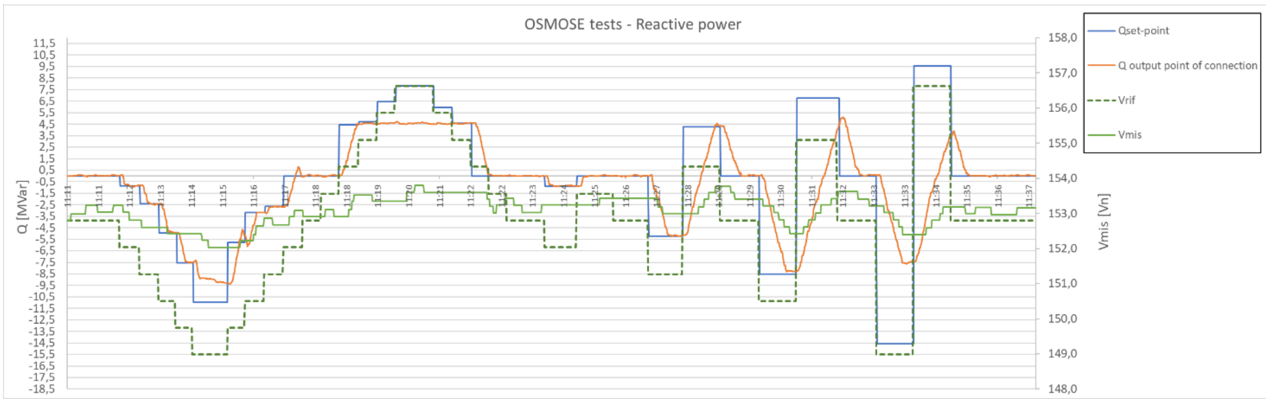

Figure 9-4 V set-point test, parametrization #1

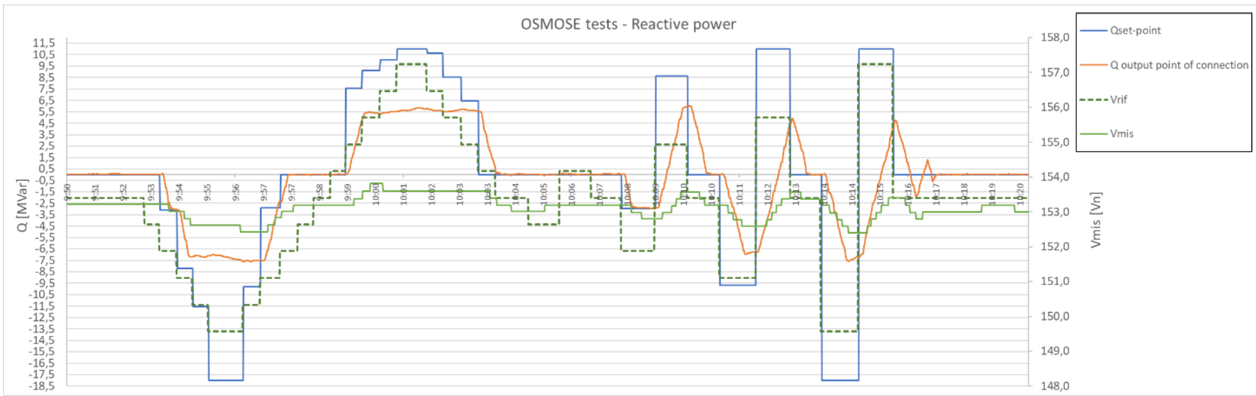

Figure 9-5 V set-point test, parametrization #2

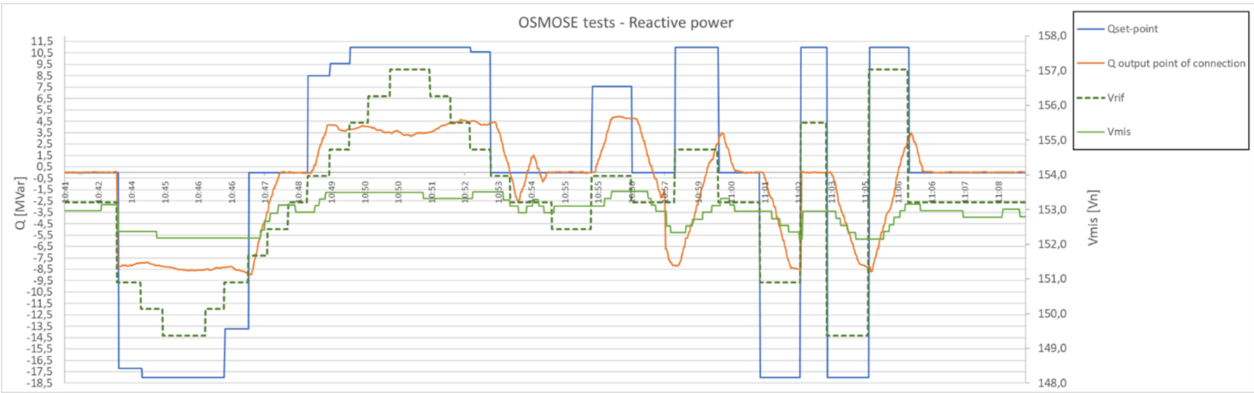

Figure 9-6 V set-point test, parametrization #3

- 10/11/2021 Remote tests (Q set-points, V set-points)

During the first part of the test, a set-point of reactive power Q value was sent from the transmission operator (Terna control room) to the concentrator of ERIN, which then sent forward the signal to the plant, where SGRE plant regulator finally implemented the setting.

The maximum reactive power Q_{max} that was instantaneously available was dependent on the active power during the test due to a lower than 10% nominal power according to each WTG capability curve. In Figure 9-7 below, P and Q values during the reactive power setpoint test are plotted.

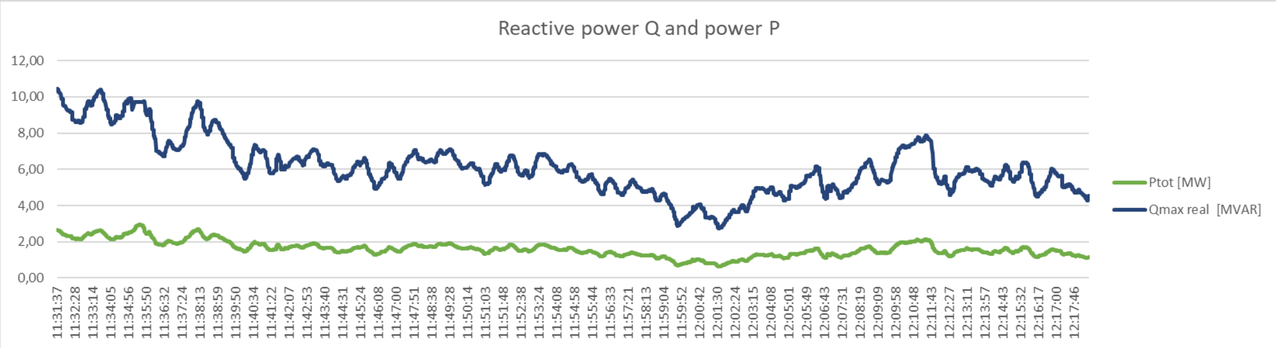

Figure 9-7 Maximum reactive power as a function of active power P

In Figure 9-8 below, the reactive power actually requested to be provided by the wind power plants, Q_{sent}, was the product of the maximum reactive power Q_{max} available at the time of the command of the transmission operator multiplied by $Q_{tso\%}$, that is the requested percentage of reactive power from Terna control room.

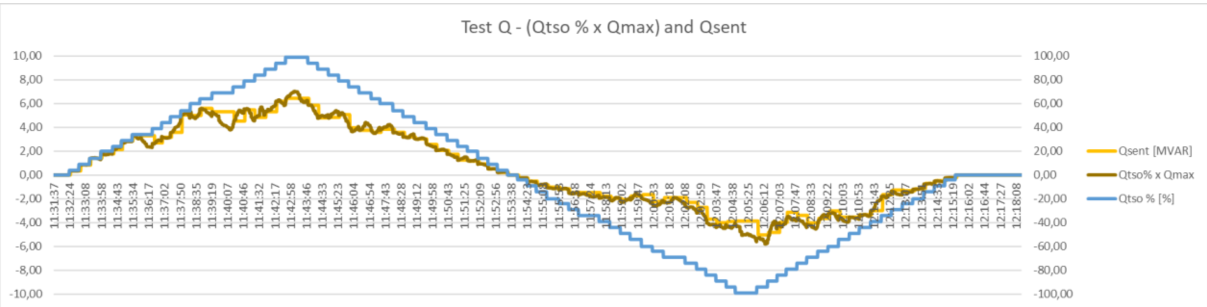

Figure 9-8 Remote test - Q set point

The step values of the profile of the reactive power requested to be provided by the wind power plant, Q_{sent}, in general match the curve of the maximum reactive power available Q_{max} multiplied by the percentage requested by the transmission service operator, $Q_{tso\%}$. The maximum reactive power output anomalous behavior was less evident due to a such low power output.

The second part of the test regarded regulation following a V set-point (Figure 9-9). As explained before, the V set-point (Vrif in Figure 9-9) sent by Terna corresponds to a certain Q set-point (through a Q=f(ΔV) parametrization curve) commanded to the turbines (Q sent); in the Figure the measured Q is then Qtot, while U1 is the measured HV voltage.

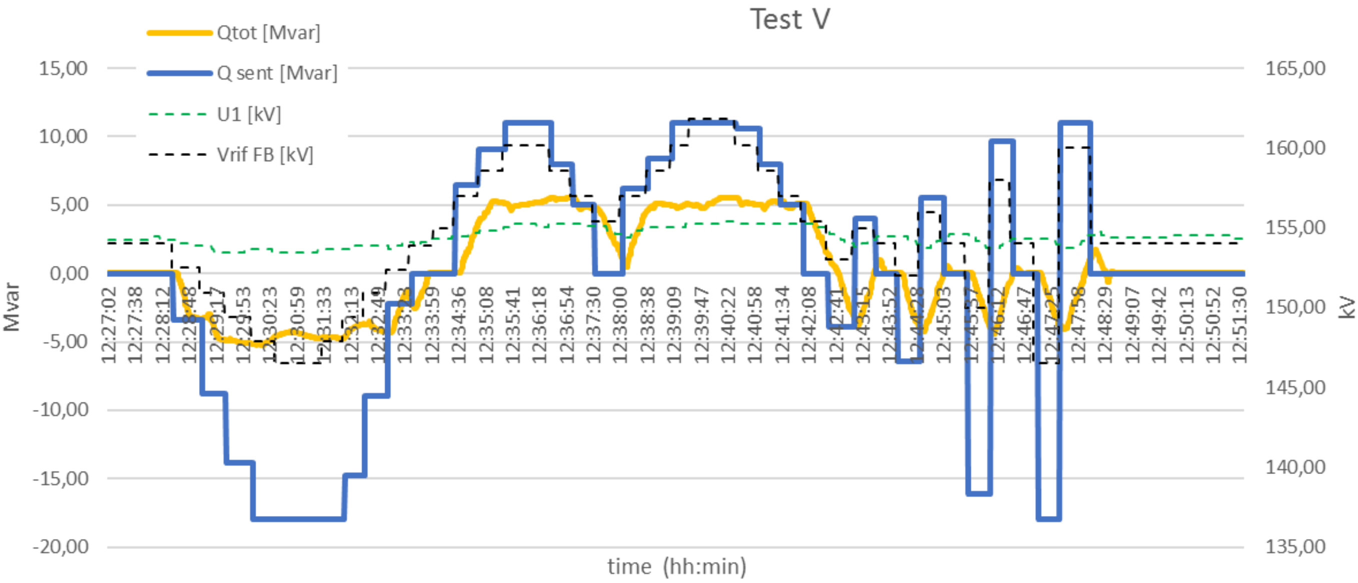

Figure 9-9 Remote test - V set-point

The “fast” parametrization implemented during these tests required the highest possible Q variations to the plant; as observed before, the plant only limitedly could follow, due both to saturation issues that blocked the plant from providing the maximum available Q and to the plant own dynamics (this can be especially seen for the last step set-points). One can still appreciate induced voltage variations in Figure 9-10.

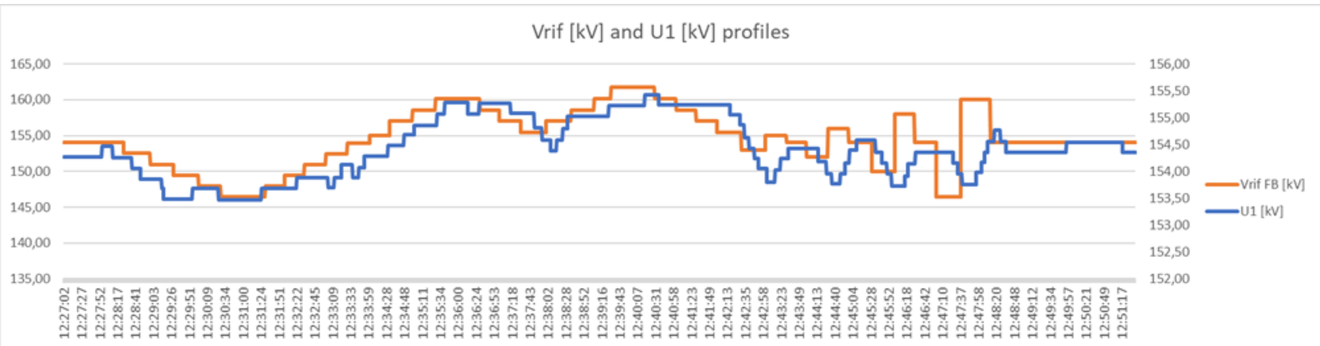

Figure 9-10 Remote test - voltage variations during V set-point test

9.2 AVC tests in Pietragalla

- 20/10/2011 Local test Pietragalla (Q set-points)

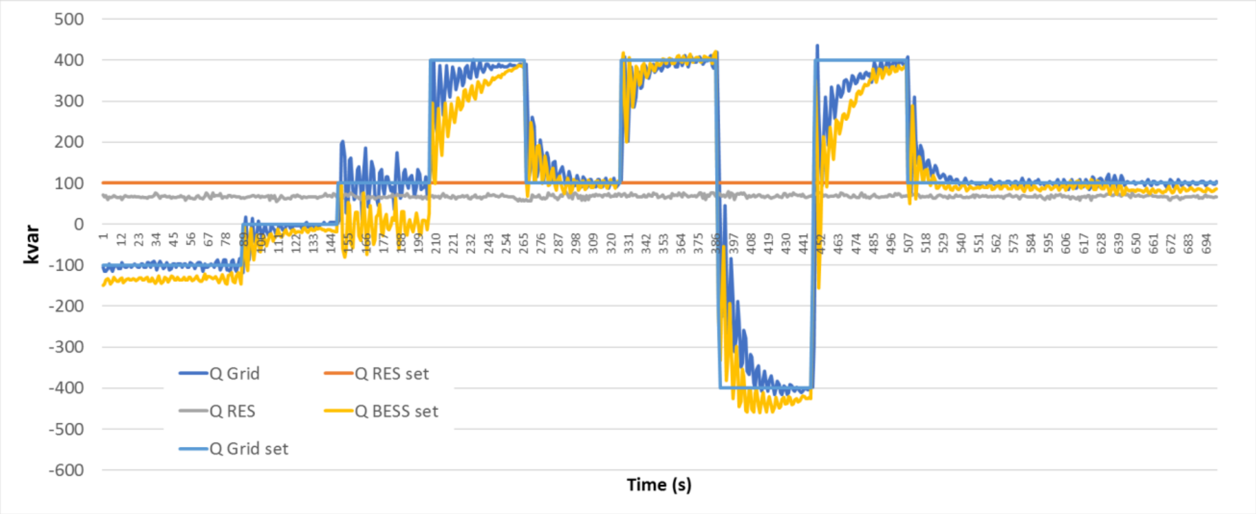

Figure 9-11 Local test - Q set-point

- 20/10/11 Remote test Pietragalla (Q set-points)

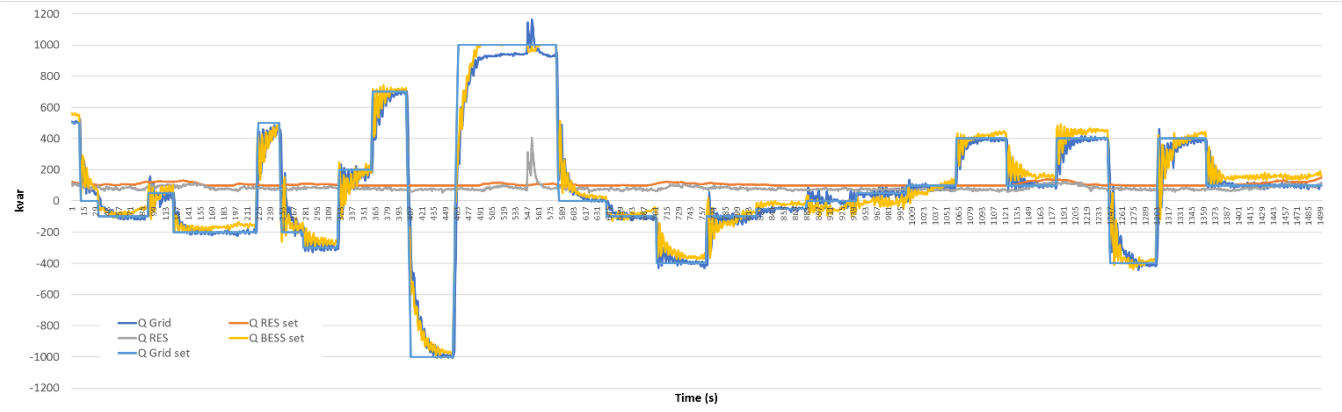

Figure 9-12 Local test - Q set-point

In both Figure 9-11 and Figure 9-12 “Q grid set” and “Q grid” represent respectively the setpoints requested to the plants and the total output at the point of connection. One can observe also the set-points requested to the storage systems and wind plants. During remote tests, Figure 9-12 the storage plant was actually asked to respond to full capability inversions (-1000 kvar to 1000 kvar); for the 100% Q setpoint, corresponding to 1000 kvar insertion, the plant was not capable to provide the requested contribution as the reactive power provided by the wind plant, QRES, was not capable by itself to compensate internal plant losses (part of Q produced by BESS was then necessary to compensate part of the internal reactive power losses).

9.3 Synthetic inertia control device parameters (Pietragalla)

Parametrization		**A**	**B**	**C**
SOC Parameters during synthetic inertia provision				
Minimum SOC	*[%]*		30	
Maximum SOC	*[%]*		70	
Objective SOC parameters				
Objective SOC Power	*[MW]*		0,1	
Objective SOC value	*[%]*		50	
SOC hysteresis	*[%]*		5	
Automatic deactivation parameters				
Minimum SOC	*[%]*		10	
Functionality dehabilitated			FALSE	
Contribute 1 (Rocof dependent)				
Maximum Power (absorption)	*[MW]*	0,8	0,8	0,8
Maximum Power (Generation)	*[MW]*	0,8	0,8	0,8
Droop	*[%]*	5	5	5
Dead band (ROCOF)	*[mHz/s]*	30	30	30
hysteresis (Rocof)	*[mHz/s]*	10	10	10
Dead band (frequency)	*[mHz]*	20	20	20
Holding time	*[ms]*	10000	10000	10000
Ramp down gradient	*[MW/s]*	0,1	0,1	0,1
Smart inertia functionality		FALSE	FALSE	VERO
Alfa coefficient		1	0	1
Contribute 2 (Frequency dependent)				
Maximum Power (absorption)	*[MW]*	0,8	0,8	0,8
Maximum Power (Generation)	*[MW]*	0,8	0,8	0,8
Droop	*[%]*	5	5	2
hysteresis (frequency)	*[mHz]*	10	10	10
Dead band (frequency)	*[mHz]*	20	20	20
Holding time	*[ms]*	10000	10000	10000
Ramp down gradient	*[MW/s]*	0,1	0,1	0,1
Beta coefficient		0	1	1

Table 9-1 Synthetic inertia control device parameters

As explained before, during experimentation only contribute 1, rocof dependent, was examined (therefore alfa coefficient is equal to 1 and beta coefficient is set to 0), meaning parametrization A was tested. The device would be capable of providing also a mixed contribution (parametrization C).